Journal of Medicinal Chemistry

Article

Discovery and Characterization of BAY 1214784, an Orally Available Spiroindoline Derivative Acting as a Potent and Selective Antagonist of the Human Gonadotropin-Releasing Hormone Receptor as Proven in a First-in-Human Study in Postmenopausal Women

Olaf Panknin, Andrea Wagenfeld, Wilhelm Bone, Eckhard Bender, Katrin Nowak-Reppel, Amaury E. Fernández-Montalván, Reinhard Nubbemeyer, Stefan Bäurle, Sven Ring, Norbert Schmees, Olaf Prien, Martina Schäfer, Christian Friedrich, Thomas M. Zollner, Andreas Steinmeyer, Thomas Mueller, and Gernot Langer

J. Med. Chem., **Just Accepted Manuscript** • DOI: 10.1021/acs.jmedchem.0c01076 • Publication Date (Web): 22 Sep 2020

is published by the American Chemical Society. 1155 Sixteenth Street N.W., Washington, DC 20036

Discovery and Characterization of BAY 1214784, an Orally Available Spiroindoline Derivative Acting as a Potent and Selective Antagonist of the Human Gonadotropin-Releasing Hormone Receptor as Proven in a First-in-Human Study in Postmenopausal Women

Olaf Panknin,[#] Andrea Wagenfeld,[#] Wilhelm Bone,[#] Eckhard Bender,[‡] Katrin Nowak-Reppel,[#] Amaury E. Fernández-Montalván,[#§] Reinhard Nubbemeyer,[#] Stefan Bäurle,[#] Sven Ring,[#] Norbert Schmees,[#] Olaf Prien,[#] Martina Schäfer,[#] Christian Friedrich,[#] Thomas M. Zollner,[#] Andreas Steinmeyer,[#] Thomas Mueller,[‡] and Gernot Langer*[#]*

[#]Bayer AG, Research & Development, Pharmaceuticals, Müllerstrasse 170, 13342 Berlin, Germany

‡Bayer AG, Research & Development, Pharmaceuticals, Aprather Weg 18a, 42113 Wuppertal, Germany

KEYWORDS. gonadotropin-releasing hormone receptor, luteinizing hormone suppression, spiroindolines, structure–activity relationship, drug metabolism and pharmacokinetics optimization, uterine fibroids, heavy menstrual bleeding

ABSTRACT. The growth of uterine fibroids is sex hormone dependent and commonly associated with highly incapacitating symptoms. Most treatment options consist of the control of these hormonal effects, ultimately blocking proliferative estrogen signaling (i.e., oral contraceptives/antagonization of human Gonadotropin-Releasing Hormone Receptor [hGnRH-R] activity). Full hGnRH-R blockade, however, results in menopausal symptoms and affects bone mineralization, thus limiting treatment duration or demanding estrogen add-back approaches. To overcome such issues, we aimed to identify novel, small-molecule hGnRH-R antagonists. This led to the discovery of compound BAY 1214784, an orally available, potent, and selective hGnRH-R

antagonist. Altering the geminal dimethylindoline core of the initial hit compound to a spiroindoline system significantly improved GnRH-R antagonist potencies across several species, mandatory for a successful compound optimization *in vivo*. In a first-in-human study in postmenopausal women, once daily treatment with BAY 1214784 effectively lowered plasma luteinizing hormone levels by up to 49%, at the same time being associated with low pharmacokinetic variability and good tolerability.

INTRODUCTION

Uterine fibroids (also known as uterine leiomyomas) are the most common benign tumors of the uterine muscle layer with a prevalence of >70% in women.[1] Although the precise genesis of uterine fibroids is still subject to current research,[2–4] their actual growth is unambiguously sex hormone dependent.[5–7] Thus, they are frequently associated with menses-related heavy menstrual bleeding (leading to dysmenorrhea; i.e., pelvic pain and pressure as well as anemia) or even infertility. Yet, despite the large number of women presenting with leiomyoma complaints (some 20–50% of women of reproductive age), the choice of treatment options available is quite limited.[8,9] The spectrum ranges from curative surgical interventions[10,11] to noncurative, symptomatic treatment of uterine fibroid associated pain (analgesics) and medications primarily controlling (heavy) bleeding symptoms,[12] namely oral contraceptives or hGnRH-R I functional antagonists, the latter widely used to also control the estrogen-dependent growth of malignant ovarian and breast cancers. However, given the induction of menopausal symptoms and effects on bone mineralization, hGnRH-R blockers currently in use are not yet entirely suitable for long-term treatment. Full antagonization of

hGnRH-R signaling results in a complete blockade of estrogen production in the vast majority of cases owing to the central role of this receptor in the production of the gonadotropins LH and FSH, which in turn control the conversion of androgen precursors in the ovary, the major source of estrogens in women of reproductive age.

Actual fine-tuning and expression of both gonadotropins is thought to be achieved by amplitude and frequency changes in GnRH secretion[13,14] and thus differential, cell-type specific hGnRH-R stimulation.[15,16] Continuous, nonpulsatile peptide agonist treatment results in a rapid development of tolerance to further stimulation, uncoupling of downstream second messenger cascades, and a complete blockade of agonist effects (functional antagonization).[17,18] In addition to parenteral administration procedures further complicating the matter, the high degree of suppression of ovarian function achieved with early peptide agonist protocols often required estrogen add-back therapies to adequately control and prevent menopausal side effects when treating patients.

All of this highly favored the search for orally available, non-peptide, small-molecule (SMOL) hGnRH-R antagonists to effectively improve treatment protocols and patient

compliance. Consequently, a number of such SMOL antagonists have been investigated.[19] In particular, two SMOL GnRH-R antagonists have already attained market approval, namely relugolix (TAK-385, Takeda; indication: uterine fibroids)[20,21] and elagolix (NBI-56418 Na, AbbVie; indication: endometriosis-related pain),[22–24] and the very same compounds are in Phase III clinical trials with regard to the respective other type of indication [i.e., elagolix (AbbVie) for uterine fibroids and relugolix (Myovant Sciences) for endometriosis], as is linzagolix (ObsEva/Kissei Pharmaceutical)[25] for both indications. Furthermore, elagolix (AbbVie) is in Phase II clinical trials for the treatment of polycystic ovary syndrome (PCOS). Table 1 gives their chemical structures and summarizes some of their reported properties.

The adverse effects reported for these compounds so far [i.e., intermenstrual and heavy menstrual bleeding (metrorrhagia/menorrhagia), hot flushes, headache, and dose-dependent loss of bone mineral density with no endometrial findings for all] are consistent with their mode of action. However, both relugolix and elagolix, when administered at higher doses, also necessitated the use of estrogen add-back therapy (ABT) – the main reason for this most likely resulting from the actual compounds' PK/PD

properties. Thus, a high unmet medical need still exists to identify hGnRH-R antagonists modulating receptor signaling behavior in favor of a partial deprivation of estradiol (E2) levels only. Therefore, we decided to initiate a comprehensive compound identification and optimization program aimed at the detection of SMOL hGnRH-R antagonists with improved, superior PK/PD properties. From the outset, we focused on compounds possessing comparable multispecies activities at both the human and the rat GnRH receptor to be able to take advantage of the use of rat animal models for further optimization. Here, we report the identification and extensive characterization of **5a** (BAY 1214784) as a novel, orally available, potent, and selective hGnRH-R antagonist with the desired pharmacological profile of partially lowering of LH levels only, in preclinical as well as first-in-human studies.

RESULTS AND DISCUSSION

HTS, Identification of Screening Hit 15 and Improved Compound 1a. A cell-based high-throughput screen of the Bayer Pharma compound library (comprising ~2.5 million compounds) led to the identification of an indoline hit cluster with borderline activities at the human GnRH receptor (see the Supporting Information for details of the hit-to-lead

examination and the removal of compounds with pan-assay interference motifs[26]). Although the members of this cluster also possess high lipophilicity and low solubility characteristics, this scaffold was considered the most promising starting point because of comparable multispecies potencies at both the human and the rat GnRH receptor, a prerequisite considered necessary for further preclinical optimization in vivo. Thus, racemic screening hit **15** (see Table 2) was chosen for resynthesis and as the starting point for a first round of SAR modifications. These efforts resulted in the identification of enantiomerically pure compound **1a** with improved potencies at both human and rat GnRH receptors [IC_{50} = 568 and 726 nM (LHRH), respectively]. Given that routine monitoring of **1a** with functional profiling in a panel of 25 GPCRs confirmed no significant off-target liabilities (data not shown), this compound was chosen for further optimization even though its lipophilicity is high (logD at pH 7.5 = 3.8), its solubility proved to be low, and compound clearance in rat hepatocytes turned out to be high [CL_b (rat female Wistar) = 3.1 L/h/kg; see the Supporting Information Table S1 for a detailed compound profile]. An overview of key compounds synthesized in the subsequent

course of the hit-to-lead and lead optimization process, along with their core properties, is given in Figure 1.

Synthesis of Screening Hit 15 and Improved Compound 1a. The racemic trimethylindoline core of **15** and **1** was prepared in two steps starting with a Fischer indole synthesis using 4-hydrazinobenzoic acid (**6**) and 3-methylbutan-2-one (**7**) under acidic conditions followed by reduction of the formed indolenine intermediate **8** with sodium borohydride to give indoline **9** (see Scheme 1). The carboxyli group at C-5 was protected as a methyl ester (intermediate **10**) which was followed by sulfonamide formation with the respective benzenesulfonyl chloride to furnish **11** and **12**. Ester saponification of **11** with aqueous lithium hydroxide and subsequent amide coupling of **13** with 1-(2-chlorophenyl)methanamine gave the racemic amide **15**. For the isolation of **1a**, an enantiomeric separation by chiral HPLC was performed at the final stage, after saponification of **12** to **14** and amide coupling to provide **1**.

Variations at N-1, C-2, and C-5 of the 3,3-Dimethylindoline Core. Numerous attempts to significantly increase compound potency by exploring extensive variations at N-1, C-

2, and C-5 of the indoline core proved unsuccessful (see Figure 2 for a brief qualitative summary).

Incorporation of a GPCR Privileged Structure: Identification of Lead 2b. In a second approach to improve compound potency, we turned towards the concept of GPCR privileged structures[27–33] (see Table 2). The incorporation of an N-acetylated spiropiperidine system at C-3 of the indoline core, as in compound **2b**, boosted antagonistic potency in all species [IC_{50} hGnRH-R/rGnRH-R = 41/29 nM (LHRH), IC_{50} cynomolgus monkey GnRH-R = 205 nM (buserelin)] and improved the LLE by approximately 2 log units relative to **1a** (see the Supporting Information Table S1 for a detailed compound profile). Therefore, compound **2b** was chosen as lead compound and starting point for further optimization with a special focus on addressing still-existing liabilities with regard to its physicochemical (i.e., low solubility: 25 mg/L at pH 6.5) and pharmacokinetic properties [i.e., high blood clearance in vivo: CL_b (rat female Wistar) = 4.7 L/h/kg and limited permeation in Caco-2 cells (P_{app} A–B = 38 nm/s, efflux ratio 2.4)].

Variations at the Spiropiperidine Nitrogen. Subsequently, a number of racemic derivatives with variations at the spiropiperidine nitrogen atom were synthesized and

tested with the aim of improving both the DMPK profile and the potency of compound **2b**. However, extensive variations including amides, sulfonamides, ureas, carbamates, and alkyl chains bearing polar groups did not lead to the desired results (data not shown). We therefore elected to retain the *N*-acetyl moiety and to continue with SAR studies at C-2, N-1, and C-5 of the spiro[piperidine-indoline] core.

Variation of the Substituent at C-2 of the Spiro[piperidine-indoline] Core. This approach confirmed that monosubstitution at C-2 has a major influence on antagonist potency (see Table 3), as the introduction of one methyl in racemic **16** increased the compound's potency in the human LHRH assay roughly fivefold compared with the C-2 unsubstituted derivative **17**. Generally, sterically less demanding hydrocarbons were preferred at C-2 and polar substituents were not well tolerated (as exemplified by the 58-fold drop in potency of hydroxyalkyl derivative **19** relative to allyl derivative **18**). Likewise, more sterically demanding residues (i.e., aryls or heteroaryls) at C-2 also led to a decrease in potency (data not shown). Overall, compound **20** containing a cyclopropyl moiety was considered to possess the best balance in terms of potency and DMPK profile. As already seen for the 3,3-dimethylindoline hit cluster, the actual

configuration at the stereogenic center had a major impact on potency, with one enantiomer being almost exclusively active only [e.g., compare the potency of racemic **16** (IC_{50} hGnRH-R = 87 nM) with distomer **16a** (IC_{50} >20 μM) and eutomer **16b** (IC_{50} = 21 nM), LHRH assay; absolute stereochemistry not elucidated].

Variations at N-1 of the Spiro[piperidine-indoline] Core. As already observed for the 3,3-dimethyl hit cluster, quite a steep SAR was found at the indoline nitrogen atom (N-1, see Table 4). Only aryl sulfonamides were tolerated while truncation to a methyl sulfonamide led to an almost complete loss of potency (cf. **21** and **22**). In addition, amide and benzyl substituents were also significantly less potent than their sulfonamide counterparts (cf. **16** with **23** and **24**). Heteroaryl sulfonamide substituents (e.g., in **25**) and sterically small substituents at the meta or para position of the phenyl sulfonamide (i.e., methoxy, fluoro, cyano) were tolerated (data not shown) while the introduction of a *para*-trifluoromethyl moiety as in **26** led to a surprisingly low potency. On the other hand, the *para*-fluoro substituent at the phenyl sulfonamide as in **16** improved potency roughly two- to threefold when compared with the corresponding methoxy derivative **2** (see

Table 2) without adding additional lipophilicity to the system (clogD of **16** = 3.25 vs clogD of **2** = 3.15).

Variations at C-5 of the Spiro[piperidine-indoline] Core. When evaluating the influence of substituents at C-5 (see Table 5), we noticed that benzamides consisting of lipophilic benzylic amines and incorporating an *ortho* substituent at the aromatic residue were preferred. The introduction of an *ortho*-chloro group as in **20** improved antagonist potency roughly 8- to 12-fold compared with the unsubstituted derivative **27**. Furthermore, benzylic amides with an additional para substituent at the aromatic residue were also tolerated (see *para*-fluoro derivative **28**). Blocking of the benzylic position with a quaternary carbon shifted the preference of monosubstitution at the aromatic residue from the ortho to the para position (cf. **29** vs **30**). However, this approach did not improve the in vitro clearance of these derivatives. Generally, NH amides were more potent than the corresponding *N*-methyl amides, and anilides were tolerated as well (data not shown). Of note, the connection of the carboxamide function to the core could be reversed. In this subseries, meta-substituted benzamides were preferred and heteroaryls were also tolerated (see **31** and **32**). Notwithstanding the

excellent potencies achieved this way, we nevertheless decided to discontinue further investigation of aniline core derivatives, having a potentially mutagenic profile upon metabolic deacylation in mind.

Identification of 3a Suitable for In Vivo Experiments. Returning to further options for spiro[piperidine-indoline] variations we chose to (a) remove the *N*-acetyl residue in compound **2b** (otherwise exhibiting favorable potencies at both the human and the rat receptor) with the aim of improving solubility, and (b) also exchange the *para*-methoxy residue at the phenyl sulfonamide in an attempt to block potential metabolism (see **3a** in Table 6). Indeed, these modifications significantly improved the solubility of the resulting compound **3a** (from 25 mg/L for **2b** to 271 mg/L for **3a** at pH 6.5) and led to a decrease in in vivo blood clearance (from 4.7 L/h/kg for **2b** to 1.4 L/h/kg for **3a**). Along with an acceptable antagonist potency [IC_{50} rGnRH-R = 27 nM (LHRH) and IC_{50} hGnRH-R = 172 nM (buserelin)], these data were considered reasonably sufficient to initiate a first animal study in rats. Nevertheless, **3a** had to be administered parenterally because of its limited oral bioavailability in rats (F <2%; see the Supporting Information Table S1 for details). To prove any blockade in GnRH/GnRH-R signaling, **3a** was tested in

ovariectomized (OVX) rats, a well-established animal model to study compound effects on OVX-induced increased gonadotropin release leading to elevated plasma LH levels. A single intraperitoneal injection of **3a** at 30 mg/kg lowered plasma LH levels in these animals significantly (i.e. approximately 74% reduction after 1 h) and reversibly in comparison with animals treated with either the peptidic GnRH antagonist cetrorelix (0.1 mg/kg, sc, long-lasting LH reduction) or vehicle (no effect; see the Supporting Information Figure S6).

Towards Orally Available Compounds. Even though treatment with **3a** resulted in a successful lowering of plasma LH levels in vivo for the first time, it transpired that the compound (apart from its already known basic and lipophilic properties as well as oral bioavailability and Caco-2 issues) suffered from off-target effects at several ion channels, including hERG (IC_{50} = 1.1 μM), clearly requiring additional improvements to reduce its basicity and lipophilicity. Thus, guided by the results of in vitro investigations in human hepatocytes which revealed the benzylic amide as the main spot of oxidative metabolism, we firstly aimed to decrease the lipophilicity and electron density in this part of the molecule by introducing heteroatoms to further improve the compound's

clearance profile. Although not very effective in terms of potency initially, unsubstituted pyridylmethyl amides clearly showed a lower metabolic clearance in human hepatocytes compared to the corresponding benzylic amides. Next, the introduction of a substituent at C-3 of the pyridyl ring, for example chloro, led to a sufficient recovery in antagonist potency while retaining an improved clearance profile in both human hepatocytes and rats in vivo (see Table 7, compounds **20b** and **33a**).

In additional experiments aimed at improving the off-target profile, we investigated the influence of basicity at the spiropiperidine nitrogen atom. However, all attempts to reduce basicity and to simultaneously improve the pharmacokinetic profile by employing extensive substituent variations at this nitrogen failed to provide the desired outcome (see 'variations at the spiropiperidine nitrogen' section above). Thus, we decided to evaluate non-nitrogen-containing structural modifications of the spiropiperidine core itself. A broad range of different spirocarbocyclic and spiroheterocyclic systems at C-3 of the indoline core was synthesized and tested (see Table 8). Whereas secondary and tertiary alcohols (e.g., **37**, **38**) and (thio)pyrans (e.g., **39**, **40**) were tolerated, but somewhat less potent than **20**, oxidized thiopyran derivatives (i.e., sulfoximines,

sulfoxides, and sulfones; see **34a**/**b**, **35**, and **36**) proved to be most promising with clear indications of a link between the absolute configuration at the stereogenic sulfur and the actual potency achieved.

Identification of Orally Available Compound 4a. In addition to having advantages in terms of synthetic access (such as less stereochemistry issues than sulfoximines or sulfoxides), *sulfones* in general were finally considered as resulting in the best balance between potency, clearance, and permeation. Consequently, the combination of (a) the chloropyridylmethyl amide at C-5 with (b) the spirocyclic sulfone at C-3 of the indoline and (c) a cyclopropyl at C-2 resulted in compound **4a** which was chosen for a first experiment making use of po administration in OVX rats. Table 9 summarizes the technical profile of **4a** (for the full profile, see the Supporting Information Table S1; note that oral bioavailability in this structural class is strongly dependent on the actual formulation vehicle used).

Thus, single po administrations of **4a** in a range of 1 to 30 mg/kg suppressed tested plasma LH levels in OVX rats in a dose-dependent manner. At doses ≥10 mg/kg, a suppression of LH levels comparable to the peptidic GnRH antagonist cetrorelix (dosed

at 0.1 mg/kg, sc) was achieved for 6 hours at least (calculated ED_{50} ca. 5.5 mg/kg, see Figure 3).

Identification of the Clinical Candidate 5a. Based on the encouraging findings with compound **4a**, we started a final round of lead optimization efforts to achieve compound characteristics having the potential of becoming a clinical candidate. Once more, we primarily focused on further improvements in antagonistic potency and oral bioavailability, in addition to overcoming the CYP3A4 interactions observed for **4a** (for details regarding the CYP profile, see the Supporting Information Table S1). As most of the structural parts of **4a** had already been optimized, we returned to modifications of the pyridylmethyl amide by synthesizing and testing various substitution patterns (see Table 10). We found that double substitution at C-3 and C-5 of the pyridyl ring had a beneficial effect on potency (buserelin assay), while single C-3 or C-5 substitution alone was less effective (cf. **5** vs **4** and **41**). Whereas the unsubstituted pyridyl derivative **45** had a far lower potency (buserelin assay), introduction of both a chloro at C-3 and a trifluoromethyl moiety at C-5 of the pyridyl ring resulted in the most potent combination (cf. **5** vs **42**, **43**, and **44**). In summary, the additional substituents not only increased

antagonist potency, but also resulted in a further improvement in the compound's clearance and CYP interaction profile. Upon enantiomeric separation of **5** (in our view, with the combination of modifications best suited for thorough preclinical evaluation), we finally managed to obtain, extensively characterize, then prepare larger quantities of eutomer **5a** which was subsequently nominated as clinical candidate.

General Synthetic Access to Spiroindolines and Synthesis of Clinical Candidate 5a. The spiroindoline analogues **53** were generally prepared according to the procedures outlined in Scheme 2. Indolenines **48** were prepared from bromophenylhydrazine **46** and carbonyl compounds **47** under acidic conditions in a Fischer indole synthesis.[34] Indolenines **48** could either be reduced with sodium borohydride to give indolines **49** (R^2 = H) or reacted with Grignard reagents under Lewis acid catalysis to introduce different residues R^2 (≠ H). Functionalization at the indoline NH was accomplished under standard acylation or alkylation conditions to furnish aryl bromides **50**. The aryl bromides were either carbonylated in the presence of carbon monoxide, methanol, and a palladium catalyst to give esters **51**, which was followed by standard saponification to carboxylic acids **52** then amide coupling with amines (R^{1a})(R^{1b})NH to give spiroindoline

analogues **53**. Alternatively, spiroindolines **53** could be obtained directly upon palladium-catalyzed carbonylation of aryl bromides **50** with molybdenum hexacarbonyl in the presence of the respective amine.

Compound **5a** specifically was synthesized as outlined in Scheme 3. Starting from commercially available thiopyran **54**, a masked aldehyde moiety was introduced by Wittig reaction to give the stable and storable enol ether intermediate **55**. The indoline system was built up via a Fischer indole synthesis as described above to give indolenine **56**. Lewis acid catalyzed Grignard reaction of indolenine **56** employing cyclopropylmagnesium bromide furnished the spiroindoline core system **57** as a racemic mixture. Sulfonamide formation and subsequent oxidation gave bromo sulfone **59**. The amide side chain at C-5 was introduced by a three-step protocol starting with a palladium-catalyzed carbonylation to give ester **60** followed by saponification and amide formation. Separation of the amide enantiomers by HPLC on a chiral phase yielded **5a**.

Characterization of 5a: Absolute Configuration. The separated enantiomers **5a** and **5b** of racemate **5** were individually tested to clarify the role of the C-2 stereocenter. This revealed that **5a** is the (only) physiologically relevant enantiomer (**5a**: IC_{50} hGnRH-R =

21 nM, **5b**: IC_{50} hGnRH-R = 2.43 μM, buserelin assay) (see Table 10). We were able to obtain diffracting crystals of eutomer **5a** (Figure 4) possessing *S*-configuration, as determined by X-ray analysis [see the Supporting Information Table S6 for details].

Pharmacological, Physicochemical, Safety, and DMPK Properties of 5a. Figure 5 summarizes the major findings of our in-depth studies of **5a**. Compound **5a** exhibited potent, double-digit nanomolar antagonism at the human, rat, and cynomolgus monkey (h/r/c)GnRH-R while it showed no agonistic activity at the human GnRH-R up to 20 μM (data not shown). Nonetheless, the aqueous solubility of **5a** at pH 6.5 continued to be limited whereas its in vitro clearance proved to be moderate to low (in human, rat, dog, and cynomolgus monkey hepatocytes). In our view, a combination of limited solubility and low to moderate absorptive permeability can also account for the species- (rat, cynomolgus monkey) and formulation-dependent low to high oral bioavailabilities observed. Total blood clearance in vivo was low in rat and low to moderate in dog and monkey, and compound half-life was intermediate in monkey and long in rat and dog. Then again, overlaying effects of irreversible CYP3A4 inhibition in human liver microsomes as well as CYP3A4 induction in human hepatocytes were detected in vitro,

still. Of particular importance, **5a** was inactive in a cell-based panel of 25 GPCRs ('Bayer Panel', Millipore GPCRProfiler, now Eurofins; see the Supporting Information Table S2), none of which was activated or inhibited >70% at 10 μM compound concentration, indicative of an excellent selectivity within the target family. Additional off-target profiling of **5a** (Ricerca, now Eurofins) confirmed the absence of relevant activities in the respective assays [see the Supporting Information Table S5 for significant responses (i.e., ≥50%)].

Drug–Target Residence Time of 5a. In addition to the typical focus on ligand potency and efficacy, drug candidate optimization programs increasingly rely on data regarding the modulation of the actual duration of ligand–receptor interactions (i.e., drug–target residence time[35]) owing to the fact that compounds with differentiated pharmacological profiles often display unique binding properties[36,37] and very much become a focus of attention.[38-40] In GPCR research longer residence times have been demonstrated to result in a prolonged duration of drug actions[41,42] as a consequence of continued receptor modulation.[43] In other cases, transient binding behavior resulted in potent compounds with an improved side effect profile.[44-46]

Based on the established *in vivo* pharmacology of **5a**, we therefore asked ourselves how its drug–target residence time would compare to other known hGnRH-R antagonists. To address this question, we used an assay previously established in our group[47,48] to characterize the hGnRH-R binding kinetic parameters of **5a** and several reference compounds (see Table 11). In terms of target recognition, **5a** is, alongside elagolix, among the fastest associating ligands known. On the other hand, its target residence time of 7 minutes is significantly shorter than the other SMOL antagonists (relugolix and elagolix) or peptide antagonist (cetrorelix) tested, and within the range of the fastest dissociating peptide antagonists evaluated so far, but still superior to the residence time of GnRH itself.[49] The ability of **5a** to saturate the GnRH receptor nearly 20 times faster than its physiological ligand, while dissociating from it at only a slightly slower rate is a unique feature that might be linked to the compound's *in vivo* activity profile. This hypothesis deserves further investigation in follow-up studies: For instance, a systems pharmacology approach similar to the one reported in[50] could be envisioned, taking into account hGnRH-R's atypical desensitization properties[51-53] as well as the agonist pulse frequency and amplitude dependent nature of receptor signaling.[54,55]

Reduction of LH Levels in Rat and Monkey Animal Models *In Vivo*. The *in vivo* efficacy of **5a** upon po administration was determined in the well-established rat OVX and cynomolgus monkey orchiectomy (ORX) models reliably allowing for the study of compound effects on increased gonadotropin release and elevated plasma LH levels as a consequence of these surgical procedures. At doses (**5a**) of 10 and 30 mg/kg po (calculated ED_{50} ca. 4.5 mg/kg), a clear reduction of plasma LH levels was noticed, and comparable to that obtained upon treatment with cetrorelix (0.1 mg/kg, sc) used as control antagonist, in the rat OVX model (Figure 6A). These results were confirmed in a subsequent study in the monkey ORX model where a suppression of baseline LH levels by up to 60% was achieved with a single dose (**5a**) of 20 mg/kg po (Figure 6B). Taken together, these outcomes clearly demonstrate that treatment with **5a** results in effects in line with the expected profile of a potent, efficacious, and reversible GnRH-R antagonist.

Maximum Reduction of LH Levels Obtained in a First-in-Human Study with 5a in Postmenopausal Women. Compound **5a** was tested in a first-in-human study using a multicenter, randomized, double-blind, parallel-group, placebo-controlled design. Single

doses of 5 mg, 20 mg, 60 mg, 150 mg, 300 mg and 450 mg of **5a** in a self-microemulsifying drug delivery system (SMEDDS) formulation were administered to six postmenopausal women each.

Compound **5a** was well tolerated and safe at the doses tested in this study. Using the SMEDDS formulation, a low variability in pharmacokinetics in terms of AUC was observed (mean CV for AUC: about 29%). Based on a cross-study comparison, this is considerably better than the variability in AUC previously reported for elagolix (~40%; $p = 0.03$).[56] Suppression of plasma LH levels reached a maximum of about 49% reduction at the 300 mg dose of **5a**, with no further increase in effect observed with the higher dose of 450 mg (Figure 7). Further details of the clinical study will be reported elsewhere.

CONCLUSION

Extensive hit-to-lead and lead optimization activities led to the identification of spiroindoline derivative **5a** (BAY 1214784) and its characterization as a potent and selective antagonist of the human GnRH receptor, finally proving efficacious in a first-in-human study in postmenopausal women. Spiroindolines represent a new class of selective GnRH-R antagonists exhibiting multispecies activity and high potency in human, rat, and cynomolgous monkey models both in vitro and in vivo, a crucial factor for project success. By introducing a spiropiperidine moiety in the barely potent, yet multispecies active, HTS hit **15** and controlling the stereochemistry at C-2, we were able to achieve a major improvement in potency and LLE in lead compound **2b**. Still-existing DMPK liabilities (i.e., high clearance, inhibition of CYP isoforms, and low oral bioavailability) of the indoline hit cluster were tackled by careful optimization of the core towards a spirocyclic sulfone and the introduction of a chlorinated pyridyl moiety in the amide side chain. This resulted in advanced compound **4a** with a far more balanced DMPK profile, while simultaneously retaining sufficient potency for profiling in animal models in vivo. Single oral dosing of **4a** resulted in a dose-dependent lowering of

plasma LH levels in OVX rats (ED_{50} ca. 5.5 mg/kg). Fine-tuning of the pyridyl amide side chain finally led to the identification of potent, transiently binding and selective **5a** exhibiting a superior DMPK profile (i.e., improved oral bioavailability, potency, and CYP interaction), along with excellent safety properties. Thus, **5a** was advanced to clinical development and shown to suppress plasma LH levels by up to 45% in a first-in-human study in postmenopausal women. In addition, low pharmacokinetic variability and good tolerability was noted at single doses of up to 450 mg po once daily.

Finally, **5a** (probe code BAY-784) meets the criteria for chemical probes[57] established by the Structural Genomics Consortium (SGC)[58] and was thus handed over to the SGC as a 'donated chemical probe' to be freely available for future studies. We trust these studies will elucidate BAY-784's unique binding behavior, and its potential usefulness for the prevention of the development of a hypoestrogenic state in the long term – a prerequisite for a substantially improved treatment of uterine fibroids. All in all, we are confident that making BAY-784 available to the scientific community will open up a wide range of opportunities for *in vitro* and *in vivo* studies thereby contributing to the future progress in field of hGnRH-receptor research.

EXPERIMENTAL SECTION

Chemistry

General Methods and Materials. All solvents and chemicals were used as purchased without further purification. The progress of all reactions was monitored by TLC on Merck precoated silica gel plates (with fluorescence indicator UV254) using EtOAc/*n*-hexane or DCM/MeOH as the solvent system or by UPLC (see Methods 1 and 2). TLC spots were visualized by irradiation with UV light (254 nm). Column chromatography was performed on Biotage chromatography systems with the solvent mixtures specified in the corresponding experiment. Proton (^{1}H) NMR, ^{13}C NMR and ^{19}F NMR spectra were recorded on Bruker Avance 300, 400, or 500 MHz instruments using $CDCl_3$ or DMSO-d_6 as solvent. Chemical shifts are given in parts per million (δ relative to the residual solvent peak). In case of enantiomeric separations the given retention times for each enantiomer refer to the respective analytical method.

Analytical (UP)LC-MS was performed using Methods 1–3. The masses (*m*/*z*) are reported from electrospray ionization in the positive mode, unless the negative mode is indicated (ESI–).

Method 1. Instrument: Waters Acquity UPLC-MS SQD 3001; column: Acquity UPLC BEH C18 1.7 μm, 50 × 2.1 mm; eluent A: H_2O + 0.1 vol % formic acid, eluent B: MeCN; gradient: 0–1.6 min 1–99% B, 1.6–2.0 min 99% B; flow rate: 0.8 mL/min; temperature: 60 °C; injection: 2 μL; DAD scan: 210–400 nm; ELSD.

Method 2. Instrument: Waters Acquity UPLC-MS SQD 3001; column: Acquity UPLC BEH C18 1.7 μm, 50 × 2.1 mm; eluent A: H_2O + 0.2 vol % NH_3, eluent B: MeCN; gradient: 0–1.6 min 1–99% B, 1.6–2.0 min 99% B; flow rate: 0.8 mL/min; temperature: 60 °C; injection: 2 μL; DAD scan: 210–400 nm; ELSD.

Preparative HPLC was performed using Method 3.

Method 3. Instrument: Waters autopurification system with pump 2545, sample manager 2767, CFO, DAD 2996, ELSD 2424, SQD; column: XBridge C18 5 µm 100 × 30 mm; eluent A: H_2O + 0.1 vol % formic acid, eluent B: MeCN; gradient: 0–8 min 10-100% B, 8-10 min 100% B; flow rate: 50 mL/min; temperature: rt; loading: 250 mg / 2.5 mL DMSO or DMF; injection: 1 x 2.5 mL; detection: DAD scan range 210–400 nm; MS ESI+, ESI-, scan range: 160-1000 m/z.

The purity of all compounds tested in vitro and in vivo is ≥ 95% as determined by UPLC-MS (Method 1 or Method 2).

Relugolix[20] (CAS-RN: [737789-87-6]) and elagolix[22] (CAS-RN: [834153-87-6]) were synthesized according to the published procedures. Cetrorelix (CAS-RN: [120287-85-6]) was purchased from Bachem.

General Synthetic Procedures

General Procedure for Indolenine Formation (GP 1) (see Scheme 2, step a). *Method 1 (GP 1.1, using TFA).*[34] To a stirred solution of hydrazine (1 equiv) and carbonyl compound or enol ether (1 equiv) in $CHCl_3$ at 0 °C, TFA (3.3 equiv) was added dropwise. The reaction mixture was heated to 50 °C until TLC and/or LC-MS indicated complete consumption of the starting material (4–18 h), and then cooled to rt. A 25% aq NH_3 solution was carefully added to reach pH ~8. The mixture was poured into H_2O and extracted with DCM. The combined organic layers were washed with H_2O, dried with Na_2SO_4, and the solvents were removed in vacuo. The crude product was taken to the next step without further purification.

Method 2 (GP 1.2, using HOAc/aq HCl). To a stirred solution of hydrazine (1 equiv) in HOAc (2 mL/mmol), concd $HCl_{(aq)}$ (1 equiv) was added at rt. After 5 min of stirring, carbonyl compound or enol ether (1–4 equiv) was added at rt, and the reaction mixture was heated to 100 °C until TLC and/or LC-MS indicated (nearly) complete consumption of the starting material (1–24 h), and then cooled to rt. A 25% aq NH_3 solution was carefully added to reach pH ~8. The mixture was poured into H_2O and extracted with DCM. The combined organic layers were washed with H_2O, dried with Na_2SO_4, and the solvents were removed in vacuo. The crude product was taken to the next step without further purification.

General Procedure for Indolenine Reduction (GP 2) (see Scheme 2, step b). To a stirred solution of the indolenine in MeOH, $NaBH_4$ (4 equiv) was carefully added at 0 °C or rt. The reaction mixture was stirred at 0 °C or rt until TLC and/or LC-MS indicated complete consumption of the starting material (1 h), and then concentrated in vacuo. The residue was taken up with H_2O, acidified with 1 M aq HCl to pH ~5, and extracted with EtOAc. The combined organic layers were washed with brine, dried with Na_2SO_4,

and the solvents were removed in vacuo. The crude product was purified by flash chromatography or preparative HPLC.

General Procedure for the Grignard Reaction (GP 3) (see Scheme 2, step b). To a stirred solution of the indolenine in THF, $BF_3{\cdot}OEt_2$ (1 equiv) was added dropwise at 0 °C. After 5 min of stirring, the corresponding Grignard reagent (commercial solution in THF or prepared from the respective alkyl bromide according to standard procedures, 3 equiv) was added dropwise, keeping the temperature of the mixture at 5–10 °C. The mixture was allowed to warm to rt and stirred until TLC and/or LC-MS indicated complete consumption of the starting material (1–3 h). Then, sat. aq NH_4Cl solution was added and the mixture was partitioned between EtOAc and H_2O. The aqueous phase was extracted with EtOAc, and the combined organic phases were washed with brine, dried with Na_2SO_4, concentrated, and purified by flash chromatography (silica gel, hexane/EtOAc).

General Procedure for Sulfonamide Formation (GP 4) (see Scheme 2, step c). *Method 1 (GP 4.1, at elevated temperatures).* To a solution of the indoline in DCE or DCM or MeCN, sulfonyl chloride (1–2 equiv) and Et_3N or DIPEA (3–5 equiv) were added

at 0 °C or rt, and the mixture was stirred at rt or up to 80 °C for 18–24 h. If needed, further sulfonyl chloride (2 equiv), Et_3N (3 equiv), and a catalytic amount of DMAP may be added, and the mixture stirred for an additional 18 h. The reaction mixture was partitioned between H_2O or aq NH_4Cl solution and DCM, extracted with DCM, and the combined organic layers were washed with H_2O, dried with Na_2SO_4, concentrated, and purified by flash chromatography (silica gel, hexane/EtOAc).

Method 2 (GP 4.2, in pyridine). A mixture of the indoline, sulfonyl chloride (1–2 equiv), and pyridine (6–10 equiv) was stirred at rt for 18–24 h. The reaction mixture was partitioned between H_2O and DCM, extracted with DCM, and the combined organic layers were washed with H_2O, dried with Na_2SO_4, concentrated, and purified by flash chromatography (silica gel, hexane/EtOAc).

General Procedure for the Oxidation to Sulfone (GP 5). TFAA (6 equiv) was dissolved in MeCN (5–6 mL/mmol) at 0 °C and urea hydrogen peroxide (8 equiv) was slowly added. After 20 min of stirring at rt, a solution of the sulfide (1 equiv) in MeCN (3.5 mL/mmol) was added dropwise and the mixture was stirred for 30 min or up to 2 h at rt. In the case of incomplete conversion, further urea hydrogen peroxide (up to

8 equiv) and the according amount of TFAA may be added. After complete conversion, the mixture was partitioned between H_2O and DCM. The aqueous layer was extracted with DCM, and the combined organic layers were washed with H_2O, dried with Na_2SO_4, and the solvents were removed in vacuo. Alternatively, upon complete conversion, the reaction mixture was cooled, and the formed precipitate was collected by filtration, washed with H_2O, and taken up with DCM. The organic phase was washed with sat. aq $NaHCO_3$ and sat. aq $Na_2S_2O_3$ solution, dried with $MgSO_4$, and concentrated under reduced pressure. If appropriate, the sulfone product was purified by preparative HPLC or flash chromatography.

General Procedure for Carbonylation To Yield Methyl Ester (GP 6) (see Scheme 2, step d). The aryl bromide was placed into a steel autoclave under argon atmosphere and dissolved in a 10:1 mixture of MeOH and DMSO (ca. 30 mL/mmol). $PdCl_2(PPh_3)_2$ (0.2 equiv) and Et_3N (2–2.5 equiv) were added and the mixture was purged with CO (3 ×). The mixture was stirred at 20 °C for 30 min under a CO pressure of ca. 9–11 bar. The autoclave was evacuated, then a CO pressure of ca. 9–11 bar was applied and the mixture was heated to 100 °C until TLC and/or LC-MS indicated complete consumption

of the starting material (18–24 h), yielding a maximum pressure of ca. 10–13 bar. The autoclave was cooled to rt, the pressure was released, and the reaction mixture was concentrated in vacuo then dissolved in EtOAc/H_2O. The layers were separated, the aqueous phase was extracted with EtOAc, and the combined organic layers were washed with H_2O and brine, then dried with Na_2SO_4. The solvents were removed in vacuo and the crude product was purified by flash chromatography (silica gel, hexane/EtOAc).

General Procedure for Ester Saponification (GP 7) (see Scheme 2, step e). The methyl ester was dissolved in a 1:1 mixture of THF and 2 M aq LiOH or NaOH (ca. 30 mL/mmol) and the mixture was stirred at rt until TLC and/or LC-MS indicated complete consumption of the starting material (18 h). For some substrates, MeOH was used as a cosolvent. The mixture was acidified to pH ~2–4 by the addition of 2 M aq HCl and extracted with EtOAc. The combined organic layers were washed with brine, dried with Na_2SO_4, and concentrated in vacuo. Alternatively, the precipitate which formed upon acidification was collected by filtration and dried. The product was used without further purification.

General Procedure for Amide Formation (GP 8) (see Scheme 2, step f). *Method 1 (GP 8.1, formation in situ).* The carboxylic acid was dissolved in DMF and the corresponding amine component (1.5–3 equiv), HATU (1.5 equiv), and Et_3N (1.5–5 equiv) were added. The reaction mixture was stirred at rt until TLC and/or LC-MS indicated complete consumption of the starting material (2–24 h), then H_2O was added. The formed precipitate was collected by filtration, washed with H_2O, and taken up with DCM. The organic phase was washed with H_2O, dried with $MgSO_4$, and the solvent was removed in vacuo. Alternatively, upon reaction completion, the reaction mixture was diluted with H_2O and EtOAc. The layers were separated and the aqueous layer was extracted with EtOAc. The combined organic layers were washed with brine, dried with Na_2SO_4, and concentrated in vacuo. If appropriate, the crude product was purified by preparative HPLC or flash chromatography.

Method 2 (GP 8.2, formation after isolation of the active HOAt ester). The carboxylic acid was dissolved in DMF, and HATU (1.5 equiv) and Et_3N (1.5 equiv) were added. The reaction mixture was stirred at rt until TLC and/or LC-MS indicated complete consumption of the starting material (2–3 h), then H_2O was added. The formed

precipitate was collected by filtration, washed with H_2O, dissolved in DCM or EtOAc or a mixture thereof, dried with Na_2SO_4, and concentrated in vacuo to give the HOAt ester. The HOAt ester, the corresponding amine component (2 equiv), and (if a hydrochloride is used as the amine component) Et_3N (1.5 equiv) were stirred in MeCN or a mixture of MeCN and NMP at 55–80 °C until TLC and/or LC-MS indicated complete consumption of the HOAt ester (1–30 h). Then, the reaction mixture was partitioned between EtOAc and H_2O. The layers were separated, the aqueous phase was extracted with EtOAc, the combined organic layers were washed with H_2O and brine, then dried with Na_2SO_4, and the solvents were removed in vacuo. If appropriate, the product was purified by preparative HPLC or flash chromatography.

General Procedure for Carbonylation To Yield Amide Directly (GP 9) (see Scheme 2, step g). To a solution of aryl bromide in 1,4-dioxane (containing ca. 1% H_2O), the corresponding amine (3 equiv), molybdenum hexacarbonyl (1 equiv), Na_2CO_3 (3 equiv), tri-*tert*-butylphosphonium tetrafluoroborate (0.1 equiv), and $Pd(OAc)_2$ (0.1 equiv) were added. The reaction mixture was vigorously stirred at 120–140 °C until TLC and/or LC-MS indicated complete consumption of the starting material (2–36 h). Alternatively,

microwave irradiation (200 W, 20 min, 140 °C, 1.2 bar) can be applied. The mixture was cooled to rt, and the solids were filtered off and rinsed with EtOAc. The filtrate was washed with H_2O and brine, dried with Na_2SO_4, and concentrated in vacuo. The crude product was purified by flash chromatography (silica gel, hexane/EtOAc) and, if appropriate, additionally by preparative HPLC.

General Procedure for the Oxidation of Sulfide to Sulfoxide (GP 10). To a solution of the sulfide in MeCN, $FeCl_3$ (0.13 equiv) was added at rt. After 15 min of stirring, periodic acid (1.1 equiv) was added and the mixture was stirred for a further 45 min. The mixture was partitioned between H_2O and EtOAc. The pH was adjusted to pH ~10 by the addition of sat. aq $NaHCO_3$ solution. The layers were separated, the aqueous phase was extracted with EtOAc, the combined organic layers were washed with brine and dried with Na_2SO_4, and the solvents were evaporated. The crude product was purified by flash chromatography or preparative HPLC.

General Procedure for the Deprotection of Benzyloxycarbamate (GP 11). The Cbz-protected amine was treated with HBr (33% in HOAc, 25–100 equiv) at 0 °C until TLC and/or LC-MS indicated complete consumption of the starting material (0.5–2 h). The

reaction mixture was poured into Et_2O and the formed precipitate was collected by filtration. The filter cake was dissolved in a mixture of DCM and Et_3N, and the solvent was removed in vacuo. The residue was taken up with DCM and washed with H_2O, the organic layer was dried with Na_2SO_4, and the solvent was removed in vacuo to give the unprotected amine which was used without further purification.

General Procedure for the Acetylation of Spiropiperidine (GP 12). A solution of the corresponding amine in THF was cooled to 0 °C, treated with Et_3N (1.5–6 equiv) and AcCl (1–5 equiv), and stirring at 0 °C was continued until TLC and/or LC-MS indicated complete consumption of the starting material (0.5–2 h). The mixture was concentrated in vacuo and the residue was taken up with DCM and H_2O. The layers were separated and the aqueous layer was extracted with DCM. The combined organic layers were washed with brine, dried with Na_2SO_4, and concentrated under reduced pressure. If appropriate, the product was purified by preparative HPLC or flash chromatography.

***rac*-*N*-(2-Chlorobenzyl)-2,3,3-trimethyl-1-(phenylsulfonyl)-2,3-dihydro-1*H*-indole-5-carboxamide (15)**

Step 15.1. 2,3,3-Trimethyl-2,3-dihydro-1*H*-indole-5-carboxylic Acid (9). Prepared according to GP 1.2 and GP 2: A mixture of 4-hydrazinobenzoic acid (**6**; 25.0 g, 164 mmol, 1.0 equiv) in HOAc (250 mL) was treated with concd $HCl_{(aq)}$ (37 wt %, 14 mL, 160 mmol, 1.0 equiv) and stirred for 5 min at rt. 3-Methylbutan-2-one (**7**; 72 mL, 670 mmol, 4.1 equiv) was added, and the resulting mixture was stirred at reflux for 1 h, cooled to rt, and concentrated under reduced pressure to give crude indolenine **8**. The residue was taken up with MeOH (200 mL), cooled to 0 °C, and treated portionwise with $NaBH_4$ (24.9 g, 657 mmol, 4.0 equiv). The reaction mixture was stirred at 0 °C for 1 h, carefully quenched with H_2O, and concentrated under reduced pressure. The obtained material was acidified with 1 M aq HCl to pH 4 and extracted with EtOAc (4 ×). The combined organic phases were washed with brine, dried with Na_2SO_4, filtered, and concentrated under reduced pressure to give crude **9** (31.4 g) which was taken to the next step without further purification. UPLC-MS (Method 1): t_R = 0.96 min. MS (ESI+): m/z = 206 $[M+H]^+$. ^{1}H NMR (300 MHz, $CDCl_3$): δ = 1.10 (s, 3H), 1.20 (d, J = 6.59 Hz, 3H), 1.32 (s, 3H), 3.64 (q, J = 6.59 Hz, 1H), 6.57 (d, J = 8.10 Hz, 1H), 7.75 (d, J = 1.51 Hz, 1H), 7.85 (dd, J = 1.79, 8.20 Hz, 1H).

Step 15.2. Methyl 2,3,3-Trimethyl-2,3-dihydro-1*H*-indole-5-carboxylate (10). A mixture of acid **9** (12.7 g, 61.8 mmol, 1.0 equiv) from step 15.1 in MeOH (130 mL) at 0 °C was treated with thionyl chloride (5.0 mL, 68 mmol, 1.1 equiv) and stirred at rt for 1 h and subsequently stirred at reflux for 4 h. The reaction mixture was concentrated under reduced pressure and the obtained material subjected to flash chromatography (silica gel, hexane/EtOAc/MeOH = 1:0:0 to 70:30:0 to 0:0:1) to give **10** (1.51 g, 11% over 3 steps). UPLC-MS (Method 1): t_R = 1.21 min. MS (ESI+): *m/z* = 220 $[M+H]^+$. ^{1}H NMR (400 MHz, $CDCl_3$): δ = 1.30 (s, 3H), 1.45 (s, 3H), 1.69 (d, *J* = 6.06 Hz, 3H), 3.93–3.96 (m, 4H), 7.71 (br d, *J* = 7.58 Hz, 1H), 7.98 (d, *J* = 1.01 Hz, 1H), 8.05 (br d, *J* = 7.07 Hz, 1H), 12.00 (br s, 1H).

Step 15.3. Methyl 2,3,3-Trimethyl-1-(phenylsulfonyl)-2,3-dihydro-1*H*-indole-5-carboxylate (11). Prepared according to GP 4.1: Indoline **10** (1.00 g, 4.56 mmol, 1.0 equiv) from step 15.2 was reacted with DIPEA (2.4 mL, 14 mmol, 3.0 equiv) and benzenesulfonyl chloride (610 μL, 4.8 mmol, 1.1 equiv) in DCM (40 mL) at rt overnight. Further benzenesulfonyl chloride (610 μL, 4.8 mmol, 1.1 equiv) and DMAP (28 mg, 0.23 mmol, 5.0 mol%) were added and the reaction was continued for 5 d. Workup and

flash chromatography (silica gel, hexane/EtOAc = 1:0 to 1:1) gave **11** (920 mg, 56%). UPLC-MS (Method 1): ^{t}R = 1.41 min. MS (ESI+): *m/z* = 360 $[M+H]^+$.

Step 15.4. 2,3,3-Trimethyl-1-(phenylsulfonyl)-2,3-dihydro-1*H*-indole-5-carboxylic Acid (13). Prepared according to GP 7: Methyl ester **11** (300 mg, 835 μmol, 1.0 equiv) from step 15.3 was reacted with 2 M aq LiOH (20 mL, 40 mmol, 48 equiv) in a 3:2 mixture of MeOH and THF (50 mL) at rt overnight. Upon acidification with 2 M aq HCl a precipitate formed and was collected by filtration and dried to give **13** (60 mg, 21%) which was taken to the next step without further purification. UPLC-MS (Method 1): ^{t}R = 1.20 min. MS (ESI+): *m/z* = 346 $[M+H]^+$.

Step 15.5. *N*-(2-Chlorobenzyl)-2,3,3-trimethyl-1-(phenylsulfonyl)-2,3-dihydro-1*H*-indole-5-carboxamide (15). Prepared according to GP 8.1: Acid **13** (20 mg, 58 μmol, 1.0 equiv) from step 15.4 was treated with HATU (33 mg, 87 μmol, 1.5 equiv), Et_3N (40 μL, 290 μmol, 5.0 equiv), and 1-(2-chlorophenyl)methanamine (CAS-RN: [89-97-7]; 21 μL, 170 μmol, 3.0 equiv) in DMF (1.5 mL) at rt overnight. Aqueous workup with EtOAc and purification of the crude product by preparative HPLC (Method 3) gave **15** (5 mg, yield: 18%, purity > 98%). UPLC-MS (Method 1): ^{t}R = 1.40 min. MS (ESI+): *m/z*

= 469/471 $[M+H]^+$ (CI isotope pattern). ^{1}H NMR (400 MHz, $CDCl_3$): δ = 0.57–0.60 (m, 3H), 1.23–1.24 (m, 3H), 1.36–1.39 (m, 3H), 3.89 (s, 1H), 3.92–3.98 (m, 1H), 4.72–4.74 (m, 1H), 6.50–6.53 (m, 0.5H), 7.25–7.27 (m, 2.5H)*, 7.39–7.50 (m, 3H), 7.51–7.59 (m, 2H), 7.67–7.74 (m, 1.5H), 7.78–7.83 (m, 2H), 7.93–7.96 (m, 0.5H); * (partially) hidden by the residual $CDCl_3$ peak. ^{13}C NMR (100 MHz, $CDCl_3$): δ = 18.3, 21.2, 31.1, 42.1, 43.5, 69.9, 114.9, 122.6, 126.7, 126.8, 127.2, 129.07, 129.09, 129.6, 130.1, 130.6, 133.3, 133.7, 135.6, 138.1, 141.1, 142.4, 166.9. HRMS (ESI+, $[M+H]^+$): calc.: 469.1353, found: 469.1363.

rac-N-(2-Chlorobenzyl)-1-[(4-methoxyphenyl)sulfonyl]-2,3,3-trimethyl-2,3-dihydro-1_H_-indole-5-carboxamide (1) and Its Enantiomers 1a and 1b

Step 1.1. Methyl 1-[(4-Methoxyphenyl)sulfonyl]-2,3,3-trimethyl-2,3-dihydro-1_H_-indole-5-carboxylate (12). Prepared according to GP 4.1: Indoline **10** (12.3 g, 56.1 mmol, 1.0 equiv) from step 15.2 was reacted with DIPEA (29 mL, 170 mmol, 3.0 equiv), 4-methoxybenzenesulfonyl chloride (17.4 g, 84.1 mmol, 1.5 equiv), and DMAP (340 mg, 2.8 mmol, 5.0 mol%) in DCE (570 mL) at rt overnight. Further DIPEA (10 mL, 58 mmol, 1.0 equiv), 4-methoxybenzenesulfonyl chloride (17.4 g, 84.1 mmol, 1.5 equiv), and

DMAP (340 mg, 2.8 mmol, 5.0 mol%) were added, and stirring was continued at reflux for 4 h and subsequently at rt for 2 d. Aqueous workup and purification of the obtained material by flash chromatography (silica gel, hexane/EtOAc = 1:0 to 7:3 to 6:4) then recrystallization from hexane/EtOAc gave **12** (6.1 g, 28%). UPLC-MS (Method 1): ^{t}R = 1.40 min. MS (ESI+): *m/z* = 390 $[M+H]^+$. ^{1}H NMR (300 MHz, $CDCl_3$): δ = 0.68 (s, 3H), 1.24 (s, 3H), 1.38 (d, *J* = 6.59 Hz, 3H), 3.82 (s, 3H), 3.89 (s, 3H), 3.91–3.97 (m, 1H), 6.87–6.92 (m, 2H), 7.67–7.71 (m, 2H), 7.72–7.77 (m, 2H), 7.93 (dd, *J* = 1.70, 8.48 Hz, 1H).

Step 1.2. 1-[(4-Methoxyphenyl)sulfonyl]-2,3,3-trimethyl-2,3-dihydro-1*H*-indole-5-carboxylic Acid (14). Prepared according to GP 7: Methyl ester **12** (4.50 g, 11.6 mmol, 1.0 equiv) from step 1.1 was reacted with 2 M aq LiOH (100 mL, 200 mmol, 17 equiv) in a 3:2 mixture of MeOH and THF (250 ml) at rt overnight to give, after workup, **14** (4.2 g, 91% purity, 88%) which was taken to the next step without further purification. UPLC-MS (Method 1): ^{t}R = 1.20 min. MS (ESI+): *m/z* = 376 $[M+H]^+$. ^{1}H NMR (300 MHz, $CDCl_3$): δ = 0.70 (s, 3H), 1.26 (s, 3H), 1.39 (d, *J* = 6.82 Hz, 3H), 3.82 (s, 3H), 3.96 (q,

J = 6.82 Hz, 1H), 6.90–6.92 (m, 2H), 7.71–7.77 (m, 4H), 8.01 (dd, *J* = 1.52, 8.59 Hz, 1H).

Step 1.3. *N*-(2-Chlorobenzyl)-1-[(4-methoxyphenyl)sulfonyl]-2,3,3-trimethyl-2,3-dihydro-1*H*-indole-5-carboxamide (1). Prepared according to GP 8.1: Acid **14** (600 mg, 1.60 mmol, 1.0 equiv) from step 1.2 was reacted with HATU (911 mg, 2.40 mmol, 1.5 equiv), Et_3N (1.1 mL, 8.0 mmol, 5.0 equiv), and 1-(2-chlorophenyl)methanamine (580 μL, 4.8 mmol, 3.0 equiv) in DMF (35 mL) at rt overnight. Aqueous workup and purification of the obtained material by flash chromatography (silica gel, hexane/EtOAc = 1:0 to to 4:6) gave **1** (750 mg, purity: > 98%). UPLC-MS (Method 1): t_R = 1.42 min. MS (ESI+): *m/z* = 499/501 $[M+H]^+$ (Cl isotope pattern). ^{1}H NMR (400 MHz, $CDCl_3$): δ = 0.65 (s, 3H), 1.23 (s, 3H), 1.36 (d, *J* = 6.57 Hz, 3H), 3.82 (s, 3H), 3.91 (q, *J* = 6.57 Hz, 1H), 4.68–4.77 (m, 2H), 6.53 (t, *J* = 5.81 Hz, 1H), 6.86–6.90 (m, 2H), 7.23–7.28 (m, 2H), 7.38–7.42 (m, 1H), 7.46–7.49 (m, 1H), 7.52 (d, *J* = 1.77 Hz, 1H), 7.57 (dd, *J* = 1.90, 8.47 Hz, 1H), 7.68 (d, *J* = 8.34 Hz, 1H), 7.71–7.74 (m, 2H). ^{13}C NMR (100 MHz, $CDCl_3$): δ = 18.2, 21.3, 31.2, 42.1, 43.5, 55. 6, 69.8, 114.2, 114.8, 122.5,

126.7, 127.2, 128.9, 129.1, 129.2, 129.6, 129.93, 129.96, 130.4, 130.6, 133.7, 135.6, 141.1, 142.7, 163.3, 166.9. HRMS (ESI+, $[M+H]^+$): calc.: 499.1380, found: 499.1458.

The enantiomers of racemic **1** were separated by chiral preparative HPLC [system: Dionex P580 pump, Gilson 215 liquid handler, Knauer K-2501 UV detector; column: Chiralpak AS-H 5 μm, 250 × 20 mm; eluent: hexane/EtOH (60:40) + 0.1% Et_2NH; flow rate: 17 mL/min; temperature: 25 °C; detection: UV 254 nm] and analytically characterized by chiral HPLC [system: Dionex 680 pump, Dionex ASI 100, Waters 2487 UV detector; column: Chiralpak AS-H 5 μm, 150 × 4.6 mm; eluent: hexane/EtOH (60:40) + 0.1% Et_2NH; flow rate: 1.0 mL/min; temperature: 25 °C; detection: UV 254 nm] and specific rotation. **1a** (eutomer): ^{t}R = 4.01 min. $[\alpha]_D^{20}$ –199.1 ± 0.40 (*c* 1.0, $CHCl_3$). Yield: 282 mg (42% from **14**). Enantiomeric Purity: 99%. **1b** (distomer): ^{t}R = 6.07 min. Yield: 261 mg (39% from **14**). Enantiomeric Purity: 99%.

***rac*-1'-Acetyl-*N*-(2-chlorobenzyl)-1-[(4-methoxyphenyl)sulfonyl]-2-methyl-1,2-dihydrospiro[indole-3,4'-piperidine]-5-carboxamide (2) and Its Enantiomers 2a and 2b**

Step 2.1. 1'-Acetyl-2-methyl-1,2-dihydrospiro[indole-3,4'-piperidine]-5-carboxylic Acid. Prepared according to GP 1.2 and GP 2: 4-Hydrazinobenzoic acid (**6**; 450 mg, 97%

purity, 2.87 mmol, 1.0 equiv) was reacted with 1,1'-piperidine-1,4-diyldiethanone (CAS-RN: [162368-01-6]; 500 mg, 97% purity, 2.87 mmol, 1.0 equiv) and concd $HCl_{(aq)}$ (37 wt %, 240 μL, 2.9 mmol, 1.0 equiv) in HOAc (6 mL) and the obtained indolenine intermediate subsequently reduced with $NaBH_4$ (434 mg, 11.5 mmol, 4.0 equiv) in MeOH (6 mL) to give the crude title compound (733 mg) which was taken to the next step without further purification. UPLC-MS (Method 1): ^{t}R = 0.75 min. MS (ESI+): *m/z* = 289 $[M+H]^+$.

Step 2.2. Methyl 1'-Acetyl-2-methyl-1,2-dihydrospiro[indole-3,4'-piperidine]-5-carboxylate. According to the preparation in step 15.2, crude 1'-acetyl-2-methyl-1,2-dihydrospiro[indole-3,4'-piperidine]-5-carboxylic acid (733 mg, 2.54 mmol) from step 2.1 was reacted with thionyl chloride (200 μL, 2.8 mmol, 1.1 equiv) in MeOH (14 mL) to give, upon flash chromatography (silica gel, EtOAc), the title compound (445 mg, 90% purity, 51% over 2 steps). UPLC-MS (Method 1): ^{t}R = 0.92 min. MS (ESI+): *m/z* = 303 $[M+H]^+$. ^{1}H NMR (300 MHz, DMSO-d_6): δ = 1.03 (d, *J* = 6.40 Hz, 3H), 1.23–1.34 (m, 0.5H), 1.40–1.49 (m, 0.5H), 1.59–1.77 (m, 2.5H), 1.86–1.92 (m, 0.5H), 2.02–2.05 (m, 3H), 2.89–2.98 (m, 0.5H), 3.10–3.26 (m, 1H), 3.39–3.48 (m, 0.5H), 3.60–3.73 (m, 4H),

3.80–3.86 (m, 1H), 3.97–4.11 (m, 1H), 6.47–6.50 (m, 1H), 7.58 (br d, *J* = 7.72 Hz, 1H), 7.62 (dd, *J* = 1.70, 8.10 Hz, 1H).

Step 2.3. Methyl 1'-Acetyl-1-[(4-methoxyphenyl)sulfonyl]-2-methyl-1,2-dihydro-spiro[indole-3,4'-piperidine]-5-carboxylate. Prepared according to GP 4.1: Methyl 1'-acetyl-2-methyl-1,2-dihydrospiro[indole-3,4'-piperidine]-5-carboxylate (445 mg, 90% purity, 1.32 mmol, 1.0 equiv) from step 2.2 was reacted with DIPEA (690 μL, 4.0 mmol, 3.0 equiv) and 4-methoxybenzenesulfonyl chloride (861 mg, 4.17 mmol, 3.15 equiv) in MeCN (35 mL) at 60 °C to give, upon flash chromatography (silica gel, DCM/MeOH = 100:0 to 95:5), the title compound (294 mg, 42%). UPLC-MS (Method 1): t_R = 1.15 min. MS (ESI+): *m/z* = 473 $[M+H]^+$. ^{1}H NMR (400 MHz, DMSO-d_6): δ = 0.00–0.16 (m, 1H), 0.77–0.85 (m, 0.5H), 1.01–1.12 (m, 1H), 1.27–1.29 (m, 3H), 1.73–1.77 (m, 1H), 1.78–1.86 (m, 0.5H), 1.93–2.01 (m, 3H), 2.04–2.12 (m, 0.5H), 2.55–2.62 (m, 0.5H), 2.67–2.74 (m, 0.5H), 3.05–3.12 (m, 0.5H), 3.22–3.29 (m, 0.5H), 3.80–3.81 (m, 6.5H), 3.86–3.89 (m, 0.5H), 4.36–4.40 (m, 0.5H), 4.51–4.59 (m, 1H), 7.08–7.10 (m, 2H), 7.60 (d, *J* = 8.59 Hz, 1H), 7.66–7.71 (m, 1H), 7.77–7.81 (m, 2H), 7.89 (dd, *J* = 1.52, 8.59 Hz, 1H).

Step 2.4. 1'-Acetyl-1-[(4-methoxyphenyl)sulfonyl]-2-methyl-1,2-dihydrospiro[indole-3,4'-piperidine]-5-carboxylic Acid. Prepared according to GP 7: According to the preparation of **13**, methyl 1'-acetyl-1-[(4-methoxyphenyl)sulfonyl]-2-methyl-1,2-dihydrospiro[indole-3,4'-piperidine]-5-carboxylate (100 mg, 212 μmol, 1.0 equiv) from step 2.3 was reacted with 2 M aq NaOH (160 μL, 320 μmol, 1.5 equiv) in a 2:1 mixture of THF and MeOH (1.5 mL) at rt overnight to give the title compound (84 mg, 80% purity, 70%) which was taken to the next step without further purification. UPLC-MS (Method 1): ^{t}R = 1.00 min. MS (ESI+): *m/z* = 459 $[M+H]^+$.

Step 2.5. 1'-Acetyl-*N*-(2-chlorobenzyl)-1-[(4-methoxyphenyl)sulfonyl]-2-methyl-1,2-dihydrospiro[indole-3,4'-piperidine]-5-carboxamide (2). Prepared according to GP 8.1: 1'-Acetyl-1-[(4-methoxyphenyl)sulfonyl]-2-methyl-1,2-dihydrospiro[indole-3,4'-piperidine]-5-carboxylic acid (59 mg, 130 μmol, 1.0 equiv) from step 2.4 was reacted with HATU (74 mg, 190 μmol, 1.5 equiv), Et_3N (27 μL, 190 μmol, 1.5 equiv), and 1-(2-chlorophenyl)methanamine (23 μL, 190 μmol, 1.5 equiv) in DMF (1 mL) at rt overnight. Flash chromatography (silica gel, hexane/EtOAc = 3:1 to 0:1) gave **2** (59 mg, yield: 77%, purity: > 98%). UPLC-MS (Method 1): ^{t}R = 1.23 min. MS (ESI+): *m/z* = 582/584

[M+H]$^+$ (CI isotope pattern). ^{1}H NMR (400 MHz, DMSO-d_6): δ = 0.03–0.20 (m, 1H), 0.77–0.85 (m, 0.5H), 0.99–1.06 (m, 0.5H), 1.28–1.30 (m, 3H), 1.75–1.84 (m, 1.5H), 1.93–2.02 (m, 3.5H), 2.58–2.64 (m, 0.5H), 2.71–2.77 (m, 0.5H), 3.08–3.14 (m, 0.5H), 3.22–3.29 (m, 0.5H), 3.81–3.88 (m, 4H), 4.38–4.41 (m, 0.5H), 4.50–4.57 (m, 3.5H), 7.08–7.11 (m, 2H), 7.26–7.35 (m, 3H), 7.43–7.46 (m, 1H), 7.56 (d, *J* = 8.59 Hz, 1H), 7.73 (dd, *J* = 1.26, 10.11 Hz, 1H), 7.77–7.81 (m, 2H), 7.89 (ddd, *J* = 1.77, 3.28, 8.34 Hz, 1H), 8.90 (t, *J* = 5.69 Hz, 1H). ^{13}C NMR (100 MHz, $CDCl_3$): δ = 18.0, 21.4, 28.2, 29.1, 37.7, 42.1, 44.2, 46.0, 55.6, 64.3, 114.4, 115.4, 122.8, 127.2, 127.4, 127.8, 128.5, 128.7, 129.2, 129.6, 130.1, 130.2, 130.7, 133.7, 135.5, 138.8, 142.4, 163.6, 166.6, 168.9. HRMS (ESI+, [M+H]$^+$): calc.: 582.1751, found: 582.1832.

The enantiomers of racemic **2** were separated by chiral preparative HPLC [system: Dionex P580 pump, Gilson 215 liquid handler, Knauer K-2501 UV detector; column: Chiralpak IA 5 μm, 250 × 30 mm; eluent: hexane/EtOH (50:50); flow rate: 20 mL/min; temperature: 25 °C; detection: UV 210 nm] and analytically characterized by chiral HPLC [system: Waters Alliance 2695, DAD 996, ESA Corona; column: Chiralpak IA 5 μm, 150 × 4.6 mm; eluent: hexane/EtOH (50:50); flow rate: 1.0 mL/min; temperature:

25 °C; detection: DAD scan at 210 nm] and specific rotation. **2a** (distomer): ^{t}R = 4.78 min. Yield: 15 mg (20%). Enantiomeric Purity: > 99%. **2b** (eutomer): ^{t}R = 5.68 min. $[\alpha]_D^{20}$ –165.45 ± 0.29 (*c* 1.0, $CHCl_3$). Yield: 17 mg (22%). Enantiomeric Purity: 97%.

***rac*-*N*-(2-Chlorobenzyl)-1-[(4-fluorophenyl)sulfonyl]-2-methyl-1,2-dihydrospiro[indole-3,4'-piperidine]-5-carboxamide (3) and Its Enantiomers 3a and 3b**

Step 3.1. Benzyl 5-Bromo-1'*H*-spiro[indole-3,4'-piperidine]-1'-carboxylate. Prepared according to GP 1.1: A mixture of 4-bromophenylhydrazine hydrochloride (1:1) (**46**, CAS-RN: [622-88-8]; 23.4 g, 105 mmol, 1.0 equiv) and benzyl 4-formylpiperidine-1-carboxylate (25.9 g, 105 mmol, 1.0 equiv) in $CHCl_3$ (755 mL) was treated with TFA (27 mL, 350 mmol, 3.3 equiv) at 0 °C and subsequently at 50 °C for 4 h to give, upon workup, the crude title compound (40 g) which was taken to the next step without further purification. UPLC-MS (Method 1): ^{t}R = 1.38 min. MS (ESI+): *m*/*z* = 399/401 $[M+H]^+$ (Br isotope pattern).

Step 3.2. Benzyl 5-Bromo-2-methyl-1,2-dihydro-1'*H*-spiro[indole-3,4'-piperidine]-1'-carboxylate. Prepared according to GP 3: Benzyl 5-bromo-1'*H*-spiro[indole-3,4'-piperidine]-1'-carboxylate (12.5 g, 82% purity, 25.6 mmol) from step 3.1 was reacted

with $BF_3 \cdot OEt_2$ (6.2 mL, 49 mmol, 1.9 equiv) and 1.4 M MeMgBr in a 1:3 mixture of THF/toluene (55 mL, 77 mmol, 3.0 equiv) in THF (292 mL) for 1 h 45 min to give, upon workup and flash chromatography (silica gel, hexane/EtOAc = 8:2 to 7:3), the title compound (7.4 g, 92% purity, 63%). UPLC-MS (Method 1): t_R = 1.41 min. MS (ESI+): *m/z* = 415/417 $[M+H]^+$ (Br isotope pattern). ^{1}H NMR (300 MHz, DMSO-d_6): δ = 0.99 (d, *J* = 6.22 Hz, 3H), 1.32–1.42 (m, 1H), 1.62–1.82 (m, 3H), 3.01–3.20 (m, 1H), 3.30–3.37 (m, 1H*), 3.67–3.84 (m, 3H), 5.09 (s, 2H), 5.69 (s, 1H), 6.43 (d, *J* = 8.29 Hz, 1H), 7.04 (dd, *J* = 1.98, 8.20 Hz, 1H), 7.18 (d, *J* = 1.88 Hz, 1H), 7.29–7.41 (m, 5H); * (partially) hidden by H_2O peak.

Step 3.3. Benzyl 5-Bromo-1-[(4-fluorophenyl)sulfonyl]-2-methyl-1,2-dihydro-1'*H*-spiro[indole-3,4'-piperidine]-1'-carboxylate. Prepared according to GP 4.1: Benzyl 5-bromo-2-methyl-1,2-dihydro-1'*H*-spiro[indole-3,4'-piperidine]-1'-carboxylate (6.5 g, 16 mmol, 1.0 equiv) from step 3.2 was reacted with Et_3N (13 mL, 94 mmol, 6.0 equiv), 4-fluorobenzenesulfonyl chloride (CAS-RN: [349-88-2]; 9.1 g, 47 mmol, 3.0 equiv), and DMAP (96 mg, 0.78 mmol, 5.0 mol%) in DCE (60 mL) at 80 °C for 5 h and subsequently at rt for 3 d to give, upon workup and flash chromatography (silica gel, hexane/EtOAc =

1:0 to 55:45), the title compound (9.6 g, quant.). UPLC-MS (Method 1): t_R = 1.60 min. MS (ESI+): *m/z* = 573/575 $[M+H]^+$ (Br isotope pattern). ^{1}H NMR (400 MHz, DMSO-d_6): δ = –0.06 (br s, 1H), 0.95 (br s, 1H), 1.26 (d, *J* = 5.81 Hz, 3H), 1.69–1.72 (m, 1H), 1.94 (dt, *J* = 4.38, 13.39 Hz, 1H), 2.77–3.11 (m, 2H), 3.48–3.52 (m, 1H), 3.97–4.00 (m, 1H), 4.49 (q, *J* = 6.32 Hz, 1H), 5.05–5.07 (m, 2H), 7.32–7.47 (m, 10H), 7.88–7.91 (m, 2H).

Step 3.4. 1'-Benzyl 5-Methyl 1-[(4-Fluorophenyl)sulfonyl]-2-methyl-1,2-dihydro-1'*H*-spiro[indole-3,4'-piperidine]-1',5-dicarboxylate. Prepared according to GP 6: Benzyl 5-bromo-1-[(4-fluorophenyl)sulfonyl]-2-methyl-1,2-dihydro-1'*H*-spiro[indole-3,4'-piperidine]-1'-carboxylate (13.6 g, 23.6 mmol) from step 3.3 was reacted with $PdCl_2(PPh_3)_2$ (2.5 g, 3.5 mmol, 15 mol%) and Et_3N (7.2 mL, 52 mmol, 2.2 equiv) under a CO pressure of 13 bar in a mixture of MeOH (500 mL) and DMSO (50 mL) at 100 °C for ~23 h. Deviating from GP 6, the concentrated crude reaction mixture was taken up with DCM, filtered, and washed with 1 M aq HCl. The layers were separated and the aqueous layer was extracted with DCM (3 ×). The combined organic layers were washed with brine, dried with Na_2SO_4, and concentrated under reduced pressure. The crude product was purified by flash chromatography (silica gel, hexane/EtOAc = 1:0 to 1:1) to give the title

compound (12.5 g, 95%). UPLC-MS (Method 1): t_R = 1.48 min. MS (ESI+): *m/z* = 553 $[M+H]^+$. ^{1}H NMR (400 MHz, DMSO-d_6): δ = 0.03 (br s, 1H), 0.97 (br s, 1H), 1.27 (d, *J* = 6.06 Hz, 3H), 1.74–1.78 (m, 1H), 1.97 (dt, *J* = 4.04, 13.14 Hz, 1H), 2.80–3.18 (m, 2H), 3.51–3.54 (m, 1H), 3.80 (s, 3H), 4.00–4.05 (m, 1H), 4.58 (q, *J* = 6.32 Hz, 1H), 5.07 (br s, 2H), 7.32–7.36 (m, 5H), 7.42–7.47 (m, 2H), 7.62 (d, *J* = 8.59 Hz, 1H), 7.70 (d, *J* = 1.52 Hz, 1H), 7.90 (dd, *J* = 1.77, 8.34 Hz, 1H), 7.92–7.96 (m, 2H).

Step 3.5. 1'-[(Benzyloxy)carbonyl]-1-[(4-fluorophenyl)sulfonyl]-2-methyl-1,2-dihydro-spiro[indole-3,4'-piperidine]-5-carboxylic Acid. Prepared in a variation to GP 7: 1'-Benzyl 5-methyl 1-[(4-fluorophenyl)sulfonyl]-2-methyl-1,2-dihydro-1'*H*-spiro[indole-3,4'-piperidine]-1',5-dicarboxylate (12.5 g, 22.7 mmol) from step 3.4 was reacted with LiOH (2.70 g, 114 mmol, 5.0 equiv) in a mixture of THF (120 mL) and H_2O (40 mL) at rt overnight. Due to incomplete conversion, further LiOH (2.70 g, 114 mmol, 5.0 equiv) was added, and stirring was continued for 7 h at 50 °C and subsequently at rt overnight to give, upon workup, the title compound (12.9 g, quant.) which was taken to the next step without further purification. UPLC-MS (Method 1): t_R = 1.31 min. MS (ESI+): *m/z* = 539 $[M+H]^+$. ^{1}H NMR (400 MHz, DMSO-d_6): δ = 0.04 (br s, 1H), 0.96 (br s, 1H), 1.27 (d,

J = 6.06 Hz, 3H), 1.74–1.78 (m, 1H), 1.91–1.98 (m, 1H), 2.82–3.16 (m, 2H), 3.50–3.54 (m, 1H), 4.00–4.05 (m, 1H), 4.57 (q, *J* = 6.32 Hz, 1H), 5.06–5.07 (m, 2H), 7.31–7.36 (m, 5H), 7.42–7.47 (m, 2H), 7.59 (d, *J* = 8.34 Hz, 1H), 7.68 (d, *J* = 1.52 Hz, 1H), 7.88 (dd, *J* = 1.77, 8.34 Hz, 1H), 7.92–7.96 (m, 2H), 12.54 (br s, 1H).

Step 3.6. Benzyl 5-[(2-Chlorobenzyl)carbamoyl]-1-[(4-fluorophenyl)sulfonyl]-2-methyl-1,2-dihydro-1'*H*-spiro[indole-3,4'-piperidine]-1'-carboxylate. Prepared according to GP 8.1: 1'-[(Benzyloxy)carbonyl]-1-[(4-fluorophenyl)sulfonyl]-2-methyl-1,2-dihydrospiro[indole-3,4'-piperidine]-5-carboxylic acid (2.6 g, 58% purity, 2.8 mmol) from step 3.5 was reacted with HATU (1.6 g, 4.2 mmol, 1.5 equiv), Et_3N (0.59 mL, 4.2 mmol, 1.5 equiv), and 1-(2-chlorophenyl)methanamine (0.51 mL, 4.2 mmol, 1.5 equiv) in DMF (50 mL) at rt overnight to give, upon aqueous workup with DCM and flash chromatography (silica gel, hexane/EtOAc = 1:0 to 1:1), the title compound (645 mg, 34%). UPLC-MS (Method 1): ^{t}R = 1.47 min. MS (ESI+): *m*/*z* = 662/664 $[M+H]^+$ (Cl isotope pattern). ^{1}H NMR (300 MHz, DMSO-d_6): δ = 0.05–0.09 (m, 1H), 0.90–1.01 (m, 1H), 1.29 (d, *J* = 6.22 Hz, 3H), 1.77–1.82 (m, 1H), 1.93–2.00 (m, 1H), 2.81–3.19 (m, 2H), 3.51–3.56 (m, 1H), 4.01–4.06 (m, 1H), 4.50–4.59 (m, 3H), 5.06 (d, *J* = 5.46 Hz,

2H), 7.26–7.36 (m, 8H), 7.42–7.48 (m, 3H), 7.57 (d, *J* = 8.48 Hz, 1H), 7.77 (s, 1H), 7.86 (dd, *J* = 1.70, 8.48 Hz, 1H), 7.90–7.97 (m, 2H), 8.89 (t, *J* = 5.65 Hz, 1H).

Step 3.7. *N*-(2-Chlorobenzyl)-1-[(4-fluorophenyl)sulfonyl]-2-methyl-1,2-dihydro-spiro[indole-3,4'-piperidine]-5-carboxamide (3). Prepared according to GP 11: Benzyl 5-[(2-chlorobenzyl)carbamoyl]-1-[(4-fluorophenyl)sulfonyl]-2-methyl-1,2-dihydro-1'*H*-spiro[indole-3,4'-piperidine]-1'-carboxylate (694 mg, 1.05 mmol) from step 3.6 was reacted with HBr (33% in HOAc; 17 mL, 105 mmol, 100 equiv) at 0 °C for 1 h to give, upon workup, the title compound (470 mg, yield: 76%, purity: > 95%) which was used in the next step without further purification. UPLC-MS (Method 1): t_R = 0.93 min. MS (ESI+): *m/z* = 528/530 $[M+H]^+$ (Cl isotope pattern). ^{1}H NMR (300 MHz, DMSO-d_6): δ = –0.02 to 0.03 (m, 1H), 0.90 (dt, *J* = 4.27, 12.53 Hz, 1H), 1.27 (d, *J* = 6.59 Hz, 3H), 1.64–1.69 (m, 1H), 1.90 (dt, *J* = 4.02, 13.05 Hz, 1H), 2.41–2.59 (m, 3H*), 2.90–2.94 (m, 1H), 4.39–4.46 (q, *J* = 6.59 Hz, 1H), 4.52 (d, *J* = 5.84 Hz, 2H), 7.26–7.36 (m, 3H), 7.38–7.47 (m, 3H), 7.57 (d, *J* = 8.29 Hz, 1H), 7.73 (d, *J* = 1.51 Hz, 1H), 7.85 (dd, *J* = 1.79, 8.39 Hz, 1H), 7.90–7.95 (m, 2H), 8.95 (t, *J* = 5.75 Hz, 1H); * (partially) hidden by the residual DMSO-d_6 solvent peak. ^{13}C NMR (100 MHz, $CDCl_3$): δ = 17.6, 29.1, 31.2, 38.9, 42.1,

43.8, 46.1, 65.4, 115.1, 116.4, 116.6, 122.8, 127.2, 127.6, 129.11, 129.13, 129.2, 129.6, 130.4, 130.5, 133.7, 135.0, 135.5, 139.8, 141.9, 164.2, 166.7. ^{19}F NMR (375 MHz, $CDCl_3$: δ = -104.7 (s, 1F). HRMS (ESI+, $[M+H]^+$): calc.: 528.1446, found: 528.1521.

The enantiomers of racemic **3** were separated by chiral preparative HPLC [system: Dionex P580 pump, Gilson 215 liquid handler, Knauer K-2501 UV detector; column: Chiralpak AD-H 5 μm, 250 × 20 mm; eluent: hexane/*i*-PrOH (50:50) + 0.1 vol % Et_2NH; flow rate: 20 mL/min; temperature: 25 °C; detection: UV 254 nm] and analytically characterized by chiral HPLC [system: Dionex 680 pump, Dionex ASI 100, Waters 2487 UV detector; column: Chiralpak AD-H 5 μm, 150 × 4.6 mm; eluent: hexane/*i*-PrOH (50:50) + 0.1 vol % Et_2NH; flow rate: 1.0 mL/min; temperature: 25 °C; detection: UV 254 nm] and specific rotation. **3a** (eutomer): t_R = 3.30 min. $[\alpha]_D^{20}$ –149.10 ± 1.55 (*c* 1.0, $CHCl_3$). Yield: 137 mg (25%). Enantiomeric Purity: 93%. **3b** (distomer): t_R = 5.03 min. Yield: 78 mg (14%). Enantiomeric Purity: 96%.

***rac-N*-[(3-Chloropyridin-2-yl)methyl]-2-cyclopropyl-1-[(4-fluorophenyl)sulfonyl]-1,2,2',3',5',6'-hexahydrospiro[indole-3,4'-thiopyran]-5-carboxamide 1',1'-Dioxide (4) and Its Enantiomers 4a and 4b**

Step 4.1. 3,4,5,6-Tetrahydro-2*H*-thiopyran-4-carbaldehyde. A solution of oxalyl chloride (6.72 g, 52.9 mmol, 1.4 equiv) in DCM (200 mL) was cooled to –65 °C. A solution of DMSO (5.91 g, 75.6 mmol, 2.0 equiv) in DCM (30 mL) was added dropwise within 10 min at such a rate that the temperature did not exceed –50 °C. After 15 min, a solution of tetrahydrothiopyran-4-methanol (5.00 g, 37.8 mmol, 1.0 equiv) in DCM (30 mL) was added dropwise within 5 min at max. –45 °C. The mixture was stirred for 1 h, while warming to –30 °C. Et_3N (11.5 g, 113 mmol, 3.0 equiv) was added dropwise and the mixture was subsequently warmed to rt. After 1 h of stirring, the reaction mixture was poured into H_2O and extracted with DCM. The combined organic layers were washed with H_2O, dried with Na_2SO_4, and the solvents were removed in vacuo to give the crude title compound (5.70 g) which was used in the next step without further purification. MS (Thermo DSQ, NH_3, CI+): m/z = 131 $[M+H]^+$.

Step 4.2. 4-(Methoxymethylene)-3,4,5,6-tetrahydro-2*H*-thiopyran (55). A mixture of (methoxymethyl)triphenylphosphonium chloride (CAS-RN: [20763-19-3]; 885 g, 2.58 mol, 1.5 equiv) in THF (1.3 L) was cooled to –50 °C and 2 M LDA in THF/heptane/ethylbenzene (1.29 L, 2.58 mol, 1.5 equiv) was added dropwise keeping

the temperature below –20 °C. After 15 min at –20 °C, the deep red reaction mixture was cooled to –40 °C and a solution of tetrahydro-4*H*-thiopyran-4-one (**54**, CAS-RN: [1072-72-6]; 200 g, 1.72 mol, 1.0 equiv) in THF (1.0 L) was added dropwise. After 15 min at –40 °C, the mixture was warmed to rt and stirred at rt overnight. The reaction mixture was filtered, concentrated in vacuo, and filtered again. The obtained filtrate was purified by distillation (bp 60 °C/0.02 mbar) to give **55** (125 g, 50%). UPLC-MS (Method 1): t_R = 1.10 min. MS (ESI+): *m/z* = 145 $[M+H]^+$. ^{1}H NMR (300 MHz, $CDCl_3$): δ = 2.25–2.29 (m, 2H), 2.50–2.54 (m, 2H), 2.58–2.62 (m, 4H), 3.54 (s, 3H), 5.81 (s, 1H).

Step 4.3. 5-Bromo-2',3',5',6'-tetrahydrospiro[indole-3,4'-thiopyran] (56). 4-Bromo-phenylhydrazine hydrochloride (1:1) (**46**; 8.96 g, 40.1 mmol, 1.0 equiv) and either 3,4,5,6-tetrahydro-2*H*-thiopyran-4-carbaldehyde (5.2 g, 40 mmol, 1.0 equiv) from step 4.1 or, alternatively, enol ether **55** (5.8 g, 40 mmol, 1.0 equiv) from step 4.2 were dissolved in $CHCl_3$ (250 mL). The solution was cooled to 0 °C and TFA (10 mL, 130 mmol, 3.3 equiv) was added dropwise. The reaction mixture was heated to 50 °C for 18 h, cooled to rt, and carefully treated with a 25% aq NH_3 solution to reach pH ~8. The mixture was poured into H_2O, the layers were separated, and the aqueous layer

was extracted with DCM. The combined organic layers were washed with H_2O, dried with Na_2SO_4, and the solvents were removed under reduced pressure to give **56** (9.6 g) which was used in the next step without further purification. UPLC-MS (Method 1): ^{t}R = 1.21 min. MS (ESI+): *m*/*z* = 282/284 $[M+H]^+$ (Br isotope pattern). ^{1}H NMR (300 MHz, DMSO-d_6): δ = 1.64 (ddd, *J* = 2.74, 5.00, 13.47 Hz, 2H), 2.00–2.10 (m, 2H), 2.73 (dt, *J* = 4.05, 13.94 Hz, 2H), 3.04–3.13 (m, 2H), 7.53 (s, 2H), 7.78 (t, *J* = 1.23 Hz, 1H), 8.74 (s, 1H).

Step 4.4. 5-Bromo-2-cyclopropyl-1,2,2',3',5',6'-hexahydrospiro[indole-3,4'-thiopyran] (57). An ice-cooled solution of crude indolenine **56** (9.6 g, 80% purity) from step 4.3 in THF (100 mL) was successively treated with $BF_3{\cdot}OEt_2$ (3.4 mL, 27 mmol, 1.0 equiv) and 0.50 M cyclopropylmagnesium bromide in THF (163 mL, 81 mmol, 3.0 equiv) and stirring was continued at rt for 2 h. Then, sat. aq NH_4Cl solution was added and the mixture was partitioned between EtOAc and H_2O. The aqueous phase was extracted with EtOAc, the combined organic phases were washed with H_2O and brine, dried with Na_2SO_4, concentrated under reduced pressure, and purified by flash chromatography (silica gel, hexane/EtOAc = 1:0 to 55:45) to give **57** (3.2 g, 25% over 2 steps). UPLC-

MS (Method 1): t_R = 1.48 min. MS (ESI+): *m/z* = 324/326 $[M+H]^+$ (Br isotope pattern). ^{1}H NMR (300 MHz, DMSO-d_6): δ = 0.13–0.24 (m, 1H), 0.35–0.46 (m, 2H), 0.48–0.58 (m, 1H), 0.80–0.92 (m, 1H), 1.61–1.70 (m, 1H), 1.85–1.93 (m, 1H), 1.95–2.04 (m, 1H), 2.16–2.24 (m, 1H), 2.62–2.79 (m, 4H), 2.83 (d, *J* = 8.67 Hz, 1H), 5.81 (s, 1H), 6.44 (d, *J* = 8.29 Hz, 1H), 7.05 (dd, *J* = 1.98, 8.20 Hz, 1H), 7.19 (d, *J* = 1.88 Hz, 1H).

Step 4.5. 5-Bromo-2-cyclopropyl-1-[(4-fluorophenyl)sulfonyl]-1,2,2',3',5',6'-hexahydro-spiro[indole-3,4'-thiopyran] (58). Prepared according to GP 4.2: Indoline **57** (3.0 g, 9.3 mmol) from step 4.4 was reacted with 4-fluorobenzenesulfonyl chloride (2.7 g, 14 mmol, 1.5 equiv) in pyridine (7 mL) at rt overnight. Deviating from GP 4.2, the reaction mixture was added to ice–water and stirring was continued for 20 min. The formed precipitate was collected by filtration, washed with H_2O, and dissolved in DCM. The organic layer was dried with $MgSO_4$, filtered, and the solvent was removed under reduced pressure to give **58** (4.4 g, ca. 95%) which was not further purified. UPLC-MS (Method 1): t_R = 1.60 min. MS (ESI+): *m/z* = 482/484 $[M+H]^+$ (Br isotope pattern). ^{1}H NMR (300 MHz, DMSO-d_6): δ = 0.20–0.24 (m, 1H), 0.33–0.49 (m, 2H), 0.56–0.65 (m, 1H), 0.71–0.79 (m, 1H), 0.90–1.07 (m, 2H), 1.95–2.00 (m, 1H), 2.07–2.17 (m, 1H), 2.30–

2.35 (m, 1H), 2.57–2.62 (m, 1H), 2.76–2.90 (m, 2H), 4.02 (d, *J* = 7.54 Hz, 1H), 7.37–7.44 (m, 5H), 7.84–7.88 (m, 2H).

Step 4.6. 5-Bromo-2-cyclopropyl-1-[(4-fluorophenyl)sulfonyl]-1,2,2',3',5',6'-hexahydro-spiro[indole-3,4'-thiopyran] 1',1'-Dioxide (59). Prepared according to GP 5: To an ice-cooled solution of TFAA (CAS-RN: [407-25-0]; 76.5 mL, 541 mmol, 6.0 equiv) in MeCN (1.2 L), urea hydrogen peroxide (68 g, 720 mmol, 8.0 equiv) was slowly added and the resulting mixture was stirred at rt for 20 min. This mixture was slowly added to thiopyran **58** (44 g, 90 mmol, 1.0 equiv) from step 4.5 at 0 °C and the reaction mixture was stirred at rt for 30 min. H_2O (2.9 L) was added to the reaction mixture which was then stored in a refrigerator for 1 h. The formed precipitate was collected by filtration, washed with H_2O (100 mL), and taken up with DCM (700 mL). The organic layer was washed with sat. aq $NaHCO_3$ and sat. aq $Na_2S_2O_3$ solution, dried with $MgSO_4$, and concentrated under reduced pressure to give crude **59** (44.75 g) which was not further purified. UPLC-MS (Method 1): ^{t}R = 1.35 min. MS (ESI+): *m/z* = 514/516 $[M+H]^+$ (Br isotope pattern). ^{1}H NMR (300 MHz, DMSO-d_6): δ = 0.17–0.23 (m, 1H), 0.36–0.52 (m, 2H), 0.54–0.63 (m, 1H), 0.79–0.87 (m, 1H), 0.93–1.05 (m, 1H), 1.44 (dt, *J* = 2.83, 14.32 Hz, 1H), 2.38–2.44

(m, 2H*), 2.54–2.60 (m, 1H*), 3.15–3.18 (m, 2H), 3.60 (dt, *J* = 2.20, 14.04 Hz, 1H), 4.30 (d, *J* = 7.91 Hz, 1H), 7.37–7.50 (m, 5H), 7.84–7.90 (m, 2H); * (partially) hidden by the residual DMSO-d_6 solvent peak.

Step 4.7. Methyl 2-Cyclopropyl-1-[(4-fluorophenyl)sulfonyl]-1,2,2',3',5',6'-hexahydro-spiro[indole-3,4'-thiopyran]-5-carboxylate 1',1'-Dioxide (60). Prepared according to GP 6: Bromo sulfone **59** (2.40 g, 90% purity, 4.20 mmol) from step 4.6 was reacted with $PdCl_2(PPh_3)_2$ (600 mg, 0.84 mmol, 20 mol%), and Et_3N (1.5 mL, 11 mmol, 2.5 equiv) under a CO pressure of 10 bar in a mixture of MeOH (120 mL) and DMSO (12 mL) at 100 °C for ~22 h. Workup and flash chromatography (silica gel, hexane/EtOAc = 1:0 to 2:3) gave **60** (1.8 g, 83% over 2 steps). UPLC-MS (Method 1): t_R = 1.24 min. MS (ESI+): *m/z* = 494 $[M+H]^+$. ^{1}H NMR (300 MHz, DMSO-d_6): δ = 0.23–0.28 (m, 1H), 0.37–0.64 (m, 3H), 0.81–0.89 (m, 1H), 0.95–1.03 (m, 1H), 1.44 (dt, *J* = 3.39, 14.41 Hz, 1H), 2.58–2.63 (m, 3H*), 3.18–3.22 (m, 2H), 3.65 (dt, *J* = 2.64, 13.94 Hz, 1H), 3.82 (s, 3H), 4.38 (d, *J* = 7.91 Hz, 1H), 7.37–7.45 (m, 2H), 7.65 (d, *J* = 8.48 Hz, 1H), 7.70 (d, *J* = 1.51 Hz, 1H), 7.87–7.96 (m, 3H); * (partially) hidden by the residual DMSO-d_6 solvent peak.

Step 4.8. 2-Cyclopropyl-1-[(4-fluorophenyl)sulfonyl]-1,2,2',3',5',6'-hexahydro-spiro[indole-3,4'-thiopyran]-5-carboxylic Acid 1',1'-Dioxide (61). Prepared according to GP 7: Methyl ester **60** (1.9g, 90% purity, 3.5 mmol) from step 4.7 was reacted with 2 M aq LiOH (66 mL, 130 mmol, 38 equiv) in THF (65 mL) at rt overnight. Workup gave **61** (1.5 g, 85% purity, ca. 77%) which was not further purified. UPLC-MS (Method 1): t_R = 1.07 min. MS (ESI–): *m/z* = 478 $[M–H]^–$. ^{1}H NMR (400 MHz, DMSO-d_6): δ = 0.28–0.32 (m, 1H), 0.38–0.45 (m, 1H), 0.48–0.54 (m, 1H), 0.56–0.63 (m, 1H), 0.82–0.88 (m, 1H), 0.95–1.04 (m, 1H), 1.45 (dt, *J* = 2.69, 14.21 Hz, 1H), 2.50–2.62 (m, 3H*), 3.19–3.22 (m, 2H), 3.64 (dt, *J* = 2.53, 14.15 Hz, 1H), 4.37 (d, *J* = 8.08 Hz, 1H), 7.38–7.44 (m, 2H), 7.61 (d, *J* = 8.59 Hz, 1H), 7.67 (d, *J* = 1.52 Hz, 1H), 7.89–7.93 (m, 3H), 12.89 (br s, 1H); * (partially) hidden by the residual DMSO-d_6 solvent peak.

Step 4.9. *N*-[(3-Chloropyridin-2-yl)methyl]-2-cyclopropyl-1-[(4-fluorophenyl)sulfonyl]-1,2,2',3',5',6'-hexahydrospiro[indole-3,4'-thiopyran]-5-carboxamide 1',1'-Dioxide (4). Prepared according to GP 8.1: Acid **61** (2.1 g, 4.3 mmol) from step 4.8 was reacted with 1-(3-chloropyridin-2-yl)methanamine (CAS-RN: [500305-98-6]; 1.24 g, 8.68 mmol, 2.0 equiv), HATU (2.47 g, 6.51 mmol, 1.5 equiv), and Et_3N (1.8 mL, 13 mmol, 3.0 equiv)

in DMF (170 mL) at rt for 2 h. The reaction mixture was diluted with H_2O, and the formed precipitate was collected by filtration, washed with H_2O, and dried at 40 °C in vacuo to give **4** (2.4 g, , yield: 85%, purity: > 95%). UPLC-MS (Method 1): t_R = 1.19 min. MS (ESI+): *m/z* = 604/606 $[M+H]^+$ (Cl isotope pattern). ^{1}H NMR (400 MHz, DMSO-d_6): δ = 0.26–0.30 (m, 1H), 0.38–0.45 (m, 1H), 0.47–0.53 (m, 1H), 0.57–0.63 (m, 1H), 0.82–0.88 (m, 1H), 0.97–1.05 (m, 1H), 1.48 (dt, *J* = 2.53, 14.21 Hz, 1H), 2.46–2.62 (m, 3H*), 3.16–3.23 (m, 2H), 3.63 (dt, *J* = 2.53, 14.02 Hz, 1H), 4.36 (d, *J* = 7.83 Hz, 1H), 4.62–4.72 (m, 2H), 7.34–7.43 (m, 3H), 7.59 (d, *J* = 8.34 Hz, 1H), 7.85–7.93 (m, 5H), 8.48 (dd, *J* = 1.26, 4.80 Hz, 1H), 8.98 (t, *J* = 5.69 Hz, 1H); * (partially) hidden by the residual DMSO-d_6 solvent peak. ^{13}C NMR (100 MHz, DMSO-d_6): δ = 2.2, 4.7, 13.0, 27.4, 36.1, 42.2, 46.3, 46.9, 48.3, 70.2, 115.3, 116.9, 117.2, 122.0, 123.9, 129.3, 129.57, 129.62, 130.5, 134.4, 137.2, 138.6, 141.6, 147.4, 154.3, 163.8, 165.1, 166.3. ^{19}F NMR (375 MHz, DMSO-d_6): δ = -103.9 (m_c, 1F). HRMS (ESI+, $[M+H]^+$): calc.: 604.1065, found: 604.1144.

The enantiomers of racemic **4** were separated by chiral preparative HPLC [system: Dionex P580 pump, Gilson 215 liquid handler, Knauer K-2501 UV detector; column: Chiralpak IA 5 μm, 250 × 30 mm; eluent: MeOH + 0.1% Et_2NH; flow rate: 30 mL/min;

temperature: rt; injection: 0.6 mL/run, 130 mg/mL DMSO/MeOH; detection: UV 280 nm] and analytically characterized by chiral HPLC [system: Dionex 680 pump, Dionex ASI 100, Waters 2487 UV detector; column: Chiralpak IC 5 μm, 150 × 4.6 mm; eluent: MeOH + 0.1% Et_2NH; flow rate: 1.0 mL/min; temperature: 25 °C; detection: DAD scan at 280 nm] and specific rotation. **4a** (eutomer): ^{t}R = 5.10 min. $[\alpha]_D^{20}$ –109.5 ± 0.21 (*c* 0.60, $CHCl_3$). Yield: 882 mg (33%). Enantiomeric Purity: 99%. **4b** (distomer): ^{t}R = 6.58 min. $[\alpha]_D^{20}$ +108.5 ± 0.13 (*c* 0.61, $CHCl_3$). Yield: 904 mg (34%). Enantiomeric Purity: 98%.

***N*-{[3-Chloro-5-(trifluoromethyl)pyridin-2-yl]methyl}-2-cyclopropyl-1-[(4-fluorophenyl)-sulfonyl]-1,2,2',3',5',6'-hexahydrospiro[indole-3,4'-thiopyran]-5-carboxamide 1',1'-Dioxide (5) and Its Enantiomers 5a and 5b.** Prepared according to GP 8.1: Acid **61** (100 mg, 209 μmol) from step 4.8 was reacted with HATU (119 mg, 313 μmol, 1.5 equiv), Et_3N (87 μL, 630 μmol, 3.0 equiv), and 1-[3-chloro-5-(trifluoromethyl)pyridin-2-yl]methanamine hydrochloride (**62**, CAS-RN: [326476-49-7]; 77 mg, 310 μmol, 1.5 equiv) in DMF (2 mL) at rt overnight. The crude reaction mixture was directly submitted to preparative HPLC (Method 3) to give **5** (77 mg, yield: 55%, purity: > 98%). UPLC-MS (Method 1): ^{t}R = 1.36 min. MS (ESI+): *m/z* = 672/674 $[M+H]^+$ (Cl isotope

pattern). ^{1}H NMR (400 MHz, DMSO-d_6): δ = 0.26–0.30 (m, 1H), 0.38–0.45 (m, 1H), 0.47–0.53 (m, 1H), 0.57–0.64 (m, 1H), 0.82–0.88 (m, 1H), 0.97–1.05 (m, 1H), 1.47 (dt, *J* = 2.69, 14.21 Hz, 1H), 2.46–2.64 (m, 3H*), 3.17–3.23 (m, 2H), 3.64 (dt, *J* = 2.61, 14.02 Hz, 1H), 4.37 (d, *J* = 8.08 Hz, 1H), 4.68–4.79 (m, 2H), 7.38–7.43 (m, 2H), 7.59 (d, *J* = 8.34 Hz, 1H), 7.85 (d, *J* = 1.52 Hz, 1H), 7.87–7.92 (m, 3H), 8.46 (d, *J* = 1.52 Hz, 1H), 8.90 (d, *J* = 1.01 Hz, 1H), 9.11 (t, *J* = 5.69 Hz, 1H); * (partially) hidden by the residual DMSO-d_6 solvent peak. ^{13}C NMR (125 MHz, DMSO-d_6): δ = 2.3, 4.8, 13.1, 27.5, 36.2, 42.5, 46.5, 47.1, 48.4, 70.4, 115.4, 117.12, 117.12, 122.2, 123.0, 125.2, 129.5, 129.78, 129.78, 130.2, 130.4, 134.5, 134.7, 138.8, 141.9, 144.1, 159.5, 165.2, 165.4. ^{19}F NMR (375 MHz, DMSO-d_6): δ = -61.1 (s, 3F), -104.0 (m_c, 1F). HRMS (ESI+, $[M+H]^+$): calc.: 672.0939, found: 672.1016.

The enantiomers of racemic **5** were separated by chiral preparative HPLC [system: Dionex: P580 pump, Gilson 215 liquid handler, Knauer K-2501 UV detector; column: Chiralpak IC 5 μm, 250 × 30 mm; eluent: EtOH/MeOH (50:50, v/v); flow rate: 35 mL/min; temperature: rt; detection: UV 280 nm] and analytically characterized by chiral HPLC [system: Waters Alliance 2695, DAD 996, ESA Corona; column: Chiralpak

IC 3 μm, 100 × 4.6 mm; eluent: EtOH/MeOH (50:50, v/v); flow rate: 1.0 mL/min; temperature: 25 °C; detection: DAD scan at 280 nm] and specific rotation. **5a** (BAY 1214784) (eutomer), (2*S*)-enantiomer: t_R = 2.62 min. $[\alpha]_D^{20}$ –101.9 ± 0.13 (*c* 1.0, $CHCl_3$). Yield: 35 mg (45%). Enantiomeric Purity: > 99% **5b** (distomer), (2*R*)-enantiomer: t_R = 3.48 min. $[\alpha]_D^{20}$ +93.0 ± 0.25 (*c* 1.0, $CHCl_3$). Yield: 34 mg (44%). Enantiomeric Purity: 99%.

Pharmacology

General Methods. Compound Logistics. Ready-to-use test plates were used throughout hit-to-lead compound characterization and were prepared in advance by transferring 50 nL (Tag-lite assay 100 nL) of a 100-fold concentrated solution of the test compound (in 100% DMSO) into a white, small-volume microtiter plate (Greiner Bio-One, Germany) using a Hummingbird liquid handler (Digilab, MA, USA). Negative and positive control wells, typically 16 wells in a 384-well plate, received 50 nL of 100% DMSO only. For the establishment of dose–response curves, compounds were typically tested in duplicates at up to 11 concentrations (e.g., 20 μM, 5.7 μM, 1.6 μM, 0.47 μM, 0.13 μM, 38 nM, 11 nM, 3.1 nM, 0.89 nM, 0.25 nM, and 0.073 nM). Test plates were sealed and stored at –80 °C until use. **Experimental procedures.** All reagents and solutions were added using a Multidrop dispenser (Thermo Labsystems).

Frozen Cell Assays.[59] All cell lines used were routinely monitored for the presence of mycoplasma and shown to be free of any contamination. Two assay procedures were used for compound testing which differed in the time required for functional recovery of

the frozen cells at 37 °C (i.e., [a] a one-day protocol based on a short, 1 h functional recovery period in the case of hGnRH-R and cGnRH-R cells or [b] a two-day protocol employing overnight incubation of the rGnRH-R cells to achieve functional recovery; see the individual assay protocols below). Nevertheless, both procedures started with the removal of vials containing the cell line expressing the appropriate human or species-specific receptor from liquid nitrogen storage and a rapid thawing procedure by placing the vials into a 37 °C water bath. Immediately after thawing, the cells were transferred by gently decanting into a 50 mL Falcon tube containing preheated medium (see the individual assay protocols for the composition of the recovery and assay media). Any liquid remaining in the vials was gently rinsed with preheated medium and transferred into the Falcon tube as well. Next, the cells were harvested by centrifugation for 5 min at 18.0 × *g* and the supernatant was removed by gentle decanting prior to slowly adding preheated medium again and resuspending the pellet by mild swirling.

[a] One-Day Recovery Protocol (hGnRH-R and cGnRH-R Cells). Upon thawing, a small aliquot of the cells was removed for cell counting and the remaining cell stock was diluted to the final cell number in medium only (see individual assay protocols). Next, an

aliquot of the appropriate HTRF probe stock solution (prepared fresh according to the manufacturer's protocol) was added to achieve a 1:38 dilution step which was followed by a short preincubation for 1 h at 37 °C, sufficient to achieve full functionality.

[b] Two-Day Recovery Protocol (rGnRH-R Cells). Upon thawing, a small aliquot of the cells was removed for cell counting and the remaining cell stock was diluted in serum-containing medium [Ham's F12, PAA E15-016; 10% fetal calf serum (FCS), non-heat-inactivated, PAA A15-151; 10000 U/mL penicillin + 10000 μg/mL streptomycin, Gibco-Invitrogen 15140-163; 2 mM L-glutamine, Sigma G7513; 20 mM HEPES, Biochrom L1615; 1.4 mM sodium pyruvate, Gibco-Invitrogen 11360; 0.15% $NaHCO_3$, Biochrom L1713; 500 μg/mL Geneticin, Gibco-Invitrogen 10131] to achieve a seeding density of ~1.0×10^5 cells/cm^2 upon seeding into regular tissue culture flasks. The next day, the cells were harvested by Accutase treatment (Sigma-Aldrich, A6964) and a small aliquot was removed for cell counting in order to prepare the final dilution to the assay cell number in the very same, yet serum-free, medium only. Next, an aliquot of the IP1-d2 stock solution (prepared according to the manufacturer's protocol) was added to

achieve a 1:38 dilution step and the cells were incubated for 1 h at 37 °C to secure full functionality.

General Assay Procedures. Fluorescence Resonance Energy Transfer (FRET) Based Detection of (a) GnRH-R Second Messenger Signaling and (b) GnRH Binding. *(a) GnRH-R Second Messenger Signaling.* Agonist binding to the GnRH-R results in the activation of phospholipase C leading to the production of inositol-3-phosphate (IP3) and the subsequent, rapid release of intracellular Ca^{2+}. Eventually, this pathway of second messenger signaling is terminated through the stepwise conversion of IP3 into myoinositol [via dephosphorylation to inositol-2-phosphate (IP2) and inositol-1-phosphate (IP1)], a process which can be blocked at the IP1 level in the presence of LiCl. The accumulation of cellular IP1 is used in a competitive immunoassay in which IP1 competes with a fluorescent IP1 tracer (IP1-d2) for the binding to a terbium-labeled anti-IP1 antibody (HTRF IP-One HTRF assay, CisBio International).[60] A maximum signal resulting from FRET between the detection reagents is obtained in the absence of cellular IP1. Any decrease in the FRET signal is indicative of GnRH-R activation whereas antagonist activity results in signal increase once again. FRET signal

quantification is achieved with an appropriate plate reader (PHERAstar, RUBYstar, ViewLux). Following excitation at 340 nm, any reduction of FRET-induced emissions at 520 nm is indicative of agonist-induced IP1 production. In addition, a second FRET signal at 495 nm, originating from the terbium-labeled anti-IP1 antibody, is used for well internal referencing (well ratio, defined as 520 nm/495 nm·10000). *(b) GnRH Binding and Drug–Target Residence Time Determination.* HEK293 cells expressing an N-terminal SNAP-tag fusion protein of the hGnRH-R and subsequently custom-labeled with a terbium fluorophore are used in a competitive assay format detecting compound interference with the binding of a second custom-labeled Tag-lite green hGnRH-R agonist. In the absence of any interfering compound, a maximum FRET signal is obtained by binding of the Tag-lite green labeled agonist to the terbium fluorophore labeled receptor.

Data Analysis. Screen results were analyzed and IC_{50} values were calculated by four-parameter fitting using a commercial software package (Genedata Screener, Switzerland) as well as in-house developed software tools.

hGnRH-R Assay. Typically, the reaction volume was 5 μL in 384-well plates. 3 μL of a cell suspension containing 3333 cells/μL (1.0×10^4 cells/well) in Ham's F12 medium was added to all wells of the ready-to-use test plate. Following preincubation for 20 min at rt, 2 μL of a 2.5 × EC_{80} agonist solution of either LHRH (Sigma-Aldrich, L7134; stock: 80 μM in 10 mM Tris HCl, 0.01% BSA, stored at –20 °C) or buserelin (USBiological, B8995; stock: 0.1 mg/mL in Tris-Cl, 8.07×10^{-5} M, stored at –20 °C) prepared fresh in stimulation buffer (10 mM HEPES, pH 7.4, 1 mM $CaCl_2$, 0.5 mM $MgCl_2$, 4.2 mM KCl, 146 mM NaCl, 5.5 mM α-D-glucose, 0.05% BSA, 150 mM) was added to the test compound and positive control wells (low controls, [C(0)]). The actual stimulation conditions (i.e., EC_{80} values used) were determined in agonist concentration–response curve experiments performed using the same cells shortly before and had to be in accordance with published data. The negative control wells (high controls, [C(i)]) received stimulation buffer only. Following that, the plate was incubated for another 60 min at 37 °C in the presence of a 1 × EC_{80} concentration of agonist. The reaction was stopped by the addition of 2 μL of lysis buffer containing a 1:38 dilution of the terbium cryptate labeled anti-IP1 antibody stock prepared according to the manufacturer's

protocol. Another 60 min later, the cell lysate containing plate was transferred to a TR-FRET compatible reader to quantify the results.

rGnRH-R Assay. The reaction volume was 5 μL in 384-well plates. 3 μL of a cell suspension containing 3333 cells/μL (1.0×10^4 cells/well) was added to all wells of the ready-to-use test plate. Following preincubation for 20 min at rt, 2 μL of a 2.5 × EC_{80} agonist solution of either LHRH (Sigma-Aldrich, L7134; stock: 80 μM in 10 mM Tris HCl, 0.01% BSA, stored at –20 °C) or buserelin (USBiological, B8995; stock: 0.1 mg/mL in Tris-Cl, 8.07×10^{-5} M, stored at –20 °C) prepared fresh in stimulation buffer (10 mM HEPES, pH 7.4, 1 mM $CaCl_2$, 0.5 mM $MgCl_2$, 4.2 mM KCl, 146 mM NaCl, 5.5 mM α-D-glucose, 0.05% BSA, 150 mM) was added to the test compound and positive control wells (low controls, [C(0)]). The actual stimulation conditions (i.e., EC_{80} values used) were determined in agonist concentration–response curve experiments performed using the same cells shortly before and had to be in accordance with published data. The negative control wells (high controls, [C(i)]) received stimulation buffer only. Following that, the plate was incubated for another 60 min at 37 °C in the presence of a 1 × EC_{80} concentration of agonist. The reaction was stopped by the addition of 2 μL of lysis buffer

containing a 1:38 dilution of the terbium cryptate labeled anti-IP1 antibody stock prepared according to the manufacturer's protocol. Another 60 min later, the cell lysate containing plate was transferred to a TR-FRET compatible reader to quantify the results.

cGnRH-R Assay. Typically, the reaction volume was 5 μL in 384-well plates. 3 μL of cell suspension containing 1666 cells/μL (5000 cells/well) in Ham's F12 medium was added to all wells of the ready-to-use test plate. Following preincubation for 20 min at rt, 2 μL of a 2.5 × EC_{80} buserelin agonist solution (USBiological, B8995; stock: 0.1 mg/mL in Tris-Cl, 8.07 × 10^{-5} M, stored at –20 °C) prepared fresh in stimulation buffer (10 mM HEPES, pH 7.4, 1 mM $CaCl_2$, 0.5 mM $MgCl_2$, 4.2 mM KCl, 146 mM NaCl, 5.5 mM α-D-glucose, 0.05% BSA, 150 mM) was added to the test compound and positive control wells (low controls, [C(0)]). The actual stimulation conditions (i.e., EC_{80} values used) were determined in agonist concentration–response curve experiments performed using the same cells shortly before and had to be in accordance with published data. The negative control wells (high controls, [C(i)]) received stimulation buffer only. Following that, the plate was incubated for another 60 min at 37 °C in the presence of a 1 × EC_{80}

concentration of agonist. The reaction was stopped by the addition of 2 μL of lysis buffer containing a 1:20 dilution of the terbium cryptate labeled anti-IP1 antibody stock prepared according to the manufacturer's protocol. Another 60 min later, the cell lysate containing plate was transferred to a TR-FRET compatible reader to quantify the results.

hGnRH-R Tag-lite Binding Assay (Modified from[47]). To determine whether antagonist binding interferes with agonist binding transiently transfected, frozen HEK293 cells expressing an N-terminal SNAP-tag fusion protein of the hGnRH-R were obtained from CisBio in a custom, terbium-labeled Tag-lite format. Binding of a second custom-labeled Tag-lite green hGnRH-R agonist (CisBio) to the terbium-labeled receptor results in a maximum FRET signal between the interacting partners (obtained by exciting the terbium donor at 337 nm and quantifying the acceptor and donor emissions at 520 nm and 495 nm, respectively). Any specific decrease in the FRET signal is indicative of compounds competitively interfering with labeled agonist binding. FRET signal quantification is achieved with an appropriate plate reader (PHERAstar, RUBYstar,

ViewLux). In addition, the donor emission at 495 nm is used for well internal referencing (well ratio, defined as 520 nm/495 nm·10000).

Typically, the reaction volume was 16 μL in 384-well plates. 8 μL of cell suspension containing 7000 cells/μL (5.6×10^4 cells/well) in Tag-lite buffer was added to all wells of the ready-to-use test plate. Next, 4 μL of Tag-lite buffer was added to the test compound and positive control wells (high controls, [C(i)]). The negative control wells (low controls, [C(0)]) received 4 μL of unlabeled hGnRG-R agonist (buserelin, 10 μM, in Tag-lite buffer). Finally, 4 μL of the custom-labeled Tag-lite green hGnRG-R agonist (4 nM, in Tag-lite buffer) was added to all wells of the ready-to-use assay plate. Following incubation for 60 min at rt, the plate was transferred to a TR-FRET compatible reader to quantify the results.

Drug–Target Residence Time Determination. Affinity and kinetic binding parameters of compounds were measured using the Tag-lite homogeneous TR-FRET binding competition method previously described by our group for hGnRH[49] and other GPCRs.[47,]Unless otherwise indicated, experiments were conducted at rt in at least two independent equilibrium probe competition assay (ePCA) and kinetic probe competition

assay (kPCA) experiments with two replicates each (N = 2, *n* = 2). Briefly, compounds were serially diluted and transferred to the test plates following the procedures described previously.[47] Frozen cells containing the terbium (Tb^{2+})-labeled hGnRH-R were thawed, spun down (300 G, 5 min), resuspended in Tag-lite buffer (CisBio, Codolet, France) to a concentration of 1400 cells/μL, and dispensed into black, small-volume 384-well microtiter plates (Greiner Bio-One) already containing the fluorescent tracer (10 nM end concentration) and the antagonists. For the ePCA, the tracer and hGnRH-labeled cells were dispensed into the ready-to-use compound plates to a final volume of 5 μL, and the mixture was incubated for 1–2 h prior to acquisition of the steady-state TR-FRET ratiometric signals (590 nm/420 nm) upon excitation at 337 nm. Normalized values were fitted to a logistic four-parameter model using Genedata Screener software, and K_i values were calculated using the Cheng–Prusoff relationship.[61] For the kPCA, the tracer was dispensed into the ready-to-use compound plates prior to transferring to a PHERAstar FS microtiter plate reader. Then, the hGnRH-labeled cells were added to the wells to a final volume of 10 μL using the injector system of the instrument, and kinetic TR-FRET readings were made at time

zero and every 21 seconds for the times indicated previously.[47] Baseline-subtracted kinetic traces were analyzed with a competitive binding kinetics model described by Motulsky and Mahan.[62]

X-ray Structure Analysis of Compound 5a. Data for **5a** were collected at 110 K on a Rigaku Xcalibur system equipped with a CCD area detector and Cu X-ray radiation (Cu Kα, λ = 1.54178 Å). X-ray data collection and processing of data were performed using the SHELXTL package.[63] SHELXS was used for structure solution and SHELXL was used for full-matrix least-squares refinement on F^2.[64] All non-hydrogen atoms were refined anisotropically. All hydrogen atoms were placed in geometrically ideal positions using the riding model. The program XP in the Proteum software package was used for molecular representations. All experimental details are listed in Table S6 [Supporting Information]. The isotropic temperature factors of all hydrogen atoms were 1.2 and 1.5 times the size of the temperature factors of the corresponding heavy atoms. The F atoms of the CF_3 group in two of the four molecules are disordered and occupancies were refined to 55:45 (molecule B) and 60:40 (molecule C), respectively.

Colorless plates of **5a** were obtained by slow evaporation from *m*-xylene at rt. A single crystal with dimensions 0.12 × 0.06 × 0.02 mm^3 was mounted on a CryoLoop using a protective oil. Four independent molecules of **5a** and six molecules of *m*-xylene are present in the monoclinic space group *P*2(1) (*Z* = 2) with cell constants *a* = 12.1292(4) Å, *b* = 21.8511(4) Å, *c* = 29.7985(8) Å, β = 97.044(3)°. The molecular formula is 4 × $C_{29}H_{26}N_3O_5S_2ClF_4$ + 6 × C_8H_{10} with a molecular weight of 4 × 672.11 + 6 × 106.16 g/mol. A total of 71524 reflections of which 27479 are unique (R_{int} = 0.0622) were collected. The final *R* values were R_1 = 0.0753, $I > 2\sigma(I)$, and wR_2 = 0.1922 for all data. The goodness-of-fit of the data was 1.293. The absolute structure was determined with a Flack parameter of 0.028(6).[65] The crystallographic data for **5a** have been deposited with the Cambridge Crystallographic Data Centre (CCDC) with deposition code CCDC 2008704.

Physicochemical Assays

Stability of Compounds in Solution (pH 10, 7, and 1, at 37 °C). Solution stability was determined by HPLC-UV.[66] A 10 mM solution of compound in DMSO (5 μL) was dissolved in MeCN (1 mL). 100 μL of this solution was transferred to the respective

buffer (1 mL) and mixed thoroughly. Injections were made immediately after mixing for time zero injection and then again after 1, 2, and 24 h. Compounds were incubated at 37 °C. Degradation rate (recovery in %) was calculated by relating the peak areas after 1, 2, and 24 h to the time zero injection.

Aqueous Solubility of Compounds in DMSO Solutions. Aqueous solubility at pH 6.5 was determined by an orientating HTS method.[67] Test compounds were applied as 1 mM DMSO solutions. After addition of buffer pH 6.5, solutions were shaken for 24 h at rt. Undissolved material was removed by filtration. The compound dissolved in the filtrate was quantified by HPLC-MS/MS.

LogD Measurement. LogD values at pH 7.5 were recorded using an indirect method for determining hydrophobicity constants by reversed-phase HPLC.[68] A homologous series of *n*-alkan-2-ones (C_3–C_{16}, 0.02 M in MeCN) was used for calibration. Test compounds were applied as 0.67 mM DMSO stock solutions in MeCN/H_2O (1:1). The lipophilicity of compounds was then assessed by comparison to the calibration curve.

Pharmacokinetic Assays

Caco-2 Permeability Assay. Caco-2 cells [purchased from the German Collection of Microorganisms and Cell Cultures (DSMZ), Braunschweig, Germany] were seeded at a density of 4.5×10^4 cells/well on 24-well insert plates, 0.4 μm pore size, and grown for 15 d in DMEM supplemented with 10% FCS, 1% GlutaMAX (100 ×, Gibco), 100 U/mL penicillin, 100 μg/mL streptomycin (Gibco), and 1% nonessential amino acids (100 ×). Cells were maintained at 37 °C in a humidified 5% CO_2 atmosphere. Medium was changed every 2–3 d. Before the permeation assay was run, the culture medium was replaced by FCS-free HEPES carbonate transport buffer (pH 7.2) For the assessment of monolayer integrity, the transepithelial electrical resistance was measured. Test compounds were predissolved in DMSO and added either to the apical or basolateral compartment at a final concentration of 2 μM. Before and after incubation for 2 h at 37 °C, samples were taken from both compartments and analyzed by LC-MS/MS after precipitation with MeOH. Permeability (P_{app}) was calculated in the apical to basolateral (A → B) and basolateral to apical (B → A) directions. The apparent permeability was calculated using following equation: $P_{app} = (V_r/P_0)(1/S)(P_2/t)$, where V_r is the volume of medium in the receiver chamber, P_0 is the measured peak area of the test compound in

the donor chamber at $t = 0$, S is the surface area of the monolayer, P_2 is the measured peak area of the test compound in the acceptor chamber after incubation for 2 h, and t is the incubation time. The efflux ratio (ER) basolateral (B) to apical (A) was calculated as P_{app} B–A/P_{app} A–B. In addition, the compound recovery was calculated. As an assay control, reference compounds were analyzed in parallel.

***In Vitro* Metabolic Stability in Human Liver Microsomes.** The *in vitro* metabolic stability of test compounds was determined by incubation at 1 μM with a suspension of human liver microsomes (purchased from XenoTech, USA) in 100 mM phosphate buffer, pH 7.4 ($NaH_2PO_4 \cdot H_2O$ + $Na_2HPO_4 \cdot 2H_2O$) at a protein concentration of 0.5 mg/mL at 37 °C. The microsomes were activated by adding a cofactor mix containing 8 mM glucose-6-phosphate (G6P), 4 mM $MgCl_2$, 0.5 mM NADP, and 1 IU/mL G6P dehydrogenase in phosphate buffer, pH 7.4. The metabolic assay was started shortly afterwards by adding the test compound to the incubation at a final volume of 1 mL. Organic solvent in the incubations was limited to ≤0.01% DMSO and ≤1% MeCN. During incubation, the microsomal suspensions were continuously shaken at 580 rpm and aliquots were taken at 2, 8, 16, 30, 45, and 60 min, to which an equal volume of

cold MeOH was immediately added. Samples were frozen at –20 °C overnight, subsequently centrifuged for 15 min at 3000 rpm, and the supernatant was analyzed with an Agilent 1200 HPLC system with LC-MS/MS detection. The half-life of a test compound was determined from the concentration–time plot. From the half-life, the intrinsic clearance was calculated. Together with the additional parameters liver blood flow, specific liver weight, and microsomal protein content, the hepatic in vivo blood clearance (CL) and the maximal oral bioavailability (F_{max}) were calculated using the 'well-stirred' liver model.[69] The following parameter values were used: liver blood flow, 1.32 L/h/kg; specific liver weight, 21 g/kg body weight; microsomal protein content, 40 mg/g. For classification of the results, the following criteria were used: F_{max} >70% (= CL <0.4 L/h/kg) was classified as high metabolic stability (high), F_{max} 30–70% (CL 0.4–0.9 L/h/kg) as moderate stability, and F_{max} <30% (CL >0.9 L/h/kg) as low metabolic stability.

***In Vitro* Metabolic Stability in Rat Liver Microsomes.** The *in vitro* metabolic stability of test compounds was determined by incubation at 1 μM with a suspension of rat liver microsomes (purchased from XenoTech, USA) in 100 mM phosphate buffer, pH 7.4 ($NaH_2PO_4 \cdot H_2O$ + $Na_2HPO_4 \cdot 2H_2O$) at a protein concentration of 0.5 mg/mL at 37 °C. The

microsomes were activated by adding a cofactor mix containing 8 mM G6P, 4 mM $MgCl_2$, 0.5 mM NADP, and 1 IU/mL G6P dehydrogenase in phosphate buffer, pH 7.4. The metabolic assay was started shortly afterwards by adding the test compound to the incubation at a final volume of 1 mL. Organic solvent in the incubations was limited to ≤0.01% DMSO and ≤1% MeCN. During incubation, the microsomal suspensions were continuously shaken at 580 rpm and aliquots were taken at 2, 8, 16, 30, 45, and 60 min, to which an equal volume of cold MeOH was immediately added. Samples were frozen at –20 °C overnight, subsequently centrifuged for 15 min at 3000 rpm, and the supernatant was analyzed with an Agilent 1200 HPLC system with LC-MS/MS detection. The half-life of a test compound was determined from the concentration–time plot. From the half-life, the intrinsic clearance was calculated. Together with the additional parameters liver blood flow, specific liver weight, and microsomal protein content, the hepatic in vivo blood clearance (CL) and the maximal oral bioavailability (F_{max}) were calculated using the 'well-stirred' liver model.[63] The following parameter values were used: liver blood flow, 4.2 L/h/kg; specific liver weight, 32 g/kg body weight; microsomal protein content, 40 mg/g.

***In Vitro* Metabolic Stability in Rat Hepatocytes.** Hepatocytes from Han Wistar rats (purchased from Harlan, The Netherlands) were isolated via a two-step perfusion method. After perfusion, the liver was carefully removed from the rat, the liver capsule was opened, and the hepatocytes were gently shaken out into a Petri dish with ice-cold Williams' medium E (WME). The resulting cell suspension was filtered through sterile gauze into 50 mL Falcon tubes and centrifuged at 50 × *g* for 3 min at rt. The cell pellet was resuspended in WME (30 mL) and centrifuged through a Percoll gradient twice at 100 × *g*. The hepatocytes were washed again with WME and resuspended in medium containing 5% FCS. Cell viability was determined by trypan blue exclusion. For the metabolic stability assay, liver cells were distributed in WME containing 5% FCS to glass vials at a density of 1.0×10^6 vital cells/mL. The test compound was added at a final concentration of 1 μM. During incubation, the hepatocyte suspensions were continuously shaken at 580 rpm and aliquots were taken at 2, 8, 16, 30, 45, and 90 min, to which an equal volume of cold MeOH was immediately added. Samples were frozen at –20 °C overnight, subsequently centrifuged for 15 min at 3000 rpm, and the supernatant was analyzed with an Agilent 1200 HPLC system with LC-MS/MS

detection. The half-life of a test compound was determined from the concentration–time plot. From the half-life, the intrinsic clearance was calculated using the 'well-stirred' liver model[63] together with the additional parameters liver blood flow, specific liver weight and amount of liver cells in vivo and in vitro. The hepatic in vivo blood clearance (CL) and the maximal oral bioavailability (F_{max}) were calculated. The following parameter values were used: liver blood flow, 4.2 L/h/kg; specific liver weight, 32 g/kg body weight; liver cells in vivo, 1.1×10^8 cells/g liver; liver cells in vitro, 1.0×10^6/mL.

Inhibition of CYP450 Metabolism. The inhibitory potency of test compounds towards cytochrome P450 dependent metabolic pathways was determined in human liver microsomes (purchased from XenoTech, USA) by applying individual CYP isoform selective standard probes (CYP1A2, phenacetin; CYP2C8, amodiaquine; CYP2C9, diclofenac; CYP2D6, dextromethorphan; CYP3A4, midazolam). Reference inhibitors were included as positive controls. Incubation conditions (protein and substrate concentration, incubation time) were optimized with regard to linearity of metabolite formation. Assays were processed in 96-well plates at 37 °C using a Genesis Workstation (Tecan, Crailsheim, Germany). After protein precipitation, metabolite

formation was quantified by LC-MS/MS analysis, which was followed by inhibition evaluation and IC_{50} calculation.

Animal Studies. All animal studies were conducted in accordance with the German Animal Welfare Act and the ethical guidelines of Bayer AG, and were approved by the local ethics committee.

Binding to Plasma Proteins. The binding of test compounds to plasma proteins was measured using the method reported by Schuhmacher et al.[70]

***In Vivo* Pharmacokinetics in Rats.** Female and male Wistar rats were obtained from Charles River (Germany) and had access to food and water *ad libitum*. All animals were housed according to institutional guidelines under a 12 h/12 h light/dark cycle and maintained under standard conditions (20–22 °C, 50–70% humidity). Rats were housed in Makrolon cages type IV, five animals per cage, fed a pelleted diet (Ssniff, Germany), and used for in vivo studies with a weight of 200–300 g.

For *in vivo* pharmacokinetic experiments, test compounds were administered to female or male Wistar rats intravenously at a dose of 0.5 mg/kg and po at a dose of 2.0

mg/kg formulated as solutions using solubilizers such as PEG400 and EtOH in well-tolerated amounts. Blood samples were collected, for example, at 2 min (iv only), 8 min, 15 min, 30 min, 45 min, 1 h, 2 h, 4 h, 7 h, 24 h, and 48 h (if needed) after dosing from the vena jugularis into lithium heparin tubes (Monovette, Sarstedt) and centrifuged for 15 min at 3000 rpm. An aliquot of 100 μL from the supernatant (plasma) was taken and precipitated by the addition of cold MeCN (400 μL). Samples were frozen at –20 °C overnight, and subsequently thawed and centrifuged at 3000 rpm, 4 °C for 20 min. Aliquots of the supernatant were analyzed with an Agilent HPLC system with LC-MS/MS detection. Pharmacokinetic parameters were calculated by non-compartmental analysis using pharmacokinetics calculation software (e.g., Phoenix WinNonlin, Certara USA, Inc.).

***In Vivo* Pharmacokinetics in Beagle Dogs and Cynomolgus Monkeys.** Beagle dogs were obtained from Marshall BioResources (USA), cynomolgus monkeys were obtained from Hartelust (Tillburg, Netherlands). All animals were housed according to institutional guidelines under a 12 h/12 h light/dark cycle and maintained under standard conditions.

For *in vivo* pharmacokinetic experiments, test compounds were administered to female beagle dogs or female cynomolgus monkeys intravenously as a 15-min infusion at a dose of 0.5 mg/kg and po at a dose of 2.0 mg/kg formulated as solutions using solubilizers such as PEG400 and EtOH in well-tolerated amounts. Blood samples were collected, for example, at 5 min (dog only), 10 min (dog only), 15 min (prior to end of infusion), 20 min, 30 min, 1 h, 2 h, 4 h, 7 h, 24 h, and 48 h (if needed) after iv dosing, and at 5 min, 15 min, 30 min, 1 h, 2 h, 4 h, 7 h, 24 h, and 48 h (if needed) after po dosing, from the vena saphena (dog) or vena cephalia antebrachii (cynomolgus monkey) into lithium heparin tubes (Monovette, Sarstedt) and centrifuged for 15 min at 3000 rpm. An aliquot of 100 μL from the supernatant (plasma) was taken and precipitated by the addition of cold MeCN (400 μL). Samples were frozen at –20 °C overnight, and subsequently thawed and centrifuged at 3000 rpm, 4 °C for 20 min. Aliquots of the supernatant were analyzed with an Agilent HPLC system with LC-MS/MS detection. Pharmacokinetic parameters were calculated by non-compartmental analysis using pharmacokinetics calculation software (e.g., Phoenix WinNonlin, Certara USA, Inc.).

Automated hERG K^+ Current Voltage-Clamp Safety Assay. The hERG K^+ current assay is based on a recombinant HEK293 cell line with stable expression of the *KCNH2* (*HERG*) gene.[71] The cells were cultured using a humidified incubator (37 °C, 5% CO_2) and a standard culture medium [MEM with Earle's salts and L-glutamine, 10% non-inactivated FCS, 0.1 mM nonessential amino acids, 1 mM sodium pyruvate, penicillin/streptomycin (50 μg/mL each), 0.4 mg/mL Geneticin]. Ca. 0.5–8 h following cell dissociation, the cells were investigated by means of the 'whole-cell voltage-clamp' technique[72] in an automated 8-channel system (Patchliner; Nanion Technologies, Munich, Germany) with PatchControlHT software (Nanion Technologies) to control the Patchliner system and to handle data acquisition and analysis. Voltage-clamp control was provided by two EPC 10 Quadro amplifiers under control of the PatchMaster Pro software (both: HEKA Elektronik, Lambrecht, Germany) and with NPC-16 medium resistance (~2 MΩ) chips (Nanion Technologies) serving as planar substrate at rt (22–24 °C). NPC-16 chips were filled with intra- and extracellular solution [intracellular solution: 10 mM NaCl, 50 mM KCl, 60 mM KF, 20 mM EGTA, 10 mM HEPES, pH 7.2 (KOH); extracellular solution: 140 mM NaCl, 4 mM KCl, 2 mM $CaCl_2$, 1 mM $MgCl_2$,

5 mM glucose, 10 mM HEPES, pH 7.4 (NaOH)] and with cell suspension. After formation of a GΩ seal and entering whole-cell mode (including several automated quality control steps), the cell membrane was clamped to the holding potential (–80 mV). Following an activating clamp step (+20 mV, 1000 ms), exclusively hERG-mediated inward tail currents were elicited by hyperpolarizing voltage steps from +20 to –120 mV (duration 500 ms); this clamp protocol was repeated every 12 s.[73] After an initial stabilization phase (5–6 min), test compounds were added either as a single concentration (10 μM) or in ascending concentrations (0.1, 1, and 10 μM; 5–6 min per concentration), followed by several washout steps. Effects of test compounds were quantified by analyzing the amplitude of the hERG-mediated inward tail currents (in % of predrug control) as a function of test compound concentration (Igor Pro Software). Mean concentration–response data were fitted with a standard sigmoidal four-parameter logistic equation of the form: Y = Bottom+(Top–Bottom)/(1+10^((LogIC_{50}–X)*HillSlope)), where Y is the current inhibition (in % of predrug control), X is the logarithm of drug concentration, and IC_{50} is the drug concentration producing half-maximal current inhibition, and using the following constraints: Top = 100%, Bottom = 0%. No curve

fitting was performed in cases with an obvious lack of a concentration-dependent current inhibition and/or a too small effect size (ca. ≤20%).

Measurement of Plasma LH Levels. *(a) Wistar Rats.* Blood samples of ca. 1 mL were collected into plain tubes at the following time points: baseline (prior to castration), week 1, 2, 3, 4, 5, 6, 7, and 8 post castration, 1 day before dosing, on day of dosing (30 min, 1 h, 2 h, 4 h, and 8 h postdosing), and 24 h postdosing. The collected blood was allowed to clot within 1 h of collection. Serum was then separated by centrifugation at 4000 rpm, 4 °C for 10 min, divided into two aliquots (ca. 0.2 mL each), and stored at –80 °C. LH determination was conducted using the Luminex MILLIPLEX MAP Council Pituitary Kit 96-well plate assay RPT86K according to the manufacturer's specifications. *(b) Cynomolgus Monkeys.* Serum levels of LH in castrated monkeys were measured by radioimmunoassay (RIA) using a double-antibody RIA procedure similar to that described by Niswender and Spies.[74] The LH RIA kit (purchased from Dr Albert Parlow, NHPP, Harbor-UCLA Medical Center, Los Angeles, USA) is a homologous cynomolgus macaque assay with cynomolgus LH (AFP-6936A) for both iodination and standards. The rabbit anti-cynomolgus LH antibody (AFP-342994) was used at a final dilution of

1:972,973. The detection limit of the assay was 0.01 ± 0.005 ng/tube routinely. The intra- and interassay variations were less than 10%.

Reduction of Plasma LH Levels Obtained in a First-in-Human Study with 5a in Postmenopausal Women. The conduct of this clinical study met all local legal and regulatory requirements. The study was conducted in accordance with the ethical principles that have their origin in the Declaration of Helsinki and the International Conference on Harmonization (ICH) guideline E6: Good Clinical Practice (GCP). Ascending single oral doses were administered to postmenopausal women aged between 45 and 65 years. The following dosages were tested: 5 mg/20 mg/60 mg/150 mg/300 mg/450 mg of **5a** administered in a self-microemulsifying drug delivery system (SMEDDS) liquid dosage form. In each dose group, six women were treated with active drug while two women were given a matching placebo. A progression to the next higher dose level was only done after careful assessment of the safety, tolerability, and pharmacokinetics of the preceding dose level.

A standard electrochemiluminescence immunoassay (ECLIA) was used for the determination of LH levels and was undertaken by MLM Medical Labs, Mönchengladbach, Germany.

ASSOCIATED CONTENT

Supporting Information

The following Supporting Information is available free of charge on the ACS Publications Website at DOI:Xxx

Identification of SMOL hGnRH-R antagonists; summary of HTS results and IC_{50} determinations; tabular summary of essential properties and detailed off-target profiling data for **1a**, **2b**, **3a**, **4a**, and **5a** (selected molecular/physicochemical, in vitro pharmacology, safety, and pharmacokinetic properties); details of in vivo pharmacodynamic studies in rats and monkeys for **3a**, **4a**, and **5a**; crystallographic data for **5a**; synthesis of compounds **16–45**; HPLC analyses of compounds **15** and **1 - 5** including chiral HPLC analyses of **1a**/**b**, **2a**/**b**, **3a**/**b**, **4a**/**b** and **5a**/**b**; (PDF).

Molecular formula strings (CSV)

AUTHOR INFORMATION

Corresponding Authors

*E-mail: olaf.panknin@bayer.com (O.P.).

*E-mail: gernot.langer@bayer.com (G.L.).

ORCID

Olaf Panknin: 0000-0002-8352-7064

Andrea Wagenfeld: 0000-0001-9648-4318

Wilhelm Bone: 0000-0002-9432-4035

Eckhard Bender: 0000-0002-6845-0011

Katrin Nowak-Reppel: 0000-0003-4029-099X

Amaury E. Fernández-Montalván: 0000-0001-9156-0000

Reinhard Nubbemeyer: 0000-0003-0757-6064

Stefan Bäurle: 0000-0002-0560-8379

Sven Ring: 0000-0001-6548-4956

Norbert Schmees: 0000-0002-3284-3921

Olaf Prien: 0000-0003-2512-9663

Martina Schäfer: 0000-0003-3640-6435

Christian Friedrich: 0000-0001-8955-4808

Thomas M. Zollner: 0000-0001-6126-370X

Andreas Steinmeyer: 0000-0002-0294-4262

Thomas Mueller: 0000-0001-9017-4781

Gernot Langer: 0000-0001-5959-8834

Present Address

§ Boehringer Ingelheim Pharma GmbH & Co. KG, Drug Discovery Sciences, Birkendorfer Straße 65, 88397 Biberach/Riß, Germany

Author Contributions

The manuscript was written through contributions of all authors. All authors have given approval to the final version of the manuscript.

Notes

All authors declare the following competing financial interests:

O.P., A.W., W.B., E.B., K.N.-R., A.E.F.-M., R.N., S.B., S.R., N.S., O.Pr., M.S., C.F., T.M.Z., A.S., T.M. and G.L. are or have been employees and stock-holders of Bayer Aktiengesellschaft.

ACKNOWLEDGMENTS

We would like to thank Kay Greenfield for proofreading the manuscript. Particular thanks are due to Eike Gardlo (Lead Discovery Wuppertal, Cell Biology) and Marco

Sommer, Kai Steger, and Dyana Röben (Lead Discovery Berlin, Screening Cell Biology), as well as to Ina Guhrke, Marc Guttzeit, Thi-Bich-Thoa Ho, Stefan Hünicke, Jördis Luge, Sandra Miksche, and Christian Wuttke (Medicinal Chemistry, Berlin) and Dennis Brinckmann, Sabine Kern, Xandra Klein, Thomas Kuhles, and Andrea Seipp (Gynecological Therapies, Berlin), for their excellent technical assistance throughout the whole project. The authors also thank Victoria Georgi and Felix Schiele (Lead Discovery Berlin, Screening Biochemistry) for support with the binding kinetics studies. In addition, Antje Rottmann (DMPK, Berlin) and Simone Schulz (DMPK, Wuppertal) are acknowledged for their excellent support with compound metabolism studies, as are Gisbert Depke, Ursula Ganzer (Medicinal Chemistry Berlin), Adam Nitsche and Rene Spang (Medicinal Chemistry Wuppertal) for exceptional analytical and logistics support. Thanks to Stefan Klein for statistical analyses regarding the first-in-human study. We would also like to thank Jan Hübner and Marcus Koppitz for a supply of elagolix, relugolix, and cetrorelix.

The frozen cells used in this project were produced in large scale and obtained from (a) acCELLerate, Hamburg, Germany and (b) CisBio, Codolet, France.

ABBREVIATIONS

hGnRH-R, human gonadotropin-releasing hormone receptor; SMOL, small molecule; LLE, lipophilic ligand efficiency; LHRH, luteinizing hormone releasing hormone; OVX, ovariectomized; ORX, orchiectomized; TPSA, topological polar surface area; DMAP, 4-(dimethylamino)pyridine; DIPEA, *N*,*N*-diisopropylethylamine; HATU, 1-[bis(dimethylamino)methylene]-1*H*-1,2,3-triazolo[4,5-*b*]pyridinium 3-oxide hexafluorophosphate; HOAt, 1-hydroxy-7-azabenzotriazole; HTRF, homogeneous time-resolved fluorescence; TR-FRET, time-resolved fluorescence resonance energy transfer.

REFERENCES

(1) Stewart, E. A.; Laughlin-Tommaso, S. K.; Catherino, W. H.; Lalitkumar, S.; Gupta, D.; Vollenhoven, B. Uterine fibroids. *Nat. Rev. Dis. Primers* **2016**, *2*, 16043.

(2) Stewart, E. A.; Cookson, C. L.; Gandolfo, R. A.; Schulze-Rath, R. Epidemiology of uterine fibroids: a systematic review. *BJOG* **2017**, *124*, 1501–1512.

(3) Baranov, V. S.; Ivaschenko, T. E.; Yarmolinskaya, M. I. Comparative systems genetics view of endometriosis and uterine leiomyoma: two sides of the same coin? *Syst. Biol. Reprod. Med.* **2016**, *62*, 93–105.

(4) Styer, A. K.; Rueda, B. R. The epidemiology and genetics of uterine leiomyoma. *Best Pract. Res., Clin. Obstet. Gynecol.* **2016**, *34*, 3–12.

(5) Reis, F. M.; Bloise, E.; Ortiga-Carvalho, T. M. Hormones and pathogenesis of uterine fibroids. *Best Pract. Res., Clin. Obstet. Gynecol.* **2016**, *34*, 13–24.

(6) Moravek, M. B.; Yin, P.; Ono, M.; Coon V, J. S.; Dyson, M. T.; Navarro, A.; Marsh, E. E.; Chakravarti, D.; Kim, J. J.; Wei, J.-J.; Bulun, S. E. Ovarian steroids, stem cells and uterine leiomyoma: therapeutic implications. *Hum. Reprod. Update* **2015**, *21*, 1–12.

(7) Bulun, S. E. Uterine fibroids. *N. Engl. J. Med.* **2013**, *369*, 1344–1355.

(8) Sohn, G. S.; Cho, S.; Kim, Y. M.; Cho, C.-H.; Kim, M.-R.; Lee, S. R.; for the Working Group of Society of Uterine Leiomyoma. Current medical treatment of uterine fibroids. *Obstet. Gynecol. Sci.* **2018**, *61*, 192–201.

(9) Al-Hendy, A.; Myers, E. R.; Stewart, E. Uterine Fibroids: burden and unmet medical need. *Semin. Reprod. Med.* **2017**, *35*, 473–480.

(10) Stovall, D. W. Alternatives to hysterectomy: focus on global endometrial ablation, uterine fibroid embolization, and magnetic resonance-guided focused ultrasound. *Menopause* **2011**, *18*, 437–444.

(11) Donnez, J.; Donnez, O.; Dolmans, M.-M. The current place of medical therapy in uterine fibroid management. *Best Pract. Res., Clin. Obstet. Gynecol.* **2018**, *46*, 57–65.

(12) Bradley, L. D.; Gueye, N.-A. The medical management of abnormal uterine bleeding in reproductive-aged women. *Am. J. Obstet. Gynecol.* **2016**, *214*, 31–44.

(13) Stamatiades, G. A.; Kaiser, U. B. Gonadotropin regulation by pulsatile GnRH: signaling and gene expression. *Mol. Cell. Endocrinol.* **2018**, *463*, 131–141.

(14) Thompson, I. R.; Kaiser, U. B. GnRH pulse frequency-dependent differential regulation of LH and FSH gene expression. *Mol. Cell. Endocrinol.* **2014**, *385*, 28–35.

(15) Kaprara, A.; Huhtaniemi, I. T. The hypothalamus-pituitary-gonad axis: tales of mice and men. *Metabolism* **2018**, *86*, 3–17.

(16) Durán-Pastén, M. L.; Fiordelisio, T. GnRH-induced Ca^{2+} signaling patterns and gonadotropin secretion in pituitary gonadotrophs. Functional adaptations to both ordinary and extraordinary physiological demands. *Front. Endocrinol.* **2013**, *4*, 127.

(17) McArdle, C. A.; Franklin, J.; Green, L.; Hislop, J. N. Signalling, cycling and desensitisation of gonadotrophin-releasing hormone receptors. *J. Endocrinol.* **2002**, *173*, 1–11.

(18) Finch, A. R.; Sedgley, K. R.; Armstrong, S. P.; Caunt, C. J.; McArdle, C. A. Trafficking and signalling of gonadotrophin-releasing hormone receptors: an automated imaging approach. *Br. J. Pharmacol.* **2010**, *159*, 751–760.

(19) For a comprehensive review, see: Tukun, F.-L.; Olberg, D. E.; Riss, P. J.; Haraldsen, I.; Kaass, A.; Klaveness, J. Recent development of non-peptide GnRH antagonists. *Molecules* **2017**, *22*, 2188.

(20) Miwa, K.; Hitaka, T.; Imada, T.; Sasaki, S.; Yoshimatsu, M.; Kusaka, M.; Tanaka, A.; Nakata, D.; Furuya, S.; Endo, S.; Hamamura, K.; Kitazaki, T. Discovery of 1-{4-[1-(2,6-difluorobenzyl)-5-[(dimethylamino)methyl]-3-(6-methoxypyridazin-3-yl)-2,4-dioxo-1,2,3,4-tetrahydrothieno[2,3-*d*]pyrimidin-6-yl]phenyl}-3-methoxyurea (TAK-385) as a potent, orally active, non-peptide antagonist of the human gonadotropin-releasing hormone receptor. *J. Med. Chem.* **2011**, *54*, 4998–5012.

(21) Osuga, Y.; Enya, K.; Kudou, K.; Hoshiai, H. Relugolix, a novel oral gonadotropin-releasing hormone antagonist, in the treatment of pain symptoms associated with uterine fibroids: a randomized, placebo-controlled, phase 3 study in Japanese women. *Fertil. Steril.* **2019**, *112*, 922–929.e2.

(22) Chen, C.; Wu, D.; Guo, Z.; Xie, Q.; Reinhart, G. J.; Madan, A.; Wen, J.; Chen, T.; Huang, C. Q.; Chen, M.; Chen, Y.; Tucci, F. C.; Rowbottom, M.; Pontillo, J.; Zhu, Y.-F.;

Wade, W.; Saunders, J.; Bozigian, H.; Struthers, R. S. Discovery of sodium *R*-(+)-4-{2-[5-(2-fluoro-3-methoxyphenyl)-3-(2-fluoro-6-[trifluoromethyl]benzyl)-4-methyl-2,6-dioxo-3,6-dihydro-2*H*-pyrimidin-1-yl]-1-phenylethylamino}butyrate (elagolix), a potent and orally available nonpeptide antagonist of the human gonadotropin-releasing hormone receptor. *J. Med. Chem.* **2008**, *51*, 7478–7485.

(23) Shebley, M.; Polepally, A. R.; Nader, A.; Ng, J. W.; Winzenborg, I.; Klein, C. E.; Noertersheuser, P.; Gibbs, M. A.; Mostafa, N. M. Clinical pharmacology of elagolix: an oral gonadotropin-releasing hormone receptor antagonist for endometriosis. *Clin. Pharmacokinet.* **2020**, *59*, 297–309.

(24) Taylor, H. S.; Dun, E. C.; Chwalisz, K. Clinical evaluation of the oral gonadotropin-releasing hormone-antagonist elagolix for the management of endometriosis-associated pain. *Pain Manage.* **2019**, *9*, 497–515.

(25) Pohl, O.; Marchand, L.; Bell, D.; Gotteland, J.-P. Effects of combined GnRH receptor antagonist linzagolix and hormonal add-back therapy on vaginal bleeding—

delayed add-back onset does not improve bleeding pattern. *Reprod. Sci.* **2020**, *27*, 988–995.

(26) Aldrich, C.; Bertozzi, C.; Georg, G. I.; Kiessling, L.; Lindsley, C.; Liotta, D.; Merz Jr., K. M.; Schepartz, A.; Wang, S. The ecstasy and agony of assay interference compounds. *J. Med. Chem.* **2017**, *60*, 2165–2168.

(27) Duarte, C. D.; Barreiro, E. J.; Fraga, C. A. M. Privileged structures: a useful concept for the rational design of new lead drug candidates. *Mini-Rev. Med. Chem.* **2007**, *7*, 1108–1119.

(28) de Sa Alves, F. R.; Barreiro, E. J.; Fraga, C. A. M. From nature to drug discovery: the indole scaffold as a 'privileged structure'. *Mini-Rev. Med. Chem.* **2009**, *9*, 782–793.

(29) Horton, D. A.; Bourne, G. T.; Smythe, M. L. The combinatorial synthesis of bicyclic privileged structures or privileged substructures. *Chem. Rev.* **2003**, *103*, 893–930.

(30) Patchett, A. A.; Nargund, R. P.; Tata, J. R.; Chen, M.-H.; Barakat, K. J.; Johnston, D. B. R.; Cheng, K.; Chan, W. W.-S.; Butler, B.; Hickey, G.; Jacks, T.; Schleim, K.; Pong, S.-S.; Chaung, L.-Y. P.; Chen, H. Y.; Frazier, E.; Leung, K. H.; Chiu, S.-H. L.; Smith, R. G. Design and biological activities of L-163,191 (MK-0677): a potent, orally active growth hormone secretagogue. *Proc. Natl. Acad. Sci. U. S. A.* **1995**, *92*, 7001–7005.

(31) Evans, B. E.; Leighton, J. L.; Rittle, K. E.; Gilbert, K. F.; Lundell, G. F.; Gould, N. P.; Hobbs, D. W.; DiPardo, R. M.; Veber, D. F.; Pettibone, D. J.; Clineschmidt, B. V.; Anderson, P. S.; Freidinger, R. M. Orally active, nonpeptide oxytocin antagonists. *J. Med. Chem.* **1992**, *35*, 3919–3927.

(32) Evans, B. E.; Rittle, K. E.; Bock, M. G.; DiPardo, R. M.; Freidinger, R. M.; Whitter, W. L.; Lundell, G. F.; Veber, D. F.; Anderson, P. S.; Chang, R. S. L.; Lotti, V. J.; Cerino, D. J.; Chen, T. B.; Kling, P. J.; Kunkel, K. A.; Springer, J. P.; Hirshfield, J. Methods for drug discovery: development of potent, selective, orally effective cholecystokinin antagonists. *J. Med. Chem.* **1988**, *31*, 2235–2246.

(33) Mirzadegan, T.; Diehl, F.; Ebi, B.; Bhakta, S.; Polsky, I.; McCarley, D.; Mulkins, M.; Weatherhead, G. S.; Lapierre, J.-M.; Dankwardt, J.; Morgans Jr., D.; Wilhelm, R.; Jarnagin, K. Identification of the binding site for a novel class of CCR2b chemokine receptor antagonists: binding to a common chemokine receptor motif within the helical bundle. *J. Biol. Chem.* **2000**, *275*, 25562–25571.

(34) Liu, K. G.; Lo, J. R.; Robichaud, A. J. One-pot synthesis of highly substituted indolines. *Tetrahedron* **2010**, *66*, 573–577.

(35) Copeland, R. A.; Pompliano, D. L.; Meek, T. D. Drug-target residence time and its implications for lead optimization. Nature Reviews Drug Discovery **2006**, 5, 730-739.

(36) Swinney, D. C. Biochemical mechanisms of drug action: what does it take for success? Nature Reviews Drug Discovery **2004**, 3, 801-808.

(37).Swinney, D. C. Biochemical mechanisms of New Molecular Entities (NMEs) approved by United States FDA during 2001-2004: mechanisms leading to optimal efficacy and safety. Current Topics Iin Medicinal Chemistry **2006**, 6, 461-478.

(38) Guo, D.; Hillger, J. M.; IJzerman, A. P.; Heitman, L. H. Drug-target residence time—a case for G protein-coupled receptors. *Med. Res. Rev.* **2014**, *34*, 856–892.

(39) Tautermann, C. S. Impact, determination and prediction of drug–receptor residence times for GPCRs. *Curr. Opin. Pharmacol.* **2016**, *30*, 22–26.

(40) Strasser, A.; Wittmann, H.-J.; Seifert, R. Binding kinetics and pathways of ligands to GPCRs. *Trends Pharmacol. Sci.* **2017**, *38*, 717–732.

(41) Yun, Y.; Chen, J.; Liu, R.; Chen, W.; Liu, C.; Wang, R.; Hou, Z.; Yu, Z.; Sun, Y.; IJzerman A. P.; Heitman, L. H.; Yin, X.; Guo, D. Long residence time adenosine A_1 receptor agonists produce sustained wash-resistant antilipolytic effect in rat adipocytes. *Biochem. Pharmacol.* **2019**, *164*, 45–52.

(42) Bosma, R.; Witt, G.; Vaas, L. A. I.; Josimovic, I.; Gribbon, P.; Vischer, H. F.; Gul, S.; Leurs, R. The target residence time of antihistamines determines their antagonism of the G protein-coupled histamine H1 receptor. *Front. Pharmacol.* **2017**, *8*, 667.

(43) Hothersall, J. D.; Brown, A. J.; Dale, I.; Rawlins, P. Can residence time offer a useful strategy to target agonist drugs for sustained GPCR responses? *Drug Discovery Today* **2016**, *21*, 90–96.

(44) Kapur, S.; Seeman, P. Antipsychotic agents differ in how fast they come off the dopamine D2 receptors. Implications for atypical antipsychotic action. Journal of Psychiatry & Neuroscience : JPN **2000**, 25, 161-166.

(45) Sykes, D. A.; Moore, H.; Stott, L.; Holliday, N.; Javitch, J. A.; Lane, J. R.; Charlton, S. J. Extrapyramidal side effects of antipsychotics are linked to their association kinetics at dopamine D2 receptors. Nature Communications **2017**, 8, 763.

(46) van der Velden, W. J. C.; Heitman, L. H.; Rosenkilde, M. M. Perspective: Implications of Ligand-Receptor Binding Kinetics for Therapeutic Targeting of G Protein-Coupled Receptors. ACS Pharmacology & Translational Science **2020**, 3, 179-189.

(47) Schiele, F.; Ayaz, P.; Fernández-Montalván, A. A universal homogeneous assay for high-throughput determination of binding kinetics. *Anal. Biochem.* **2015**, *468*, 42–49.

(48) Georgi, V.; Andres, D.; Fernández-Montalván, A. E.; Stegmann, C. M.; Becker, A.; Mueller-Fahrnow, A. Binding kinetics in drug discovery – a current perspective. *Front. Biosci., Landmark Ed.* **2017**, *22*, 21–47

(49) Nederpelt, I.; Georgi, V.; Schiele, F.; Nowak-Reppel, K.; Fernández-Montalván, A. E.; IJzerman A. P.; Heitman, L. H. Characterization of 12 GnRH peptide agonists – a kinetic perspective. *Br. J. Pharmacol.* **2016**, *173*, 128–141.

(50) de Witte, W.E.A.; Versfelt, J.W.; Kuzikov, M.; Rolland, S.; Georgi, V.; Gribbon, P.; Gul, S.; Huntjens, D.; van der Graaf, P.H.; Danhof, M.; Fernández-Montalván, A.; Witt, G.; de Lange, E.C.M. In vitro and in silico analysis of the effects of D 2 receptor antagonist target binding kinetics on the cellular response to fluctuating dopamine concentrations. *Br. J. Pharmacol.* **2018**, 175, 4121-4136.

(51) McArdle, C. A.; Davidson, J. S.; Willars, G. B. The tail of the gonadotrophin-releasing hormone receptor: desensitization at, and distal to, G protein-coupled receptors. *Mol. Cell. Endocrinol.* **1999**, *151*, 129–136.

(52) McArdle, C. A.; Franklin, J.; Green, L.; Hislop, J. N. The gonadotrophin-releasing hormone receptor: signalling, cycling and desensitisation. *Arch. Physiol. Biochem.* **2002**, *110*, 113–122.

(53) Willars, G. B.; Heding, A.; Vrecl, M.; Sellar, R.; Blomenröhr, M.; Nahorski, S. R.; Eidne, K. A. Lack of a C-terminal tail in the mammalian gonadotropin-releasing hormone receptor confers resistance to agonist-dependent phosphorylation and rapid desensitization. *J. Biol. Chem.* **1999**, *274*, 30146–30153.

(54) Savoy-Moore, R. T.; Swartz, K. H. Several GnRH stimulation frequencies differentially release FSH and LH from isolated, perfused rat anterior pituitary cells. *Adv. Exp. Med. Biol.* **1987**, *219*, 641–645.

(55) Thompson, I. R.; Ciccone, N. A.; Zhou, Q.; Xu, S.; Khogeer, A.; Carroll, R. S.; Kaiser, U. B. GnRH pulse frequency control of *Fshb* gene expression is mediated via ERK1/2 regulation of ICER. *Mol. Endocrinol.* **2016**, *30*, 348–360.

(56) Struthers, R. S.; Nicholls, A. J.; Grundy, J.; Chen, T.; Jimenez, R.; Yen, S. S.; Bozigian, H. P. Suppression of gonadotropins and estradiol in premenopausal women

by oral administration of the nonpeptide gonadotropin-releasing hormone antagonist elagolix. *The Journal of Clinical Endocrinology and Metabolism* **2009**, 94, 545-551.

(57) Arrowsmith, C. H.; Audia, J. E.; Austin, C.; Baell, J.; Bennett, J.; Blagg, J.; Bountra, C.; Brennan, P. E.; Brown, P. J.; Bunnage, M. E.; Buser-Doepner, C.; Campbell, R. M.; Carter, A. J.; Cohen, P.; Copeland, R. A.; Cravatt, B.; Dahlin, J. L.; Dhanak, D.; Edwards, A. M.; Frederiksen, M.; Frye, S. V.; Gray, N.; Grimshaw, C. E.; Hepworth, D.; Howe, T.; Huber, K. V. M.; Jin, J.; Knapp, S.; Kotz, J. D.; Kruger, R. G.; Lowe, D.; Mader, M. M.; Marsden, B.; Mueller-Fahrnow, A.; Müller, S.; O'Hagan, R. C.; Overington, J. P.; Owen, D. R.; Rosenberg, S. H.; Ross, R.; Roth, B.; Schapira, M.; Schreiber, S. L.; Shoichet, B.; Sundström, M.; Superti-Furga, G.; Taunton, J.; Toledo-Sherman, L.; Walpole, C.; Walters, M. A.; Willson, T. M.; Workman, P.; Young, R. N.; Zuercher, W. J. The promise and peril of chemical probes. *Nat. Chem. Biol.* **2015**, *11*, 536–541.

(58) Structural Genomics Consortium (SCG). https://www.thesgc.org (accessed June 22, 2020). Note: The donated probe set complements the actual SGC probe set. Best

access for donated chemical probes given via the following SGC homepage: https://www.sgc-ffm.uni-frankfurt.de/.

(59) Langer, G. Implementation and use of state-of-the-art, cell-based in vitro assays. *Handb. Exp. Pharmacol.* **2016**, *232*, 171–190.

(60) Degorce, F. HTRF: pioneering technology for high-throughput screening. Expert Opin. Drug Discovery. **2006**, 1, 753–764.

(61) Cheng, Y.-C.; Prusoff, W. H. Relationship between the inhibition constant (K_i) and the concentration of inhibitor which causes 50 per cent inhibition (I_{50}) of an enzymatic reaction. *Biochem. Pharmacol.* **1973**, *22*, 3099–3108.

(62) Motulsky, H. J.; Mahan, L. C. The kinetics of competitive radioligand binding predicted by the law of mass action. *Mol. Pharmacol.* **1984**, *25*, 1–9.

(63) SHELXTL, version 6.14, Bruker AXS Inc., Madison, WI, USA, 2012.

(64) Sheldrick, G. M. Crystal structure refinement with *SHELXL*. *Acta Crystallogr., Sect. C: Struct. Chem.* **2015**, *71*, 3–8.

(65) Parsons, S.; Flack, H. D.; Wagner, T. Use of intensity quotients and differences in absolute structure refinement. *Acta Crystallogr., Sect. B: Struct. Sci., Cryst. Eng. Mater.* **2013**, *69*, 249–259.

(66) Kerns, E. H.; Di, L.; Carter, G. T. In vitro solubility assays in drug discovery. *Curr. Drug Metab.* **2008**, *9*, 879–885.

(67) Onofrey, T.; Kazan, G. Performance and correlation of a 96-well high throughput screening method to determine aqueous drug solubility. Application Note Lit. No. AN1731EN00; Millipore Corporation, Billerica, MA, USA, 2003.

(68) Minick, D. J.; Frenz, J. H.; Patrick, M. A.; Brent, D. A. A comprehensive method for determining hydrophobicity constants by reversed-phase high-performance liquid chromatography. *J. Med. Chem.* **1988**, *31*, 1923–1933.

(69) Pang, K. S.; Rowland, M. Hepatic clearance of drugs. I. Theoretical considerations of a “well-stirred” model and a “parallel tube” model. Influence of hepatic blood flow, plasma and blood cell binding, and the hepatocellular enzymatic activity on hepatic drug clearance. *J. Pharmacokinet. Biopharm.* **1977**, *5*, 625–653.

(70) Schuhmacher, J.; Kohlsdorfer, C.; Bühner, K.; Brandenburger, T.; Kruk, R. High-throughput determination of the free fraction of drugs strongly bound to plasma proteins. *J. Pharm. Sci.* **2004**, *93*, 816–830.

(71) Zhou, Z.; Gong, Q.; Ye, B.; Fan, Z.; Makielski, J. C.; Robertson, G. A.; January, C. T. Properties of HERG channels stably expressed in HEK 293 cells studied at physiological temperature. *Biophys. J.* **1998**, *74*, 230–241.

(72) Hamill, O. P.; Marty, A.; Neher, E.; Sakmann, B.; Sigworth, F. J. Improved patch-clamp techniques for high-resolution current recording from cells and cell-free membrane patches. *Pfluegers Arch.* **1981**, *391*, 85–100.

(73) Himmel, H. M. Suitability of commonly used excipients for electrophysiological *in-vitro* safety pharmacology assessment of effects on hERG potassium current and on rabbit Purkinje fiber action potential. *J. Pharmacol. Toxicol. Methods* **2007**, *56*, 145–158.

(74) Niswender, G. D.; Spies, H. G. Serum levels of luteinizing hormone, follicle-stimulating hormone and progesterone throughout the menstrual cycle of rhesus monkeys. *J. Clin. Endocrinol. Metab.* **1973**, *37*, 326–328.

Table 1. Overview of the Most Advanced SMOL hGnRH-R Antagonists[a]

Company	Takeda/Myovant Sciences	AbbVie/[Neurocrine Biosciences]	ObsEva/Kissei Pharmaceutical	Astellas Pharma
	Relugolix[20]	Elagolix[22]	Linzagolix[25]	Opigolix
	[TAK-385]	[NBI-56418 Na]	[OBE-2109]	[ASP-1707]
Structure	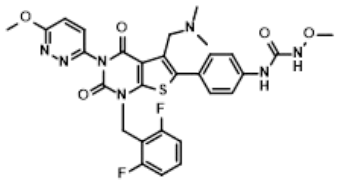	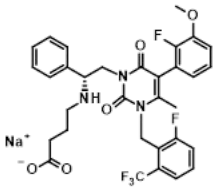	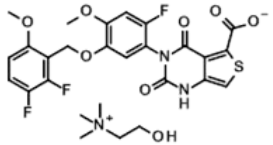	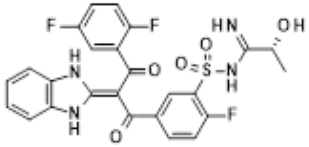
Active Indications	Uterine Fibroids	Uterine Fibroids	Uterine Fibroids	–/–
	Endometriosis	Endometriosis	Endometriosis	
		PCOS		
Development Status				
Uterine Fibroids	**Approved**: 01/2019 (JPN)	**Phase III**	**Phase III**	**Discontinued**
Endometriosis	**Phase III** (Myovant	**Approved**: 07/2018 (US)	**Phase III**	
PCOS		**Phase II**		
Chronic Use				
Uterine Fibroids	40 mg q.d./ABT	300 mg b.i.d./ABT	100 mg q.d.	
			200 mg q.d./ABT	
Endometriosis	40 mg q.d./ABT	150 mg q.d.		
		200 mg b.i.d./ABT		
MW [g/mol]	624	632 (parent)	508 (parent)	545
IC_{50} rat [nM]	9800	4400 (K_i)	Not Available	Not Available

[a]ABT = estrogen add-back therapy required.

Table 2. Potencies of Screening Hit 15, Improved Compound 1a, and Spiro[piperidine-indoline] Lead 2b

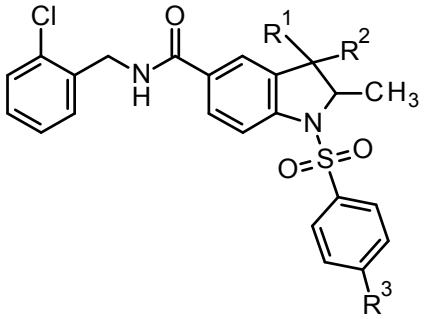

Compd	R^1	R^2	R^3	IC_{50} hGnRH-R[b]				IC_{50} rGnRH-R[b]			
				LHRH[c]		Buserelin[c]		LHRH[c]		Buserelin[c]	
				[nM]	SD [nM]	[nM]	SD [nM]	[nM]	SD [nM]	[nM]	SD [nM]
rac-**15**[a]	Me	Me	H	3059	473	1413	473	n.d.[d]	n.d.[d]	4843	455
rac-**1**	Me	Me	OMe	365	28	6616	8550	1419	319	4867	238
ent-**1a**[a]	Me	Me	OMe	568	237	1530	1263	726	246	1110	213
ent-**1b**	Me	Me	OMe	≥20E3	n.a.[e]	≥20E3	n.a.[e]	≥20E3	n.a.[e]	≥20E3	n.a.[e]

rac-**2**	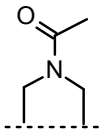	OMe	154	58	306	26	72	n.a.[e]	n.d.[d]	n.d.[d]
ent-**2a**	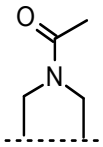	OMe	≥20E3	n.a.[e]	≥20E3	n.a.[e]	≥20E3	n.a.[e]	n.d.[d]	n.d.[d]
ent-**2b**	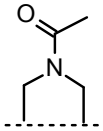	OMe	41	14	99	37	29	13	34	6.0

[a]"*rac*-" = Racemic mixture; "*ent*-" ≥ 97% enantiomerically pure by HPLC. [b]Values represent averages of at least two independent experiments done in duplicates, unless noted otherwise. [c]Agonists used to determine GnRH-R antagonist potencies: LHRH, the physiological agonist, was used in early SAR studies with less potent compounds, with a shift to buserelin, a stronger (synthetic) agonist, once more potent antagonists were available in advanced program phases to allow for a more precise characterization of compound potencies. For completeness, data for both agonists are given whenever possible. [d]Not determined. [e]Not applicable.

Table 3. SAR Investigation of the Substituent at C-2 of the Spiro[piperidine-indoline] Core

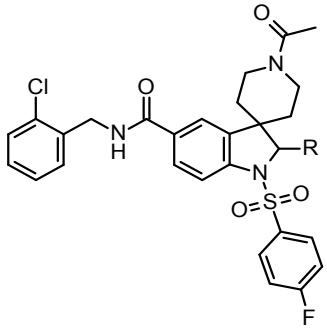

Compd	R	IC_{50} hGnRH-R[b]			
		LHRH[c]		Buserelin[c]	
		[nM]	SD [nM]	[nM]	SD [nM]
rac-**16**[a]	Me	87	54	90	10
ent-**16a**[a]	Me	>20000	n.a.[d]	>20000	n.a.[d]
ent-**16b**	Me	21	4.7	n.d.[e]	n.d.[e]
rac-**17**	H	420	322.5	1768	1943
rac-**18**	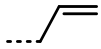	10	2.2	22	6.2
rac-**19**	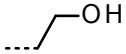	584	110	1151	310
rac-**20**		24	5.5	47	5.4

[a]"*rac*-" = Racemic mixture; "*ent*-" ≥ 97% enantiomerically pure by HPLC. [b]Values represent averages of at least two independent experiments done in duplicates, unless noted otherwise. [c]Agonists used to determine GnRH-R antagonist potencies: LHRH, the physiological agonist, was used in early SAR studies with less potent compounds, with a shift to buserelin, a stronger (synthetic) agonist, once more potent antagonists were available in advanced program phases to allow for a more precise characterization of

compound potencies. For completeness, data for both agonists are given whenever possible. [d]Not applicable. [e]Not determined.

Table 4. SAR Investigation of the Substituent at N-1 of the Spiro[piperidine-indoline] Core

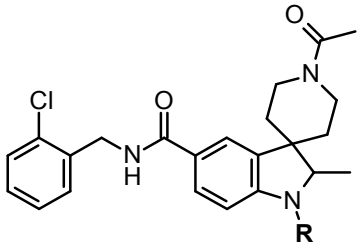

Compd	R	IC_{50} hGnRH-R[b]			
		LHRH[c]		Buserelin[c]	
		[nM]	SD [nM]	[nM]	SD [nM]
rac-**16**[a]	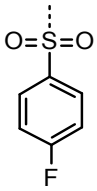	87	54	90	10
rac-**21**	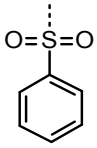	53	20	131	37
rac-**22**		10093	6346	18144	1997
rac-**23**	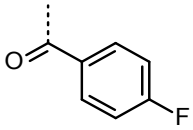	17975	2863	>20000	n.a.[d]
rac-**24**	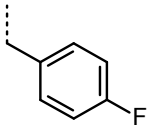	12782	6317	18241	3114

rac-**25**	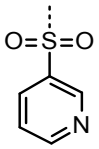	139	44	269	98
rac-**26**	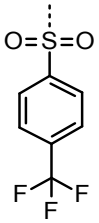	>20000	n.a.[d]	13802	8779

[a]"*rac*-" = Racemic mixture. [b]Values represent averages of at least two independent experiments done in duplicates, unless noted otherwise. [c]Agonists used to determine GnRH-R antagonist potencies: LHRH, the physiological agonist, was used in early SAR studies with less potent compounds, with a shift to buserelin, a stronger (synthetic) agonist, once more potent antagonists were available in advanced program phases to allow for a more precise characterization of compound potencies. For completeness, data for both agonists are given whenever possible. [d]Not applicable.

Table 5. SAR Investigation of the Substituent at C-5 of the Spiro[piperidine-indoline] Core

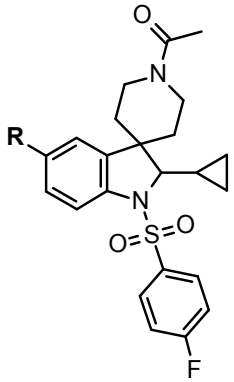

Compd	R	IC_{50} hGnRH-R[b]			
		LHRH[c]		Buserelin[c]	
		[nM]	SD [nM]	[nM]	SD [nM]
rac-20[a]	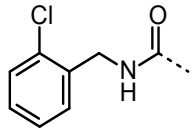	24	5.5	47	5.4
rac-27	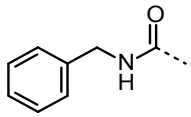	208	86	553	196
rac-28	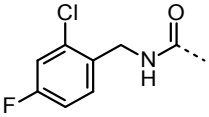	38	9.2	77	18
rac-29	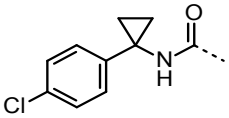	56	20	92	20
rac-30	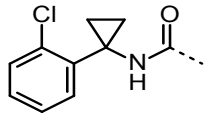	161.5	33	1047	1082
rac-31	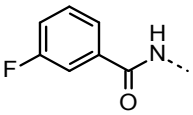	10	1.5	18	2.7

rac-**32**	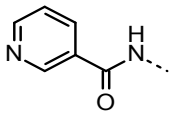	34	4.2	68	9.8

[a]"*rac*-" = Racemic mixture. [b]Values represent averages of at least two independent experiments done in duplicates, unless noted otherwise. [c]Agonists used to determine GnRH-R antagonist potencies: LHRH, the physiological agonist, was used in early SAR studies with less potent compounds, with a shift to buserelin, a stronger (synthetic) agonist, once more potent antagonists were available in advanced program phases to allow for a more precise characterization of compound potencies. For completeness, data for both agonists are given whenever possible.

Table 6. Potencies and Pharmacokinetic Profiles of Lead Compound 2b and First In Vivo Compound 3a

Compd	Structure	IC_{50} hGnRH-R[b]				IC_{50} rGnRH-R[b]		PK in vitro[d]	PK in vivo[e]	
		LHRH[c]		Buserelin[c]		LHRH[c]				
		[nM]	SD [nM]	[nM]	SD [nM]	[nM]	SD [nM]	CL_{blood} [L/h/kg]	CL_{blood} [L/h/kg]	$t_{1/2}$ [h]
ent-**2b**[a]	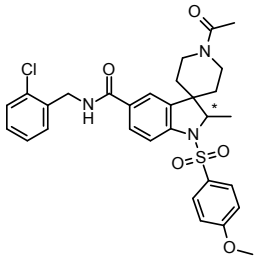	41	14	99	37	29	13	2.8	4.7	0.82
ent-**3a**	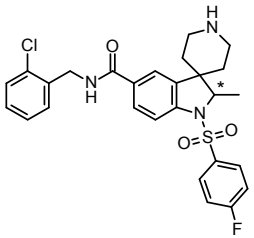	99	41	172	37	27	1.3	2	1.4	8.1

[a]"*ent*-" ≥ 93% Enantiomerically pure by HPLC. [b]Values represent averages of at least two independent experiments done in duplicates, unless noted otherwise. [c]Agonists used to determine GnRH-R antagonist potencies: LHRH, the physiological agonist, was used in early SAR studies with less potent compounds, with a shift to buserelin, a stronger

(synthetic) agonist, once more potent antagonists were available in advanced program phases to allow for a more precise characterization of compound potencies. For completeness, data for both agonists are given whenever possible. [d]In rat hepatocytes. [e]In rats at 0.5 mg/kg, iv (female Wistar)

Table 7. Potencies and Pharmacokinetic Profile of Benzylic Amide 20b vs Pyridylmethyl Amide 33a

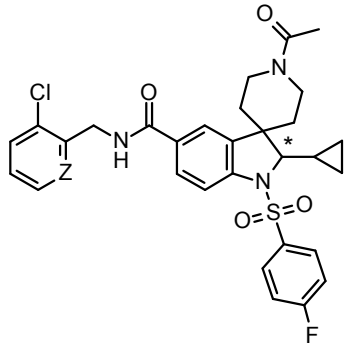

Compd	Z	IC_{50} hGnRH-R[b]				PK in vitro[d]	PK in vivo[e]	
		LHRH[c]		Buserelin[c]				
		[nM]	SD [nM]	[nM]	SD [nM]	CL_{blood} [L/h/kg]	CL_{blood} [L/h/kg]	*F* [%]
ent-**20b**[a]	CH	15	7	28	14	1.2	1.9	1.3
ent-**33a**	N	53.5	15	35	13	0.7	1.7	18

[a]"*ent*-" ≥ 96% Enantiomerically pure by HPLC. [b]Values represent averages of at least two independent experiments done in duplicates, unless noted otherwise. [c]Agonists used to determine GnRH-R antagonist potencies: LHRH, the physiological agonist, was used in early SAR studies with less potent compounds, with a shift to buserelin, a stronger (synthetic) agonist, once more potent antagonists were available in advanced program phases to allow for a more precise characterization of compound potencies. For completeness, data for both agonists are given whenever possible. [d]In human hepatocytes. [e]In rats at 0.5 mg/kg, iv (female Wistar).

Table 8. SAR Investigation at C-3 of the Spiroindoline Core (Variation of Z)

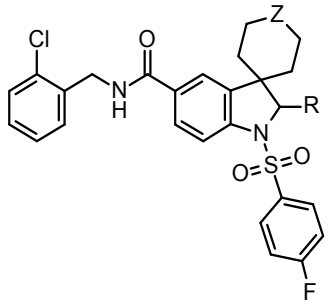

Compd	Z	R	IC_{50} hGnRH-R[b]			
			LHRH[c]		Buserelin[c]	
			[nM]	SD [nM]	[nM]	SD [nM]
rac-**20**[a]			24	5.5	47	5.4
dia-**34a**[a]	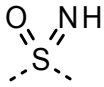		32	8.1	58.5	17
dia-**34b**	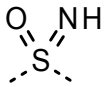		13	3.4	26	4.1
dia-**35**			18	8.2	36	12
rac-**36**			20	6.2	45	5.8
dia-**37**	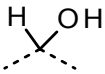		26	3.7	61	11.5
dia-**38**	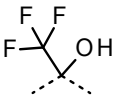		78	20	228	140
rac-**39**			48	12	132	48

rac-**40**		CH_3	53	19	140	42.5

[a]"*rac*-" = Racemic mixture; "*dia*-" = diastereomeric mixture. [b]Values represent averages of at least two independent experiments done in duplicates, unless noted otherwise. [c]Agonists used to determine GnRH-R antagonist potencies: LHRH, the physiological agonist, was used in early SAR studies with less potent compounds, with a shift to buserelin, a stronger (synthetic) agonist, once more potent antagonists were available in advanced program phases to allow for a more precise characterization of compound potencies. For completeness, data for both agonists are given whenever possible.

Table 9. Potencies and Pharmacokinetic Profile of In Vivo Compound 4a Suited for po Administration

Compd	Structure	IC_{50} hGnRH-R[b]				IC_{50} rGnRH-R[b]		PK in vitro[d]	PK in vivo[e]		
		LHRH[c]		Buserelin[c]		LHRH[c]					
		[nM]	SD [nM]	[nM]	SD [nM]	[nM]	SD [nM]	CL_{blood} [L/h/kg]	CL_{blood} [L/h/kg]	$t_{1/2}$ [h]	*F* [%][f]
ent-**4a**[a]	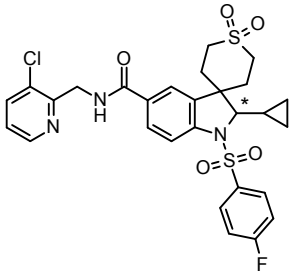	60	9.3	104	24	40	n.a.	0.25	1.8	2.1	27

[a]"*ent*-" 99% Enantiomerically pure by HPLC. [b]Values represent averages of at least two independent experiments done in duplicates, unless noted otherwise. [c]Agonists used to determine GnRH-R antagonist potencies: LHRH, the physiological agonist, was used in early SAR studies with less potent compounds, with a shift to buserelin, a stronger (synthetic) agonist, once more potent antagonists were available in advanced program phases to allow for a more precise characterization of compound potencies. For completeness, data for both agonists are given whenever possible. [d]In rat hepatocytes. [e]In rats at 0.5 mg/kg (iv) and 2.0 mg/kg (po) (male Wistar). [f]Dependent on dose and formulation vehicle (vehicle at 2.0 mg/kg: PEG400/H_2O/EtOH, 60:30:10).

Table 10. Fine-tuning of the Pyridylmethyl Amide

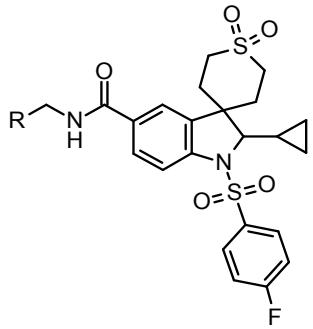

Compd	R	IC_{50} hGnRH-R[b]			
		LHRH[c]		Buserelin[c]	
		[nM]	SD [nM]	[nM]	SD [nM]
rac-**5**[a]	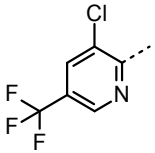	20	3	44	9.9
ent-**5a**[a] (BAY 1214784)	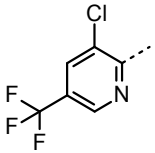	n.d.[d]	n.d.[d]	21	5.3

ent-**5b**	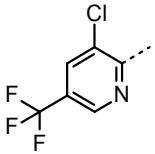	n.d.[d]	n.d.[d]	2432	2458
rac-**4**	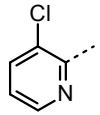	90	34	222	67
rac-**41**	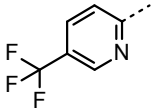	159	14	415	66
rac-**42**	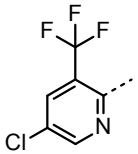	16	3	54	31
rac-**43**	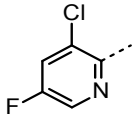	65	20.5	144	34
rac-**44**	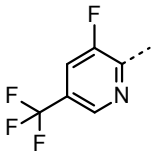	84	15	246	124
rac-**45**	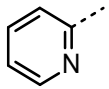	245	42	921	421

[a]"*rac*-" = Racemic mixture; "*ent*-" ≥ 99% enantiomerically pure by HPLC. [b]Values represent averages of at least two independent experiments done in duplicates, unless noted otherwise. [c]Agonists used to determine GnRH-R antagonist potencies: LHRH, the physiological agonist, was used in early SAR studies with less potent compounds, with a shift to

buserelin, a stronger (synthetic) agonist, once more potent antagonists were available in advanced program phases to allow for a more precise characterization of compound potencies. For completeness, data for both agonists are given whenever possible. [a]Not determined.

Table 11. Drug–Target Residence Time of 5a in Comparison to Known hGnRH-R Antagonists

Compd	RT[a] [min]		k_{on} [$M^{-1}s^{-1}$]		k_{off} [s^{-1}]		k_{off} calcd [s^{-1}]		K_d kinetic [M]		K_d equil.[b] [M]	
	Mean	SD	Mean	SD	Mean	SD	Mean	SD	Mean	SD	Mean	SD
5a	7	0	4.20×10^{5}	1.56×10^{4}	4.13×10^{-3}	3.34×10^{-3}	2.32×10^{-3}	1.41×10^{-5}	9.83×10^{-9}	8.03×10^{-9}	5.52×10^{-9}	1.70×10^{-10}
Cetrorelix	35	n.d.[c]	3.57×10^{6}	n.d.[c]	1.00×10^{-5}	n.d.[c]	4.80×10^{-4}	n.d.[c]	1.70×10^{-12}	n.d.[c]	1.35×10^{-10}	n.d.[c]
Relugolix	38	n.d.[c]	5.28×10^{5}	n.d.[c]	1.90×10^{-4}	n.d.[c]	4.40×10^{-4}	n.d.[c]	3.72×10^{-10}	n.d.[c]	8.40×10^{-10}	n.d.[c]
Elagolix	76	1.4	2.06×10^{5}	9.19×10^{4}	3.30×10^{-4}	3.68×10^{-4}	2.20×10^{-4}	0	3.21×10^{-9}	1.34×10^{-9}	1.19×10^{-9}	5.52×10^{-10}

[a]Drug–target residence time. [b]Equilibrium. [c]Not determined.

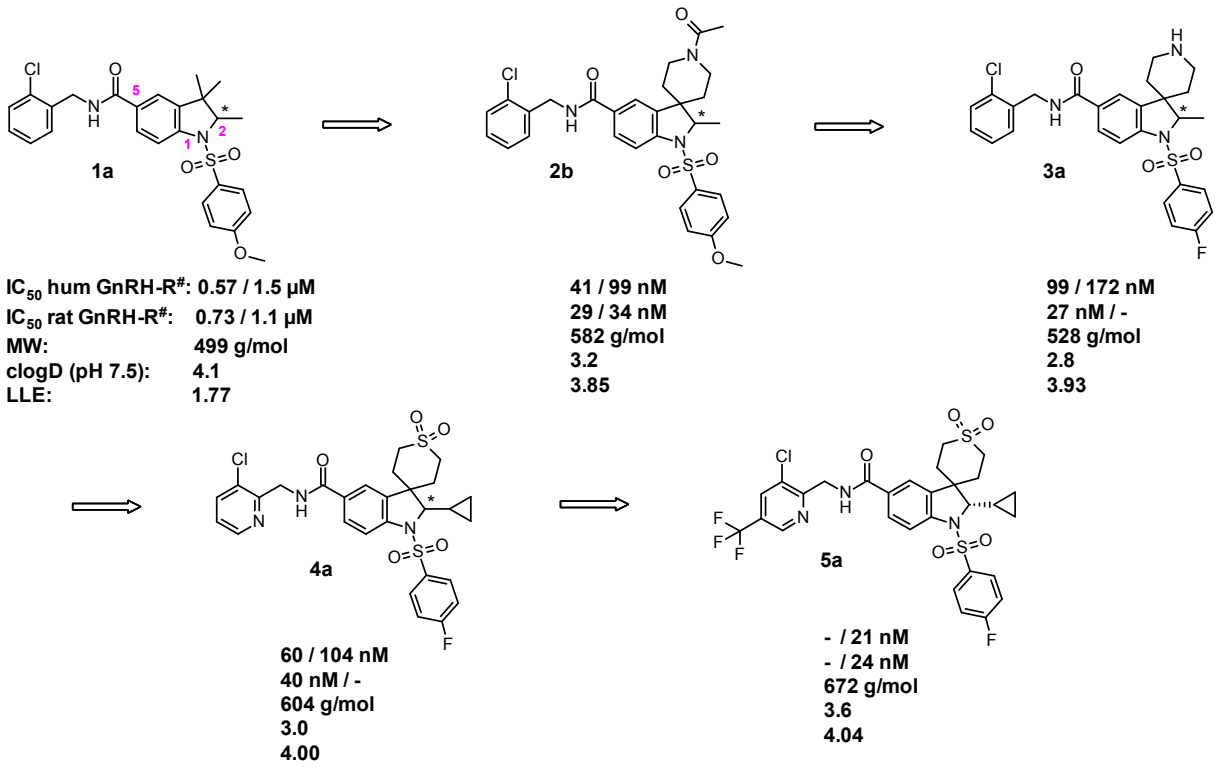

Figure 1. Overview of key compounds synthesized in the course of the hit-to-lead and lead optimization process. Replacing the geminal dimethyl unit in improved hit compound **1a** by a spiropiperidine moiety in **2b** increased antagonist potency at the human GnRH receptor roughly 15-fold (buserelin assay data) and lipophilic ligand efficiency [LLE = p(IC_{50} human) – clogD] by approximately 2 log units. Exchanging the aromatic methyl ether by fluorine and removing the *N*-acetyl moiety resulted in **3a**, the first compound suitable for in vivo experiments. The introduction of (a) a pyridylmethyl amide in combination with (b) switching to a sulfonyl spirocycle and (c) the incorporation

of a cyclopropyl moiety at the stereocenter in **4a** further improved DMPK, selectivity, and potency properties and gave rise to the first compound to be dosed orally in vivo. Final lead optimization efforts aimed at improving oral bioavailability, potency, and CYP interaction profile by fine-tuning of the pyrimidylmethyl amide moiety led to the nomination of **5a** (BAY 1214784) as clinical candidate. # LHRH / buserelin assay data.

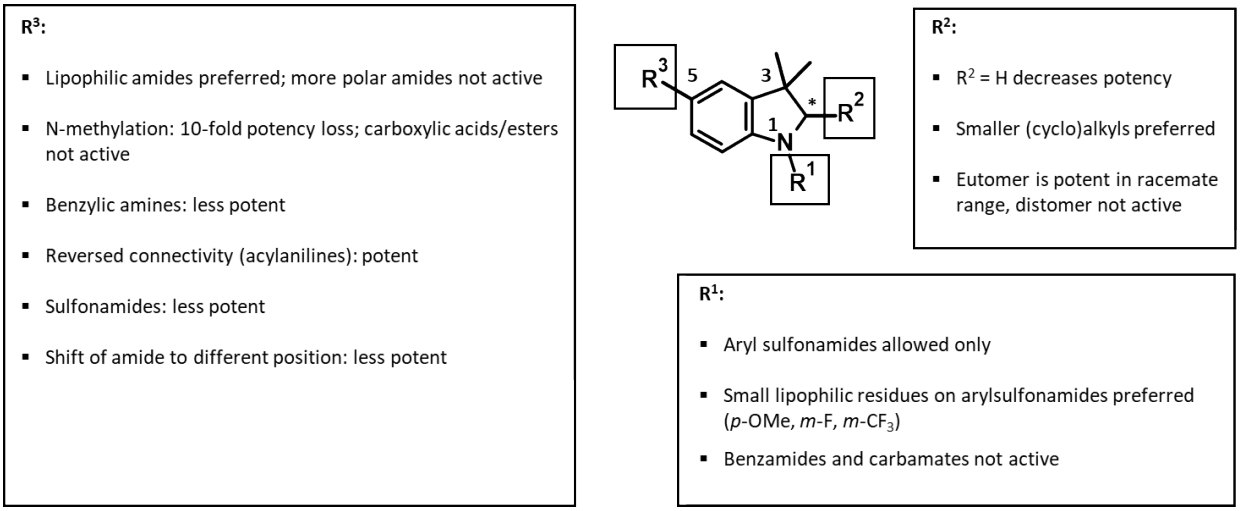

Figure 2. Short qualitative summary of the results obtained from early SAR explorations by variation of R^1, R^2, and R^3 at the indoline core. For residue R^1, only aryl sulfonamides were allowed in terms of potency though this structural element had a negative impact on the Caco-2 permeation and solubility profile of the compounds. A methyl substituent was mandatory for R^2 as the corresponding C-2 unsubstituted

derivatives were much less potent. The stereochemistry at this position had an influence on the potency as well, with the eutomers being potent in the range of the racemic mixtures and the distomers showing only residual activities. Carboxamides bearing lipophilic benzylic residues were preferred for R^3, while the corresponding carboxylic acids, esters, or more polar amides were not potent.

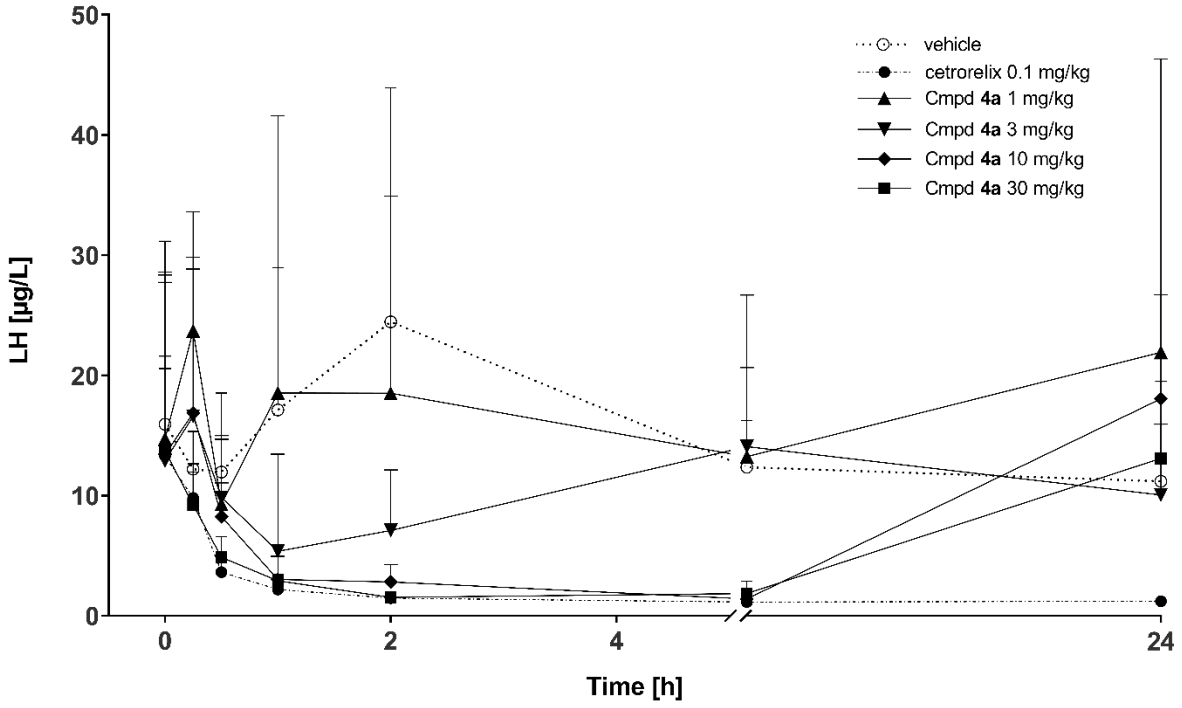

Figure 3. Reversible suppression of plasma LH levels in OVX rats following treatment with **4a**. Blood samples were collected at 0, 20, 40, and 60 min, and at 2, 6, and 24 h. Values represent means ±SEM. Significant lowering of plasma LH levels was found in animals treated with either **4a** at doses ≥10 mg/kg (po) or with the control GnRH antagonist cetrorelix (0.1 mg/kg, sc), the latter exhibiting the typical long-lasting effect expected for a peptidic antagonist (see 20 h values).

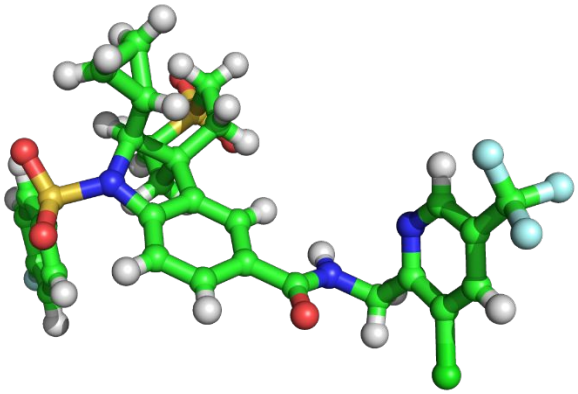

Figure 4. X-ray analysis of compound **5a** established the *S*-configuration for the eutomer.

Pharmacological In Vitro Properties	
hGnRH-R Antagonism, IC_{50}	21 nM[a]
rGnRH-R Antagonism, IC_{50}	24 nM[a]
cGnRH-R Antagonism, IC_{50}	35 nM[a]
hGnRH-R Binding	27 nM
Residence Time [min]	7
k_{on} [$M^{-1}s^{-1}$]	4.20×10^5
k_{off} [s^{-1}]	4.13×10^{-3}
h Fraction Unbound [%]	1.4
Functional GPCR Off-target profile	clean[b]
Off-target Profile (Ricerca)	3 hits[b,c]

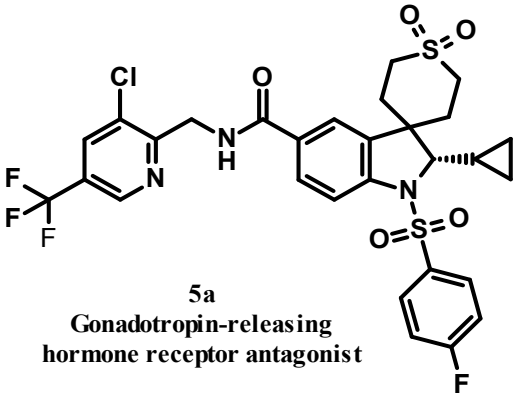

5a
Gonadotropin-releasing hormone receptor antagonist

Safety Properties	
hERG [μM]	>10 μM

Physicochemical Properties	
MW [g/mol]	672
TPSA [$Å^2$]	114
LogD @ pH 7.5	4.1
Solub. at pH 6.5 [mg/L]	7.1
Chemical Stability, pH	stable

In Vitro DMPK Properties						
Caco-2 Permeability		P_{app} A–B [nm/s]	P_{app} B–A [nm/s]		Efflux Ratio	
		13	129		10	
Metabolic Stability			CL [L/h/kg]		F_{max} [%][d]	
		Liver Microsomes (h/r/d/c)	1×10^{-4}/0.38/0.32/0.49		100/91/85/81	
		Hepatocytes (h/r/d/c)[e]	0.1/0.75/0.73/0.71		93/82/65/72	
CYP Inhibition [μM]	1A2	2C8	2C9	2D6	3A4	3A4 preinc.
	>10	1.0	>10	>10	>10	>10
CYP Induction NOEL [μg/L][f]	5000	n.d.[g]	n.d.[g]	n.d.[g]	1667	n.a.[h]
In Vivo PK Properties[i]						
CL_{blood} [L/h/kg]			$t_{1/2}$ [h]		F [%]	
0.54			16		48	

Figure 5. Summary of *in vitro* and selected *in vivo* pharmacological, physicochemical, safety, and DMPK properties of **5a**. [a]Buserelin assay data. [b]See the Supporting Information Tables S1, S2, and S5 for full details. [c]CB1: IC_{50} = 3.4 μM, MAPK3: IC_{50} =

4.9 μM, MAPK14: IC_{50} = 10.7 μM. [d]Calculated maximal oral bioavailability, F_{max} = 1 − (blood clearance divided by species-specific liver blood flow). [e]h = human, r = rat, d = dog, c = cynomolgus monkey. [f]No observed effect level. [g]Not determined. [h]Not applicable. [i]In rats at 0.5 mg/kg, iv (male Wistar; vehicle: PEG400/H_2O/EtOH, 60:30:10).

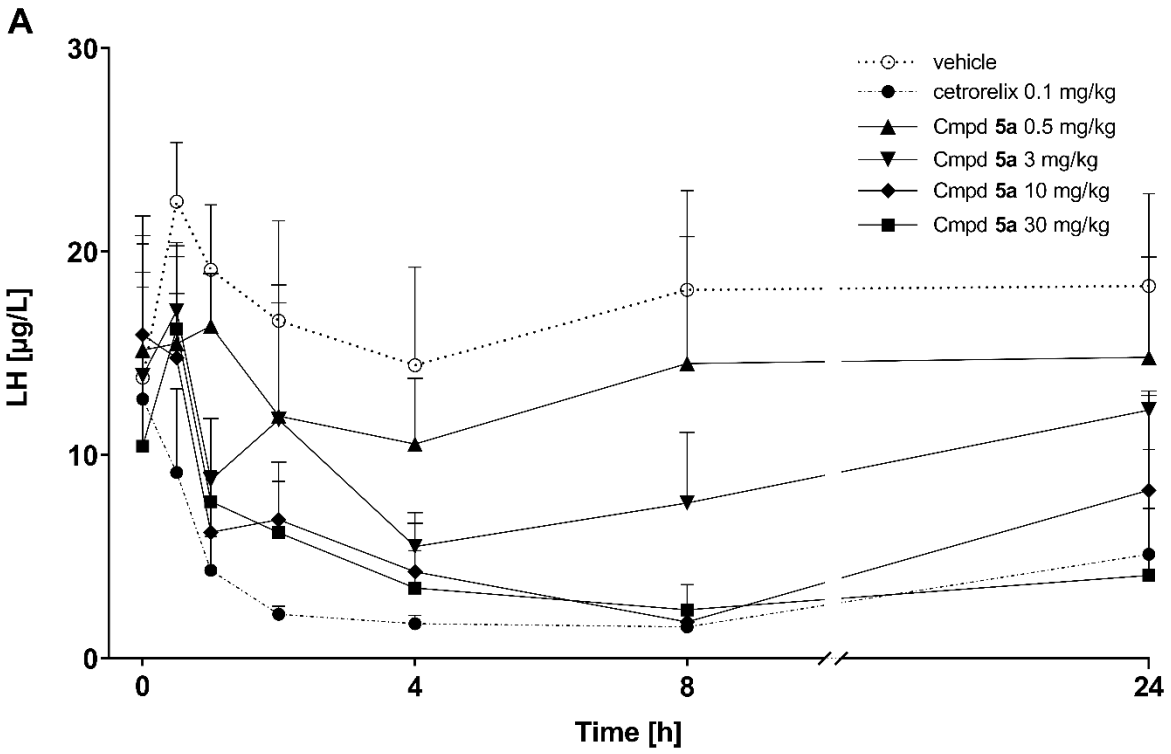
A
LH [µg/L]
30
20
10
0
0
4
8
24
Time [h]
vehicle
cetrorelix 0.1 mg/kg
Cmpd 5a 0.5 mg/kg
Cmpd 5a 3 mg/kg
Cmpd 5a 10 mg/kg
Cmpd 5a 30 mg/kg

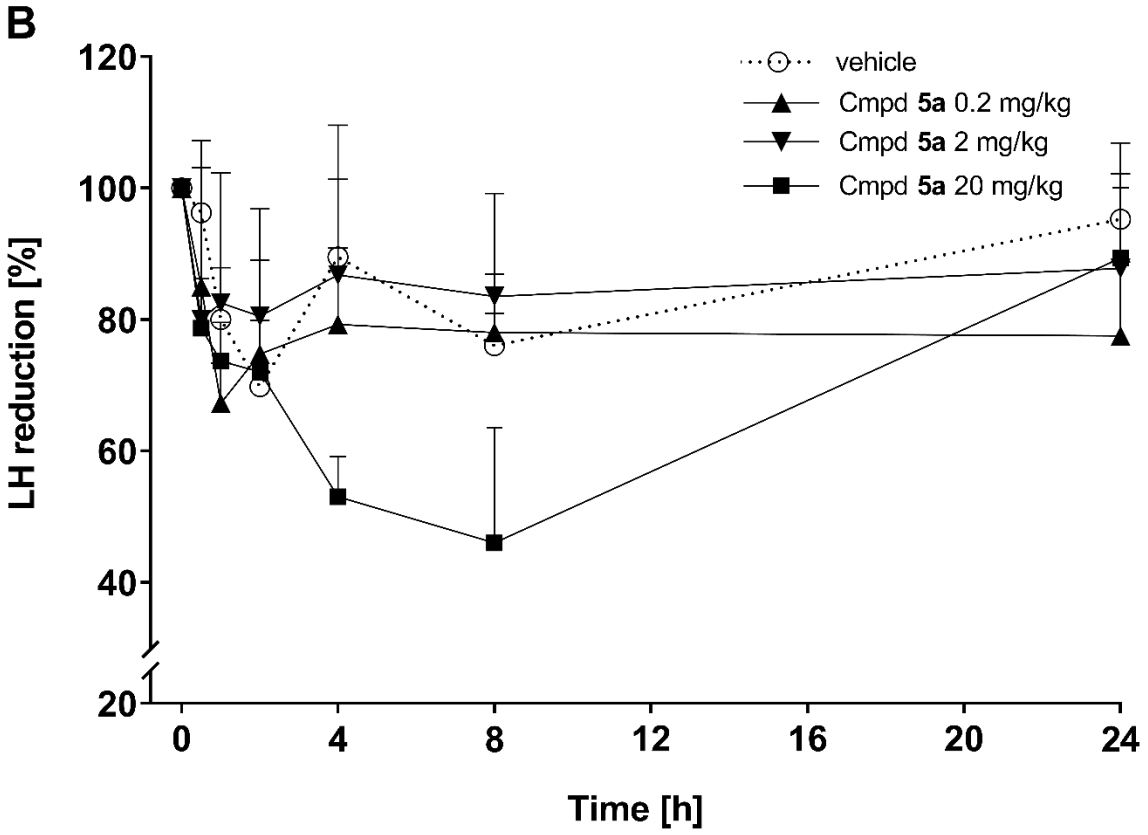

Figure 6. Suppression of plasma LH levels in OVX rats (A) and ORX cynomolgus monkeys (B) following treatment with **5a**. (A) Blood samples were collected at 0, 0.5, 1, 2, 4, 8, and 24 h. Values represent means ±SEM. Significant lowering of plasma LH levels was found in animals treated with either **5a** at doses ≥3 mg/kg (po) or with the control GnRH antagonist cetrorelix (0.1 mg/kg, sc). (B) Again, blood samples were collected at 0, 0.5, 1, 2, 4, 8, and 24 h. Values represent means ±SEM. Significant lowering of plasma LH levels was found in animals treated with **5a** at doses ≥20 mg/kg.

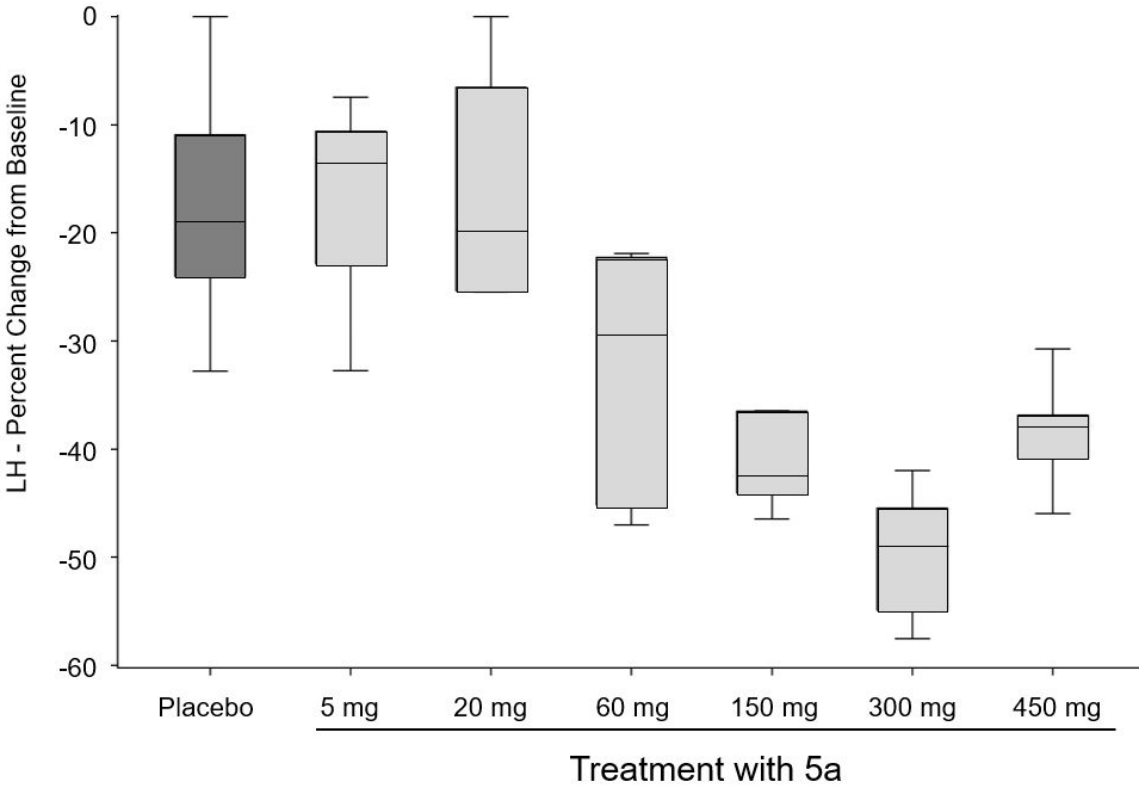

Figure 7. Maximum reduction of LH levels obtained in a first-in-human study with **5a** in postmenopausal women (n = 6 per dose group, single oral doses). Boxes represent the 25th to 75th percentile with the horizontal line indicating the median of the results. Vertical lines extend from the boxes as far as the data extends, including outliers. Suppression of plasma LH levels reached a maximum of about 49% reduction at the 300 mg dose.

Scheme 1. Synthesis of Screening Hit 15 and Improved Compound 1a[a]

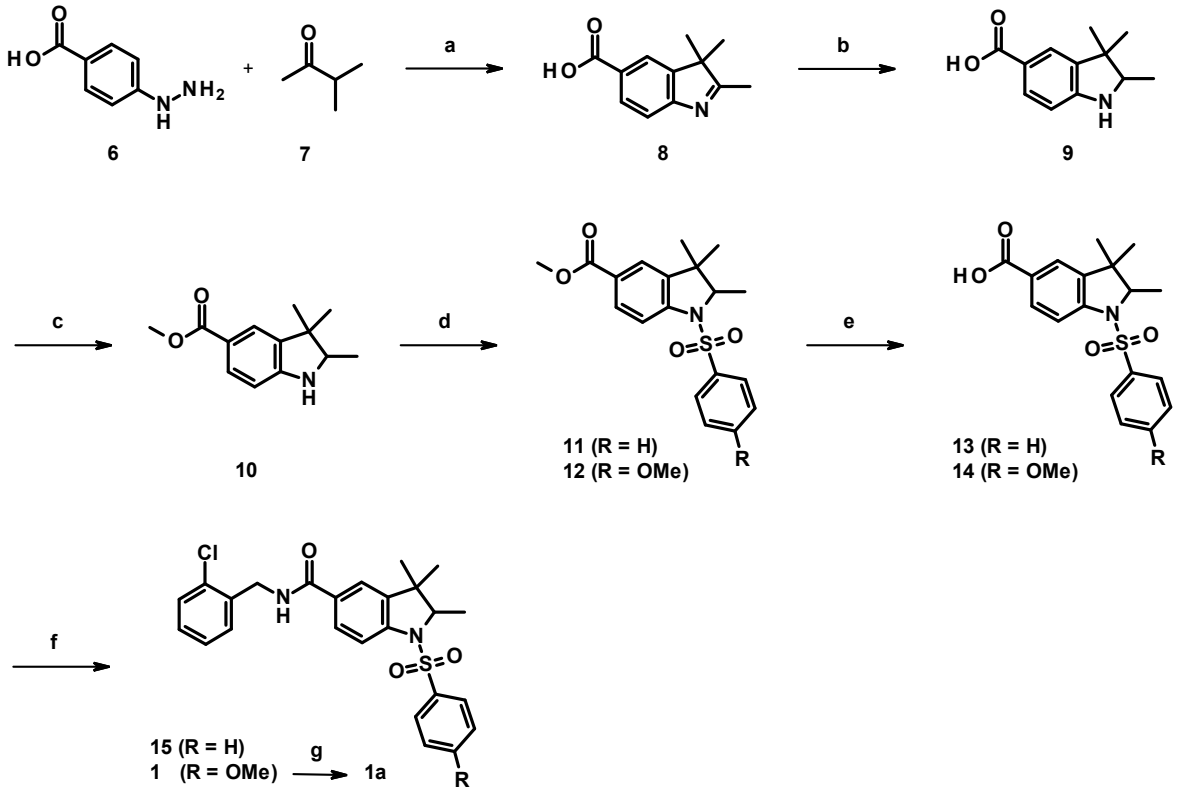

[a]Reagents and conditions: (a) concd HCl, HOAc, reflux; (b) $NaBH_4$, MeOH, 0 °C; (c) $SOCl_2$, MeOH, 0 °C to reflux, 11% (3 steps); (d) **11**: benzenesulfonyl chloride, DIPEA, DCM, rt, 56%; **12**: 4-methoxybenzenesulfonyl chloride, DIPEA, DMAP, DCE, rt to reflux, 28%; (e) 2 M aq LiOH, MeOH/THF, rt; **13**: 21%, **14**: 88%; (f) 1-(2-chlorophenyl)methanamine, HATU, Et_3N, DMF, rt, **15**: 18%; (g) chiral HPLC, **1a**: 42% (from **14**).

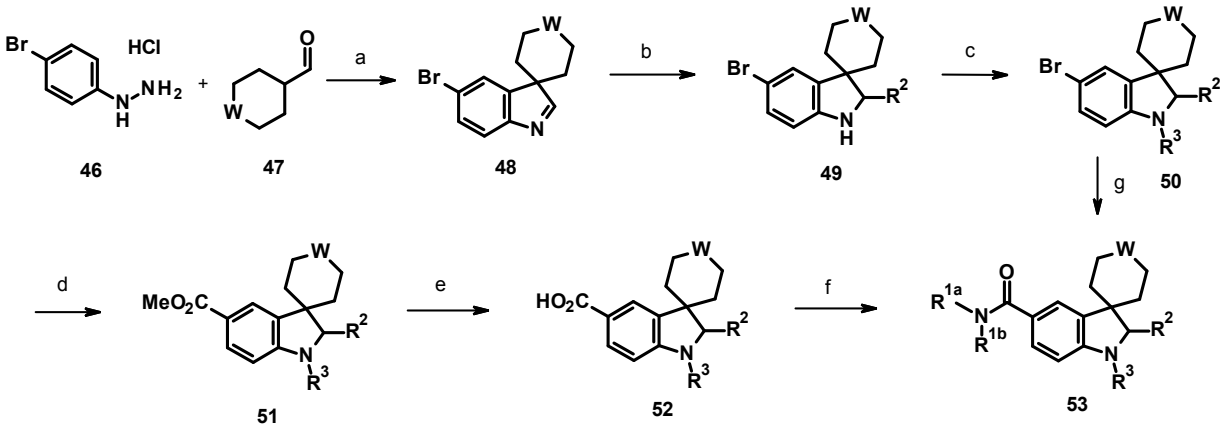

Scheme 2. General Synthetic Access to Spiroindolines[a]

[a]Reagents and conditions: (a) TFA, $CHCl_3$, 0 °C to 50 °C or concd HCl, HOAc, rt to 100 °C; (b) R^2 = H: $NaBH_4$, MeOH, rt or R^2 ≠ H: R^2MgX, $BF_3{\cdot}OEt_2$, THF, 0 °C to rt; (c) R^3Cl, Et_3N, DCE, rt to 80 °C or R^3Cl, pyridine, rt; (d) CO (9 bar), $PdCl_2(PPh_3)_2$, Et_3N, MeOH/DMSO, 100 °C; (e) LiOH, THF/H_2O, rt; (f) $(R^{1a})(R^{1b})NH$, HATU, Et_3N, DMF, rt or HATU, Et_3N, DMF, rt and then $(R^{1a})(R^{1b})NH$, NMP, MeCN, 55–80 °C; (g) $(R^{1a})(R^{1b})NH$, $Mo(CO)_6$, $Pd(OAc)_2$, $(t\text{-Bu})_3PH^+BF_4^-$, Na_2CO_3, 1,4-dioxane, 120–140 °C. W = N-Ac, N-Cbz, S, S(O), $S(O)_2$, O.

Scheme 3. Synthesis of Clinical Candidate 5a[a]

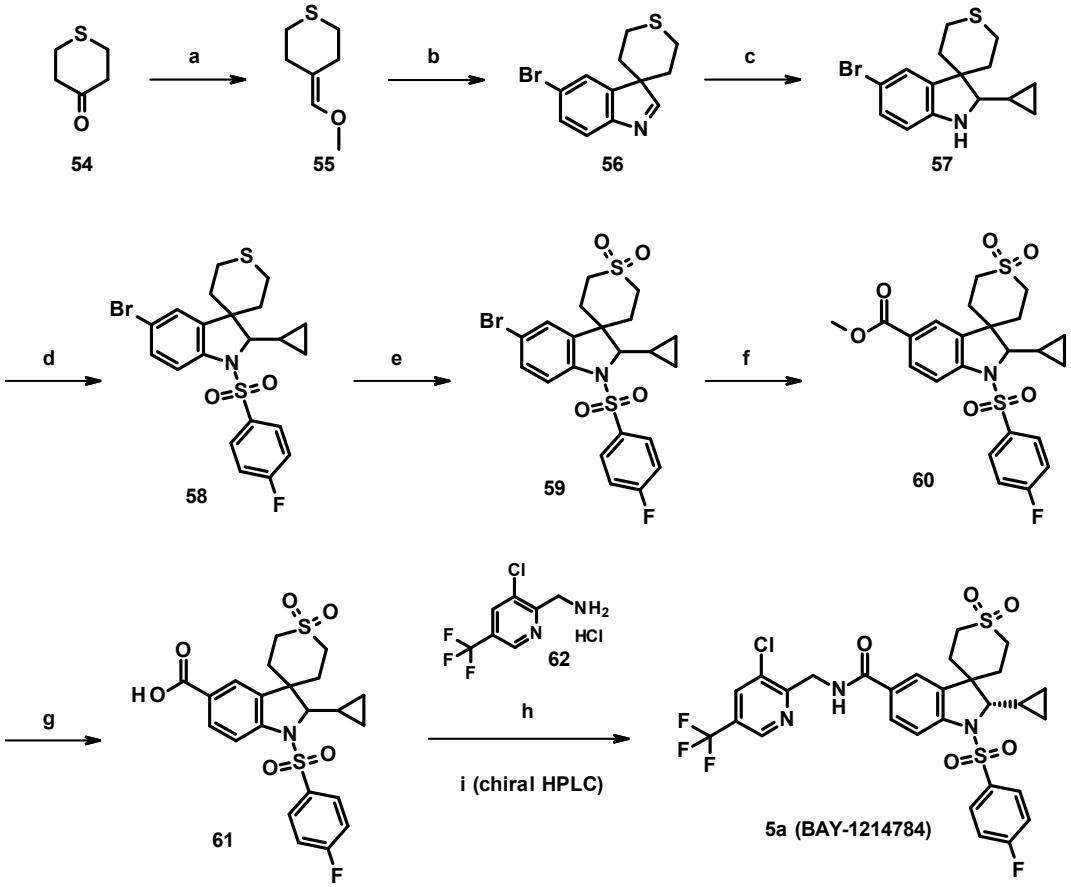

[a]Reagents and conditions: (a) $MeOCH_2PPh_3^+Cl^-$, LDA, THF, –50 °C to rt, 50%; (b) 4-bromophenylhydrazine hydrochloride, TFA, $CHCl_3$, 0 °C to 50 °C; (c) cyclopropylmagnesium bromide, $BF_3{\cdot}OEt_2$, THF, 0 °C, 25% (2 steps); (d) 4-fluorobenzenesulfonyl chloride, pyridine, rt, ca. 95%; (e) urea hydrogen peroxide, TFAA, MeCN, 0 °C to rt; (f) CO (10 bar), $PdCl_2(PPh_3)_2$, Et_3N, MeOH/DMSO, 100 °C, 83% (2 steps); (g) 2 M aq LiOH, THF, rt, ca. 77%; (h) **62**, HATU, Et_3N, DMF, rt, 55%; (i) chiral HPLC.

Table of Contents graphic

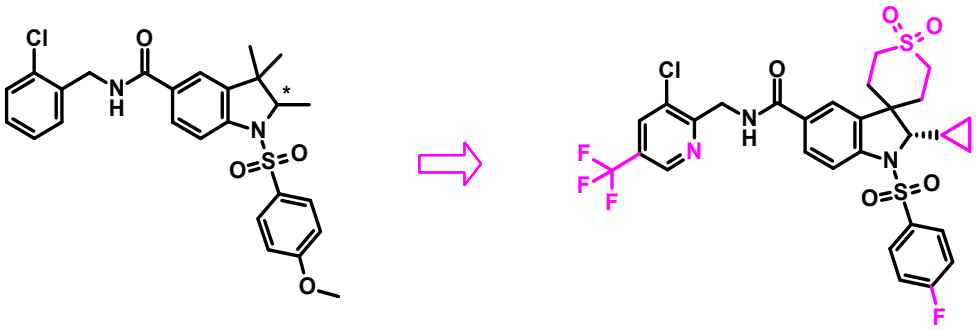

	Improved Hit (**1a**)	Final Candidate (**BAY 1214784**)
hGnRH-R	1530 nM	21 nM
CL_{blood} (rat)	3.10 L/h/kg	0.75 L/h/kg
LLE	1.8	4.0